The Molecular Organisation in Starch Based Products

The Influence of Polyols used as Plasticisers

De Moleculaire Organisatie in Zetmeelproducten

De Invloed van Polyolen als Weekmakers

(met een samenvatting in het Nederlands)

Proefschrift

Ter verkrijging van de graad van doctor aan de Universiteit Utrecht
op gezag van de Rector Magnificus, Prof. Dr. W.H. Gispen,
ingevolge het besluit van het College voor Promoties
in het openbaar te verdedigen
op woensdag 12 december 2001 des middags te 14.30 uur

door

Angela Leonarda Maria Smits

geboren op 9 mei 1974 te Den Dungen

Promotor: **Prof. Dr. J.F.G. Vliegenthart**

Verbonden aan het Bijvoet Centrum van de
Faculteit Scheikunde van de Universiteit Utrecht

Dit proefschrift werd mede mogelijk gemaakt met financiële steun van Technologiestichting STW van de Nederlandse Organisatie voor Wetenschappelijk Onderzoek NWO.

ISBN: 90393288-0

Cover: Polarised light microscopy picture of
potato starch granules and ghosts

Contents

Chapter 1

Introduction

Starch

In green plant cells and in several micro-organisms assimilation of CO_2 and H_2O takes place to form the energy-source glucose. Energy is stored in plant roots, seeds, fruits, tubers, leaves, kernels, pollen and trunks as two polymeric forms of glucose, amylose and amylopectin. Amylose is essentially a linear polymer in which glucose residues are α-D-(1→4) linked, whereas amylopectin also contains α-D-(1→6) bonds, which make it a branched polymer [1].

Amylose is linear or slightly branched, has a degree of polymerisation up to DP 6000, and a molecular mass of 10^5 to 10^6 g/mol. The chains can easily form single or double helices [2]. Amylopectin (10^7-10^9 g/mol) is highly branched and has an average DP 2.000.000, making it one of the largest molecules in nature. Chain lengths of 20-25 glucose units between branch points are typical [3]. Its structure is often described by a cluster model (Figure 1.1). The cluster model gained greater credence when Hizukuri postulated that amylopectin chains are either located within a single cluster or serve to connect two or more clusters [4,5]. Short chains (A) of DP 12-16 that can form double helices, are arranged in clusters. The clusters comprise 80-90% of the chains, and are linked by longer chains (B) that form the other 10-20% of the chains. Most B-chains extend into two (DP ~40) or three clusters (DP ~70), but some extend into more clusters (DP ~110) [4].

Amylose and amylopectin are stored as granules of 1-100 μm in diameter. The granules contain in addition water and small amounts of lipids and proteins, and the contents vary for different starch sources [6,7]. These starch granules have a high degree of radial organisation, which is established by an interference Maltese cross in polarised light microscopy. In native starch, amylose and the branching regions of amylopectin are amorphous, but the linear outer chains of amylopectin are crystalline double helices arranged in lamellae [8-18]. Crystal growth in granules probably starts in the middle and develops in an outward direction, causing the radial organisation.

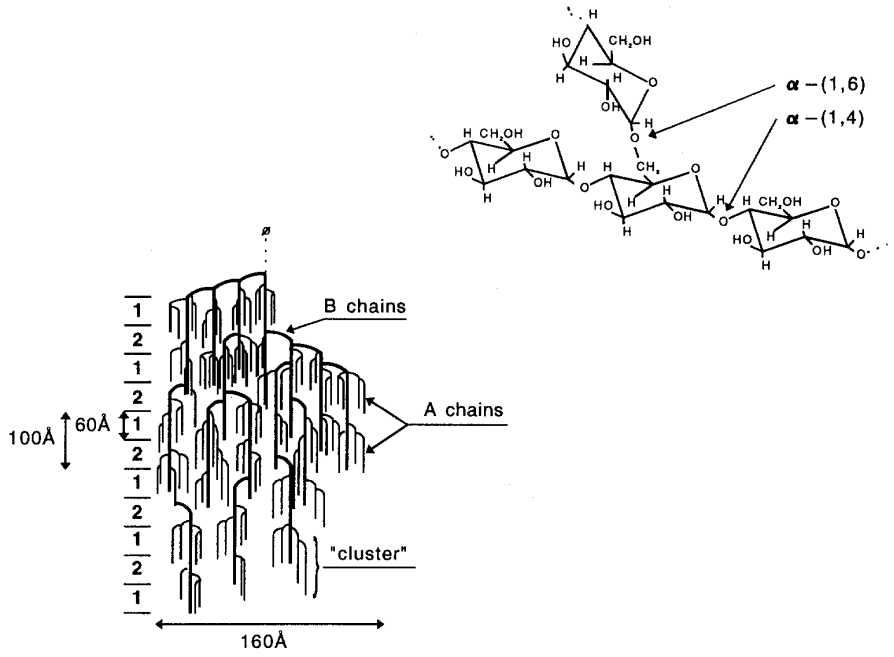

Figure 1.1 Cluster model of amylopectin.

Some different types of starch crystallinity have been observed, denoted A-, B-, C- or V- type [19]. The crystal type is determined by the amylose / amylopectin ratio, the molecular mass distribution, the degree of branching and the length of the outer amylopectin chains. These factors are different for different plant sources [7,20-24]. In general the A-type structure is found in cereal starch, and the B-type structure in tuber starch. The C-type structure is seen as an intermediate between the A- and B-structures. It is less common and can be found for example in pea starch. The A- and B-type crystal lattices both consist of parallel-stranded double helices that are packed in a hexagonal assembly [25-32]. The B-type structure has a column of water molecules in the centre of the hexagonal arrangement, whereas in the A-type structure an extra double helix is present. Both crystal unit cells contain12 glucose residues, but the more densely packed A-type structure contains 4 water molecules and the B-type structure contains 36 water molecules in the crystal unit cell. The V-type crystal structure is a single helical structure that is found for amylose complexed with lipids or other complexing agents [20,33-36]. The V-type crystal lattice has a relatively large cavity that is thought to contain the complexed compound. There are several V-type structures, varying in number of glucose residues per helix turn and in crystal packing.

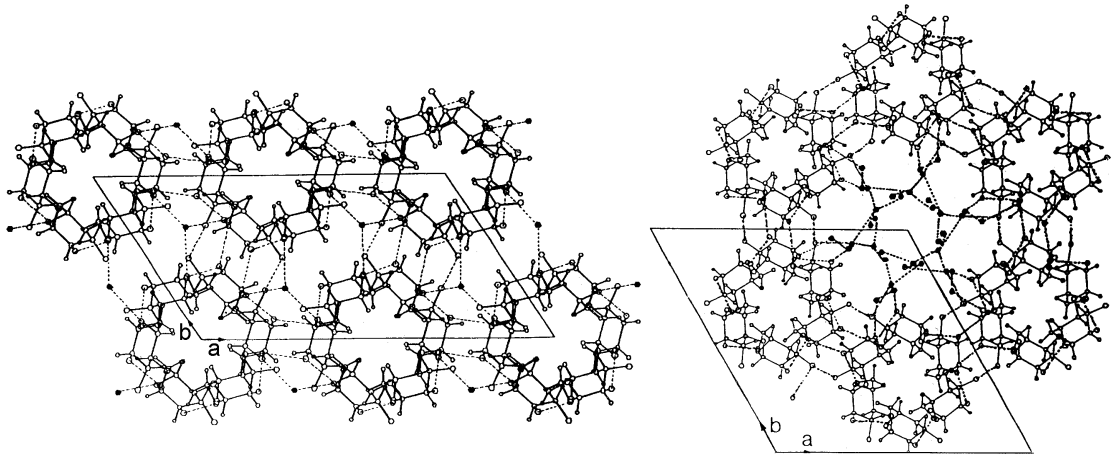

Figure 1.2 Projection on the (a,b) plane of A-type (left) and B-type (right) starch crystal structures. Hydrogen bonds are indicated as broken lines, (•) indicate water molecules [32].

Gelatinisation

Due to strong hydrogen bonding, starch granules are insoluble in cold water. But upon heating in water, the granules will gradually start swelling irreversibly. First the amorphous regions will swell, leading to disruption of the radial organisation. Then the crystalline regions begin to disrupt, the granule still being held together. Some amylose will leach out into the water, resulting in a viscosity increase until the largest hydrated swollen volume of the granules is reached. The granular remnants without polysaccharide order are known as ghosts. Then the swollen granules will begin to rupture and collapse. The viscous dispersion of granule fragments and dissolved molecules will finally become a viscous starch solution (Figure 1.3). This process is known as gelatinisation [7,37-41]. The ability of starch to produce such a viscous paste, when heated in water, is a property used in many starch applications.

In food applications, processing usually includes starch gelatinisation. Bakery doughs are processed at high water contents and are (partly) gelatinised and dried during baking to yield low water content products like bread, cookies and crackers [42]. During processing enzymes can degrade starch, producing various malto-oligosaccharides [43,44]. Much research has been done on gelatinised starch gels, amylose gels and amylopectin gels of high water contents, but for bakery products it is interesting to investigate gelatinised starch systems of low water contents.

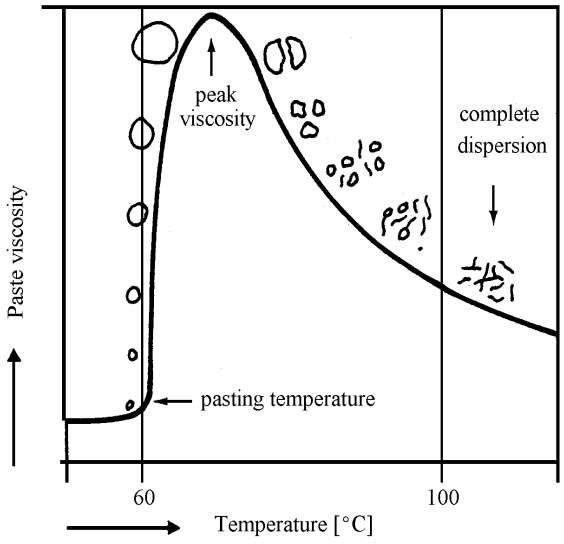

Figure 1.3 Swelling, disruption and dispersion of a starch granule during gelatinisation.

Also the influence of water and polyol plasticisers like sugars is important for these systems. The ageing of bread has been investigated, but from this multiple component system it is rather difficult to attribute features to specific constituents [45]. Therefore, in this thesis (partly) gelatinised starch is investigated with various water contents and only one polyol plasticiser for each system.

Melting

At sufficiently low temperatures, the starch polymer chains are restricted in their molecular motion, rendering a glassy, brittle material. Upon heating to gradually higher temperatures with DSC, at the so-called glass transition temperature T_g, the polymer chain mobility increases due to increasing kinetic energy, yielding a ductile material [46,47]. A stepwise change in heat capacity is observed. Upon increasing the temperature further, a crystalline melting endotherm M_1 is observed characteristic for low moisture starch. Then, a second melting endotherm M_2 is observed denoting the melting of amylose-lipid complexes [37]. Subsequently, the high-temperature endotherm HT is observed, which marks the transition into a thermoplastic melt (Figure 1.4, curve B).

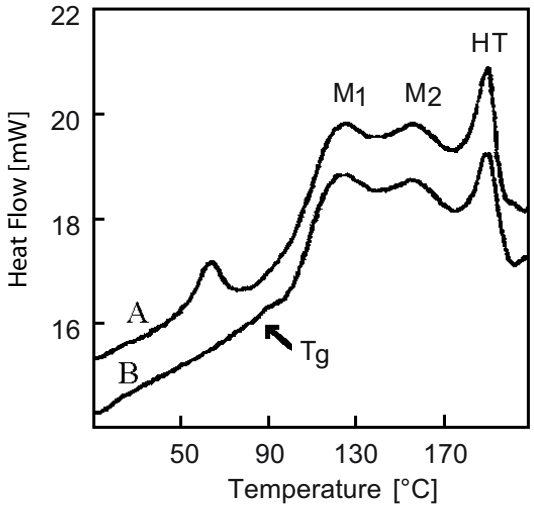

Figure 1.4 DSC curves of potato starch. A: aged below T_g, B: native PN.

During processing starch for thermoplastic starch (TPS) plastics, low water content starch systems are tailored through subjection to thermal and mechanical forces, which makes them melt. Plasticisers are added to enable melting below the decomposition temperature. This makes it important to examine (partly) melted systems with low water contents, and the influence of water and polyol plasticisers, like glycerol, on these systems. Starch melting has been investigated by using DSC, and by X-ray diffraction of starch that was previously subjected to different temperatures for certain periods of time [42,48-50]. In this thesis starch is investigated that is melted by thermal force without shear, using compression moulding.

Classification of starch products

Depending on the amount of water used during processing, starch is either gelatinised or melted. In the bakery industry, partly gelatinised starch products are obtained due to the use of high water concentrations in dough. Also in other food applications like in puddings or soups, and in non-food applications like paper sizing agents, adhesives and coatings, use is made of gelatinisation. When applied in bioplastics, either as a filler material in plastics, grafted on other polymers or as starch based plastic, low water contents are used during processing and starch is partly melted.

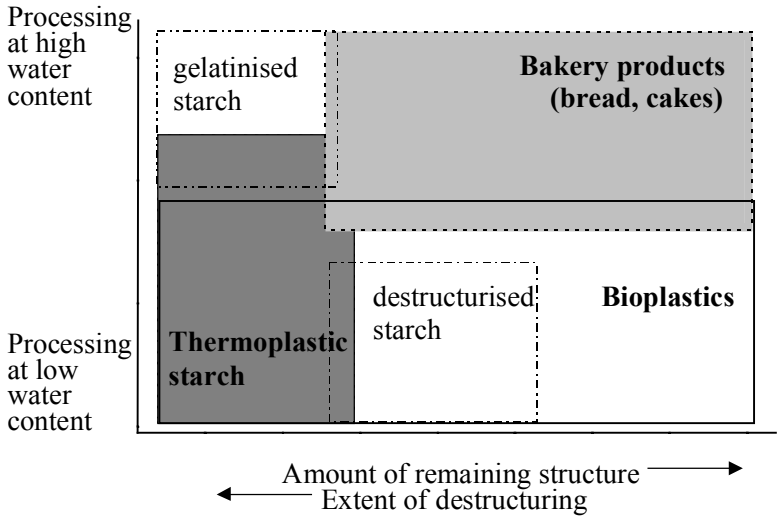

Figure 1.5 Classification of starch based systems.

In Figure 1.5 starch products are classified with respect to the processing water contents and the extent of destructuring obtained during processing. In thermoplastic starch and gelatinised starch the granular crystalline structure is substantially disrupted, whereas in starch products structure disruption can be less complete. Thermoplastic starch (TPS) is referred to when granular starch is processed at low water contents using thermal and mechanical forces, in the presence of (polyol) plasticisers that do not evaporate substantially during processing. Substantially amorphous starch is yielded. Several other additives like lipids, lecithin and glycerol monostearate are used to improve flow properties. TPS can be moulded using standard equipment used for the processing of synthetic polymers, such as injection moulding, blow moulding and compression moulding. The term destructurised starch (DS) is used for granular starch that is turned into a homogeneous, mainly amorphous starch mixture using thermal and mechanical forces, irrespective of the additives used. Little knowledge on molecular processes in starch systems has been developed regarding low water contents systems and regarding the influence of granular remnants like ghosts, remaining due to incomplete gelatinisation or melting.

Ageing

The ageing of starch systems has a major effect on the quality of many products. Because the predominantly amorphous products are not at thermodynamic equilibrium, the systems will approach this equilibrium in time. In this matter, one

should distinguish between sub T_g physical ageing and retrogradation. For starch-based foods, such as bread and dough, ageing (due to recrystallisation or retrogradation of starch) exhibits itself as staling. Especially for new products such as low-fat baked or convenience foods, sufficient practical experience and insight into mechanisms underlying ageing have not yet been built up to overcome staling. In non-food uses of starch such as in paper and adhesives applications or plastics, retrogradation affects the processing and final properties. Starch based glues (e.g. in corrugated board) may therefore break into pieces, and adhesive properties of starch based hot melts are reduced. Recently developed starch plastics have the unwanted tendency to become brittle in time. These processes are analogous to the staling process in baked goods.

Retrogradation

During storage (ageing) of starch systems, retrogradation occurs. It causes the staling of bakery products and the embrittlement of starch plastics, coatings and adhesives. The system goes from a dissolved, dissociated condition to a more ordered, associated state, which is thermodynamically more stable. In contrast to starch granules, in retrograded starch the crystalline material is mainly amylose. Amylose retrogradation involves rapid formation of helices, helix-helix aggregation and double helical crystal formation. Retrogradation of amylopectin is slow and only takes place at high starch concentrations or low temperatures. The crystals are composed of double helices formed by its short outer chains [51-55].

Retrogradation can cause a viscosity increase, opacity, turbidity, water syneresis (weeping) or the formation of a precipitate, a gel or an insoluble skin on hot pastes. The process depends on the starch type and concentration, storing time and temperature, processing and cooling procedure, pH and the presence of other compounds [56-65]. Because polymers cannot crystallise in the glassy state, retrogradation only takes place at temperatures higher than the glass transition temperature [66]. Plasticisers affect the polymer mobility and conformational behaviour in the system by increasing the distance between polymer chains and covering chains for interactions, therewith lowering T_g [67-70]. Polyol plasticisers have been found to reduce the retrogradation rate, probably as the result of starch-plasticiser interactions [71-81]. Since retrogradation causes unwanted changes in material properties during ageing, it is important to know how, why, where and when

retrogradation takes place exactly [82-84]. This has been elucidated to some extent for amylose and amylopectin gels, starch gels with various amylose to amylopectin ratios and for breadcrumbs [85-89]. The influence of plasticisers on retrogradation as well as retrogradation of melted systems have not been well investigated.

Sub T_g Physical Ageing

When an amorphous polymer is cooled below the glass transition temperature T_g its chain mobility is decreased and the thermodynamic properties can no longer follow the temperature change. There is a deviation from equilibrium linear enthalpy decrease, from a kinetic point of view. The system will gradually approach its thermodynamic equilibrium, decreasing the enthalpy. During this enthalpy relaxation the free volume between the polymer chains decreases. The material becomes stiffer and more brittle, known as physical ageing [90-99]. Upon heating the system, a sudden endothermic event can be observed [100-102]. The enthalpy loss during ageing is recovered to reach the equilibrium value (Figure 1.4, curve A).
During storage many food products are cooled or frozen. This may lower the temperature to below the glass transition temperature of the products. Other products already appear in the glassy state at room temperature. In the glassy state retrogradation does not take place, but the sub T_g relaxation phenomena become important. Sub T_g phenomena (physical ageing) have been investigated mainly for synthetic polymers [90-93]. However, some research has been done on starches and food systems [94-102], where the freezing of water becomes important at subzero temperatures [17,103].

Aim and Outline of this Thesis

The aim of this thesis is to increase fundamental insight into the molecular processes underlying the ageing of starch in order to help solving the problems of staling of baked foods and embrittlement of starch plastics, adhesives and coatings. Insight to be gained concerns the molecular behaviour of starch in the presence of water and polyol-type plasticisers, and the location and mobility of the various components. Most of the present knowledge on molecular processes in starch systems has been developed on high water systems (>50% H_2O), but because non-food starch products and baked products have low water contents (10-30%), the effect of low molecular mass additives is particularly important. Emphasis is on retrogradation, the influence

of polyol plasticisers on retrogradation, and the influence of structure remaining due to incomplete melting or gelatinisation.

For this thesis, model systems are prepared using native potato starch, because it is high in amylopectin and amylose concentrations, or wheat starch, which is mainly used in bakery products. The most important plasticisers in these model systems are glycerol and ethylene glycol, which are used in non-food starch products, and glucose, maltose and malto-oligosaccharides that are used in foods. The research combines new non-invasive solid state NMR and FT-IR spectroscopic techniques, which have moved forward the understanding of molecular phenomena in starch materials, and have shown to be applicable for determining the molecular mobility and organisation in various polymer systems. These techniques are applied in combination with X-ray diffraction and DSC, and are supported by dielectric relaxation spectroscopy.

References

1. T. Gilliard, P. Bowler, 'Morphology and composition of starch', *Critical Reports Appl. Chem.* **13** (1987), p 55-78,
2. C. Takeda, Y. Takeda, S. Hizukuri, 'Structure of amylomaize amylose', *Cereal Chem.* **66** (1989), p 22-25,
3. D.J. Manners, 'Recent developments in our understanding of amylopectin structure', *Carboh. Polym.* **11** (1989), p 87-112,
4. S. Hizukuri, 'Polymodal distribution of chain lengths of amylopectins and its significance', *Carboh. Res.* **147** (1986), p 342-347,
5. D.B. Thompson, 'On the non-random nature of amylopectin branching', *Carboh. Polym.* **43** (2000), p 223-239,
6. R. Hoover, 'Composition, molecular structure, and physicochemical properties of tuber and root starches', *Carboh. Polym.* **45** (2001), p 253-267,
7. J.J.M. Swinkels, 'Composition and properties of commercial native starches', *Starch/ Stärke* **37** (1985), p 1-5,
8. H.F. Zobel, 'Molecules to granules: a comprehensive starch review', *Starch/Stärke* **40** (1988), p 44-50,
9. G.T. Oostergetel, E.F.J. van Bruggen, 'The crystalline domains in potato starch granules are arranged in a helical fashion', *Carboh. Polym.* **21** (1993), p 7-12,
10. P.J. Jenskins, R.E. Cameron, A.M. Donald, 'A universal feature in the structure of starch granules from different botanical sources', *Starch/Stärke* **45** (1993), p 417-420,
11. P.J. Jenskins, A.M. Donald, 'The influence of amylose on starch granule structure', *Int. J. Biol. Macromol.* **17** (1995), p 315-321,
12. A. Buléon, B. Pontoire, C. Riekel, H. Chanzy, W. Helbert, R. Vuong, 'Crystalline ultrastructure of starch granules revealed by synchroton radiation microdiffraction mapping', *Macromolecules* **30** (1997), p 3952-3954,
13. H. Jacobs, N. Mischenko, M.H.J. Koch, R.C. Eerlingen, J.A. Delcour, H. Reynaers, 'Evaluation of the impact of annealing on gelatinisation at intermediate water content of wheat and potato starches: a DSC and SAXS study', *Carboh. Res.* **306** (1998), p 1-10,
14. T.A. Waigh, A.M. Donald, F. Heidelbach, C. Riekel, M.J. Gidley, 'Analysis of the native structure of starch granules with small angle X-ray microfocus scattering', *Biopolymers* **49** (1999), p 91-105,

15. R.F. Tester, S.J.J. Debon, 'Annealing of starch: a review', *Int. J. Biol. Macromol.* **27** (2000), p 1-12,
16. P.A. Perry, A.M. Donald, 'SANS study of the distribution of water within starch granules', *Int. J. Biol. Macromol.* **28** (2000), p 31-39,
17. P.A. Perry, A.M. Donald, 'The effects of low temperatures on starch granule structure', *Polymer* **41** (2000), p 6361-6373,
18. H.R. Tang, J. Godward, B. Hills, 'The distribution of water in native starch granules: a multinuclear NMR study', *Carboh. Polym.* **43** (2000), p 375-387,
19. A. Sarko, H.C.H. Wu, 'The crystal structures of A-, B-, and C-polymorphs of amylose and starch', *Starch/Stärke* **30** (1978), p 73-78,
20. H.F. Zobel, 'Starch crystal transformations and their industrial importance', *Starch/Stärke* **40** (1988), p 1-7,
21. N.W.H. Cheetham, L. Tao, 'The effects of amylose content on the molecular size of amylose, and on the distribution of amylopectin chain length in maize starches', *Carboh. Polym.* **33** (1997), p 251-261,
22. J.D. Klucinek, D.B. Thompson, 'Fractionation of high-amylose maize starches by differential alcohol precipitation and chromatography of the fractions', *Cereal Chem.* **75** (1998), p 887-896,
23. C. Gérard, V. Planchot, P. Colonna, E. Bertoft, 'Relationship between branching density and crystalline structure of A- and B-type maize mutant starches', *Carboh. Res.* **326** (2000), p 130-144,
24. C. Gérard, C. Barron, P. Colonna, V. Planchot, 'Amylose determination in genetically modified starches', *Carboh. Polym.* **44** (2001), p 19-27,
25. K. Kainuma, D. French, 'Naegeli amylodextrin and its relationship to starch granule structure', *Biopolymers* **11** (1972), p 2241-2250,
26. H.C.H. Wu, A. Sarko, 'The double-helical molecular structure of crystalline B-amylose', *Carboh. Res.* **61** (1978), p 7-25,
27. H.C.H. Wu, A. Sarko, 'The double-helical molecular structure of crystalline A-amylose', *Carboh. Res.* **61** (1978), p 27-40,
28. A. Imberty, H. Chanzy, S. Pérez, A. Buléon, V. Tran, 'New three-dimensional structure for A-type starch', *Macromolecules* **20** (1987), p 2634-2636,
29. A. Imberty, H. Chanzy, S. Pérez, A. Buléon, V. Tran, 'The double-helical nature of the crystalline part of A-starch', *J. Mol. Biol.* **201** (1988), p 365-378,
30. A. Imberty, S. Pérez, 'A revisit to the three-dimensional structure of B-type starch', *Biopolymers* **27** (1988), p 1205-1221,
31. S. Pérez, A. Imberty, R.P. Scaringe, 'Modelling of interactions of polysaccharide chains', in: *Computer modelling for carbohydrates*, A.D. French, W. Brady, eds., Am. Chem. Soc. **430** (1990),
32. A. Imberty, A. Buléon, V. Tran, S. Pérez, 'Recent advances in knowledge of starch structure', *Starch/Stärke* **43** (1991), p 375-384,
33. C.E. Snape, W.R. Morrison, M. M. Maroto-Valer, J. Karkalas, R.A. Pethrick, 'Solid state ^{13}C NMR investigation of lipid ligands in V-amylose inclusion complexes', *Carboh. Polym.* **36** (1998), p 225-237,
34. N.W.H. Cheetham, L. Tao, 'Solid state NMR studies on the structural and conformational properties of natural maize starches', *Carboh. Polym.* **36** (1998), p 285-292,
35. S. Immel, F.W. Lichtenthaler, 'The hydrophobic topographies of amylose and its blue iodine complex', *Starch/Stärke* **52** (2000), p 1-8,
36. P. Lebail, A. Buléon, D. Shiftan, R.H. Marchessault, 'Mobility of lipid in complexes of amylose-fatty acids by deuterium and ^{13}C solid state NMR', *Carboh. Polym.* **43** (2000), p 317-326,
37. R.C. Hoseney, K.J. Zeleznak, D.A. Yost, 'A note on the gelatinization of starch', *Starch/Stärke* **38** (1986), p 407-409,

38. C.G. Biliaderis, C.M. Page, T.J. Maurice, B.O. Juliano, 'Thermal characterisation of rice starches: a polymeric approach to phase transitions of granular starch', *J. Agric. Food Chem*. **34** (1986), p 6-14,
39. P.J. Jenskins, A.M. Donald, 'Gelatinisation of starch: a combined SAXS/WAXS/DSC and SANS study', *Carboh. Res.* **308** (1998), p 133-147,
40. N.J. Atkin, R.M. Abeysekera, S.L. Cheng, A.W. Robards, 'An experimentally-based predictive model for the separation of amylopectin subunits during starch gelatinization', *Carboh. Polym.* **36** (1998), p 173-192,
41. T.A. Waigh, M.J. Gidley, B.U. Komanshek, A.M. Donald, 'The phase transformations in starch during gelatinisation: a liquid crystalline approach', *Carboh. Res*. **328** (2000), p 165-176,
42. H. Levine, L. Slade, 'Water relationships in food', Plenum Press New York (1991),
43. A. Léon, E. Durán, C. Benedito de Barber, 'Firming of starch gels and amylopectin retrogradation as related to dextrin production by α-amylase', *Z. Lebensm. Unters. Forsch. A* **205** (1997), p 131-134,
44. E. Durán, A. Léon, B. Barber, C. Benedito de Barber, 'Effect of low molecular weight dextrins on gelatinization and retrogradation of starch', *Eur. Food Res. Techn.* **212** (2001), p 203-207,
45. C.C. Biliaderis, 'Structures and phase transitions of starch in food systems', *Food Technology* **46** (1992), p 98-109, 145,
46. H. Bizot, P. Le Bail, B. Leroux, J. Davy, P. Roger, A. Buléon, 'Calorimetric evaluation of the glass transition in hydrated, linear and branched polyanhydroglucose compounds', *Carboh. Polym.* **32** (1997), p 33-50,
47. R.F. Boyer, 'Structure of the amorphous state in polymers', *Ann N.Y. Acad. Sci.* **279** (1976), p 223-233,
48. V.P. Yuryev, A.N. Danilenko, I.E. Nemirovskaya, N.D. Lukin, A.I. Zushman, V.G. Karpov, 'Structure and thermodynamic parameters of melting native starch grains in various potato varieties', *Appl. Biochem. & Microbiol.* **32** (1996), p 514-518,
49. Y.I. Matveev, J.J.G. van Soest, C. Nieman, L.A. Wasserman, V.A. Protserov, M. Ezernitskaja, V.P. Yuryev, 'The relationship between thermodynamic and structural properties of low and high amylose maize starches', *Carboh. Polym.* **44** (2001), p 151-160,
50. C. Barron, A. Buléon, P. Colonna, G. Della Valle, 'Structural modifications of low hydrated pea starch subjected to high thermomechanical processing', *Carboh. Polym.* **43** (2000), p 171-181,
51. M.J. Miles, V.J. Morris, S.G. Ring, 'Gelation of amylose', *Carboh. Res.* **135** (1985), p 257-269,
52. S.G. Ring, P. Colonna, K.J. I'Anson, M.T. Kalichevsky, M.J. Miles, V.J. Morris, P.D. Orford, 'The gelation and crystallisation of amylopectin', *Carboh. Res.* **162** (1987), p 277-293,
53. D. Sievert, P. Würsch, 'Amylose chain association based on differential scanning calorimetry', *J. Food. Sci.* **58** (1993), p 1332-1334,
54. K. Ishiguro, N. Kumamoto, K. Kagoshima, O. Yamakawa, 'Retrogradation of sweetpotato starch', *Starch/Stärke* **52** (2000), p 13-17,
55. J.L. Puteaux, A. Buléon, H. Chanzy, 'Network formation in dilute amylose and amylopectin studied by TEM', *Macromolecules* **33** (2000), p 6416-6422,
56. K.J. Zeleznak, R.C. Hoseney, 'Characterisation of starch from bread aged at different temperatures', *Starch/Stärke* **39** (1987), p 231-233,
57. P.L. Russell, G. Oliver, 'The effect of pH and NaCl content on starch gel ageing; a study by DSC and rheology', *J. Cereal Sci.* **10** (1989), p 123-138,
58. M. Gudmundsson, A.C. Eliasson, 'Retrogradation of amylopectin and the effects of amylose and added surfactants/emulsifiers', *Carboh. Polym.* **13** (1990), p 295-315,
59. Y.C. Shi, P.A. Seib, 'The structure of four waxy starches related to gelatinization and retrogradation', *Carboh. Res.* **227** (1992), p 131-145,

60. M. Gudmundsson, 'Retrogradation of starch and the role of its components', *Thermochim. Acta* **246** (1994), p 329-341,
61. M.R. Jacobson, M. Obanni, J.N. Bemiller, 'Retrogradation of starches from different botanical sources', *Carbohydrates* **74** (1997), p 511-518,
62. J.J.G. van Soest, D.B. Borger, 'Structure and properties of compression-molded thermoplastic starch materials from normal and high-amylose maize starches', *J. Appl. Polym. Sci*. **64** (1997), p 631-644,
63. T.J. Lu, J.L. Jane, P.L. Keeling, 'Temperature effect on retrogradation rate and crystalline structure of amylose', *Carboh. Polym.* **33** (1997), p 19-26,
64. V. Evageliou, R.K. Richardson, E.R. Morris, 'Effect of sucrose, glucose and fructose on gelation of oxidised starch', *Carboh. Polym.* **42** (2000), p 261-272,
65. M. Stading, Å. Rindlav-Westling, P. Gatenholm, 'Humidity-induced structural transitions in amylose and amylopectin films', *Carboh. Polym.* **45** (2001), p 209-217,
66. K. Jouppila, J. Kansikas, Y.H. Roos, 'Factors affecting crystallization and crystallization kinetics in amorphous corn starch', *Carboh. Polym.* **36** (1998), p 143-149,
67. C. van den Berg, F.S. Kaper, J.A.G. Weldring, I. Wolters, 'Water binding by potato starch', *J. Food Tech.* **10** (1975), p 589-602,
68. H. Bizot, A. Buleon, N. Mouhous-Riou, J.L. Multon, 'Some facts concerning water vapour sorption hysteresis on potato starch', in: *Properties of water in foods*, D. Simatos, J.L. Multon, eds., Martinus Nijhoff Publishers, Dordrecht (1985), p 83-93,
69. D. Lourdin, L. Coignard, H. Bizot, P. Colonna, 'Influence of equilibrium relative humidity and plasticizer concentration on the water content and glass transition of starch materials', *Polymer* **38** (1997), p 5401-5406,
70. Y.I. Matveev, V.Y. Grinberg, V.B. Tolstoguzov, 'The plasticizing effect of water on proteins, polysaccharides and their mixtures: glassy state of biopolymers, food and seeds', *Food Hydrocoll.* **14** (2000), p 425-437,
71. N. Krog, S.K. Oleson, H. Toernaes, T. Joensson, 'Retrogradation of the starch fraction in wheat bread', *Cereal Foods World* **34** (1989), p 281-285,
72. K. Kohyama, K. Nishinari, 'Effect of soluble sugars on gelatinization and retrogradation of sweet potato starch', *J. Agric. Food. Chem.* **39** (1991), p 1406-1410,
73. P. Cairns, M.J. Miles, V.J. Morris, 'Studies of the effect of the sugars ribose, xylose and fructose on the retrogradation of wheat starch gels by X-ray diffraction', *Carboh. Polym.* **16** (1991), p 355-365,
74. K. Katsuta, M. Miura, A. Nishimura, 'Kinetic treatment for rheological properties and effects of saccharides on retrogradation of rice starch gels', *Food Hydrocoll.* **6** (1992), p 187-198,
75. K. Katsuta, A. Nishimura, M. Miura, 'Effects of saccharides on stabilities of rice starch gels: 1. Monosaccharides and disaccharides', *Food Hydrocoll.* **6** (1992), p 387-398,
76. K. Katsuta, A. Nishimura, M. Miura, 'Effects of saccharides on stabilities of rice starch gels: 2. Oligosaccharides', *Food Hydrocoll.* **6** (1992), p 399-408,
77. M.T. Kalichevsky, E.M. Jaroszkiewicz, J.M.V. Blanshard, 'A study of the glass transition of amylopectin-sugar mixtures', *Polymer* **34** (1993), p 346-358,
78. J.J.G. van Soest, D. de Wit, H. Tournois, J.F.G. Vliegenthart, 'The influence of glycerol on structural changes in waxy maize starch as studied by FT-IR spectroscopy', *Polymer* **35** (1994), p 4722-4727,
79. L.A. Bello-Pérez, O. Parades-López, 'Effects of solutes on retrogradation of stored starches and amylopectins: a calorimetric study', *Starch/Stärke* **47** (1995), p 83-86,
80. E. Chiotelli, A. Rolée, M. Le Meste, 'Effect of sucrose on the thermomechanical behavior of concentrated wheat and waxy corn starch-water preparations', *J. Agric. Food Chem.* **48** (2000), p 1327-1339,
81. M.A. García, M.N. Martino, N.E. Zaritzky, 'Microstructural characterization of plasticized starch-based films', *Starch/Stärke* **52** (2000), p 118-124,
82. L. Slade, H. Levine, 'Recent advances in starch retrogradation', in: *Industrial polysaccharides*, S.S. Stivala, V. Crescenzi, I.C.M. Dea, eds., Gordon & Breach Science Publishers, New York (1987),

83. J.J.G. van Soest and N. Knooren, 'Influence of glycerol and water content on the structure and properties of extruded starch plastic sheets during aging', *J. Appl. Polym. Sci*. **64** (1997), p 1411-1422,
84. C.G. Biliaderis, 'Structure and phase transitions of starch in food systems', *Food Techn.* **6** (1992), p 98-109,
85. K. Kulp, J.G. Ponte, 'Staling of white pan bread: fundamental causes', *CRC Critical Reviews in Food Science and Nutrition*, September (1981),
86. K.J. Zeleznak, R.C. Hoseney, 'The role of water in the retrogradation of wheat starch gels and bread crumb', *Cereal Chem.* **63** (1986), p 407-411,
87. P.L. Russell, 'The ageing of gels from starches of different amylose/amylopectin content studied by differential scanning calorimetry', *J. Cereal Sci.* **6** (1987), p 147-158,
88. B.J. Goodfellow, R.H. Wilson, 'A Fourier transform IR study of the gelation of amylose and amylopectin', *Biopolymers* **30** (1990), p 1183-1189,
89. A.S. Kulik, J. Haverkamp, 'Molecular mobility of polysaccharide chains in starch investigated by two-dimensional solid state NMR spectroscopy', *Carboh. Polym*. **34** (1997), p 49-54,
90. L.C.E. Struik, 'Physical ageing in amorphous glassy polymers', *Ann N.Y. Acad. Sci.* **279** (1976), p 78-85,
91. J. Heijboer, 'Molecular origin of relaxations in polymers', *Ann N.Y. Acad. Sci.* **279** (1976), p 104-116,
92. L.C.E. Struik, 'Effect of thermal history on secondary relaxation processes in amorphous polymers', *Polymer* **28** (1987), p57-68,
93. S. Wu, 'Secondary relaxation, brittle-ductile transition temperature, and chain structure', *J. Appl. Polym. Sci.* **46** (1992), p 619-624,
94. G.E. Attenburrow, A.P. Davies, R.M. Goodband, S.J. Ingman, 'The fracture behaviour of starch and gluten in the glassy state', *J. Cereal Sci.* **16** (1992), p 1-12,
95. R.J. Nicholls, I.A.M. Appelqvist, A.P. Davies, S.J. Ingman, P.J. Lillford, 'Glass transitions and the fracture behaviour of gluten and starches within the glassy state', *J. Cereal. Sci.* **21** (1995), p 25-36,
96. M. Le Meste, G. Roudaut, S. Davidou, 'Thermomechanical properties of glassy cereal foods', *J. Thermal Anal.* **47** (1996), p 1361-1375,
97. G. Roudaut, M. Maglione, D. van Dusschoten, M. Le Meste, 'Molecular mobility in glassy bread: a multispectroscopy approach', *Cereal Chem.* **76** (1999), p 70-77,
98. G. Roudaut, M. Maglione, M. Le Meste, 'Relaxations below glass transition temperature in bread and its components', *Cereal Chem.* **76** (1999), p 78-81,
99. Y.P. Chang, P.B. Cheah, C.C. Seow, 'Plasticizing-antiplasticizing effects of water on physical properties of tapioca starch films in the glassy state', *J. Food Sci.* **65** (2000), p 445-451,
100. R.L. Shogren, 'Effect of moisture-content on the melting and subsequent physical ageing of cornstarch', *Carboh. Polym.* **19** (1992), p 83-90,
101. R.L. Shogren, B.K. Jasberg, 'Ageing properties of extruded high-amylose starch', *J. Env. Polym. Degr.* **2** (1994), p 99-109,
102. H.J. Thiewes, P.A.M. Steeneken, 'The glass transition and the sub-T_g endotherm of amorphous and native potato starch at low moisture content', *Carboh. Polym.* **32** (1997), p 123-130,
103. P. Cornillon, J. Andrieu, J.C. Duplan, M. Laurent, 'Use of NMR to model thermophysical properties of frozen and unfrozen model food gels', *J. Food. Eng.* **25** (1995), p 1-19.

Chapter 2

Analytical Techniques

A combination of analytical techniques is used in order to examine the molecular organisation and molecular dynamics in starch based materials at various molecular levels. Conventional techniques used, arranged from looking at a long-range towards a short-range molecular level, are polarised light microscopy, differential scanning calorimetry (DSC), X-ray diffraction (XRD), and infrared spectroscopy (FT-IR). Less conventional techniques in carbohydrate research are solid state nuclear magnetic resonance (NMR) spectroscopy, which is growing to be more common, and dielectric relaxation spectroscopy (DRS).

Polarised Light Microscopy

With polarised light microscopy the radial orientation in starch granules is observed as a strong interference cross, the Maltese cross. Polarised light microscopy can therefore be used to see if samples contain starch in the granular form, and how sample treatment influences the granule structure [1,2].

Differential Scanning Calorimetry

In Differential Scanning Calorimetry samples are heated at a constant rate. The calorimeter consists of a sample and a reference container, both heated separately over a certain temperature range, and being kept at equal temperature. Variations in the heat capacity, enthalpy, melting and glass transition of the sample are detected by a difference in heat flow dQ/dt between reference and sample. In a DSC curve the difference in heat flow is given versus temperature or time. Heat is absorbed during melting resulting in an endothermic peak, and at the glass transition a stepwise change in heat flow is observed. For an exact determination of the melting enthalpy, calibration with a sample of known melting heat, e.g. Iridium or Indium, is necessary. The quotient of the melting enthalpy and the sample weight is called the specific melting enthalpy $\Delta\tilde{H}_m$ and indicates the amount of crystallinity of the analysed sample.

Melting of native starches and melting of recrystallised (aged) starch can be investigated to examine the extent of recrystallisation, recrystallisation kinetics, and the relationship with starch structure, such as the amylopectin chain lengths [3-8]. Recrystallised material will give melting peaks of the newly formed crystals. Thermal analysis can also be used to examine the influence of water and other plasticisers on the glass transition temperature of starches [9,10]. Furthermore, DSC can be used for investigating sub T_g ageing phenomena, since they bring about an endotherm below T_g [10-12].

X-Ray Diffraction

XRD has been used to study various existing starch crystal types [13-20], the extent of starch melting and gelatinisation [21], and the extent of retrogradation [7,8,22]. Different crystal types give their own specific diffractogram, and peak intensities are a

measure of the amount of crystalline material. The X-ray patterns of the A-, B-, and C-type crystal structures are displayed in Figure 2.1.

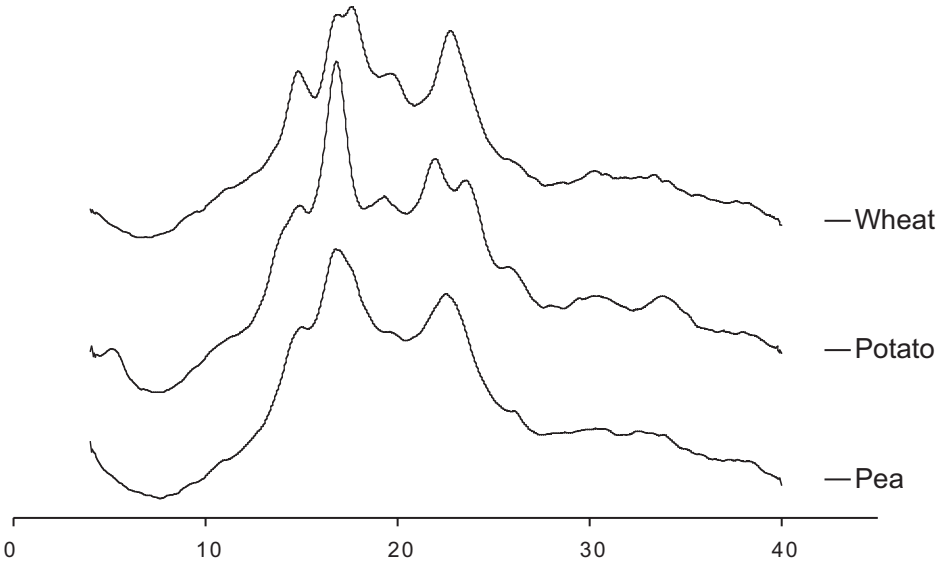

Figure 2.1 X-ray diffractograms of wheat, potato and pea starch, having A-, B-, and C-type crystallinity, respectively.

FT-IR spectroscopy

An IR absorption spectrum displays the amount of absorbed radiation as a function of the infrared wavelength or frequency. Reflection methods are divided into the classes Internal Reflectance such as Attenuated Total Reflection (ATR) and External Reflectance like Diffuse Reflectance (DRIFT).

In ATR infrared radiation is partly reflected and partly intrudes into the sample at the interface of an infrared transparent crystal (that has a high refractive index), like ZnSe, and the liquid or solid sample. The reflected radiation is internally multiple reflected within the crystal and therefore has multiple contact with the sample.

In DRIFT powder samples are diluted with non-absorbing material such as KBr. Infrared radiation penetrates into the sample and is refracted, transmitted and absorbed. It is also partly reflected at the surface, which may distort the spectrum. A Kubelka-Munk transformation is used to correct the spectra for the fact that radiation of a higher wavelength penetrates further into the sample and is thus better absorbed.

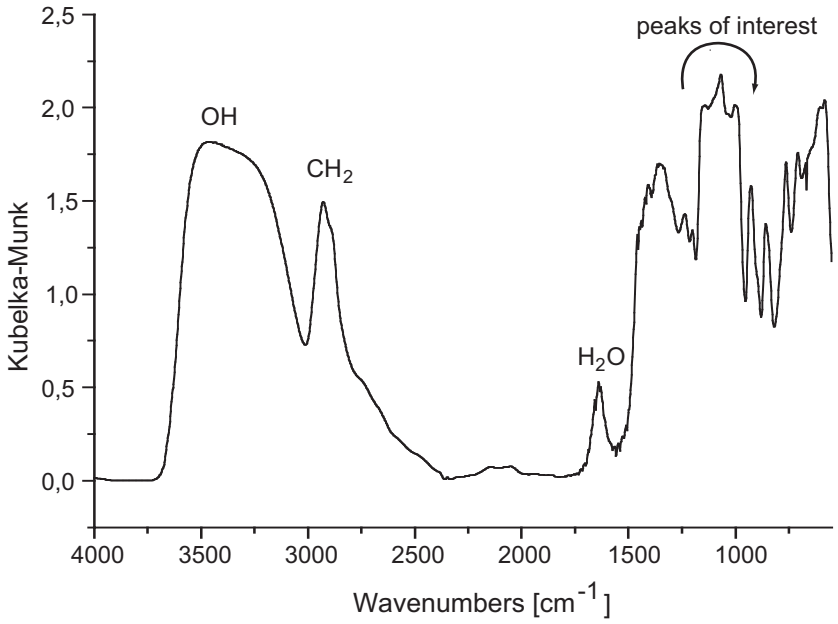

Figure 2.2 FT-IR spectrum of PN (moisture content 16.2 %).

Local interactions dominating the FT-IR spectra are effective on a sub-nanometer scale, making it possible to probe molecular order and dynamics at a microscopic level. Infrared techniques have been used for investigating retrogradation of amylose, amylopectin and starch gels, and breadcrumbs [23-28]. Peak intensities and positions vary with water contents, different extents of crystallinity and different crystal types [7,17,29-31]. Figure 2.2 displays the characteristic infrared spectrum of native potato starch. Changes in structure and crystallinity are reflected in the focus area between 1200 and 950 cm^{-1}, even though most bands arise from highly coupled and difficult to assign C-O and C-C stretching, and C-OH bending vibrations. Deconvolution can be used to enhance the resolution of individual components of these complex absorption bands [32].

Solid State NMR spectroscopy

Since 1976 it is possible to obtain solid state NMR spectra using dipolar decoupling (DD), magic angle spinning (MAS) and cross polarisation (CP) techniques [33]. Resolutions comparable to solution NMR can be obtained. Not only is it possible to analyse insoluble materials like cross-linked polymers. Solid state NMR additionally gives information on the physical properties of the material, like the specific crystal

structure, the amounts of crystalline and amorphous material and the molecular mobility and arrangement.

Using dipolar decoupling (DD), one radio frequency is used to observe signals, while an other radio frequency strongly irradiates the resonance of the nuclei to be decoupled, annulling the effective magnetic field generated by these nuclei. In ^{13}C NMR spectroscopy the protons are decoupled with ^{13}C-^{1}H DD, while homonuclear DD is not needed, because of the natural low amount of ^{13}C nuclei. In ^{1}H NMR spectroscopy pulse sequences are used for homonuclear decoupling. A higher resolution and more spectrum characteristics can be obtained by using DD.

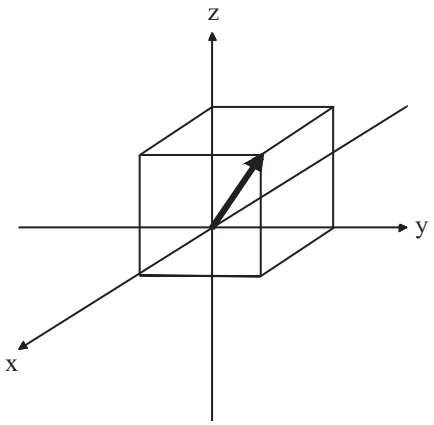

Figure 2.3 Schematic picture of the magic angle. The diagonal in a cube has an orientation of 54.7° with respect to all three axes.

By rapid spinning of samples at the so-called magic angle of 54.7° with respect to the external magnetic field (Figure 2.3), the chemical shift anisotropy is reduced to the isotropic average, as in solutions. Magic angle spinning (MAS) dramatically increases the resolution and also increases the signal intensity (Figure 2.4). Information on molecular anisotropy is lost, but can be regained by rotating the sample slower. The anisotropic coupling then appears as rotational sidebands next to the normal peak at distances of multiple times the rotation frequency.

Signal to noise ratios are increased by adding up multiple scans, alternated by spin relaxation. Using cross-polarisation (CP), polarisation is transferred from the abundant spins (^{1}H) to the dilute ^{13}C nuclei. After a 90° pulse, a spin-lock is imposed on the protons. Then, a radio frequency field on the ^{13}C channel causes the ^{13}C nuclei to spin with a frequency equal to that of the ^{1}H nuclei, transferring the proton magnetisation to the ^{13}C nuclei. CP not only reduces the measurement time because of the much shorter spin lattice relaxation time T_1 of protons, it also increases the signal intensity (Figure 2.4). Selective CP can be used by restricting the polarisation to

protonated or unprotonated carbons, in order to simplify complicated sideband spectra.

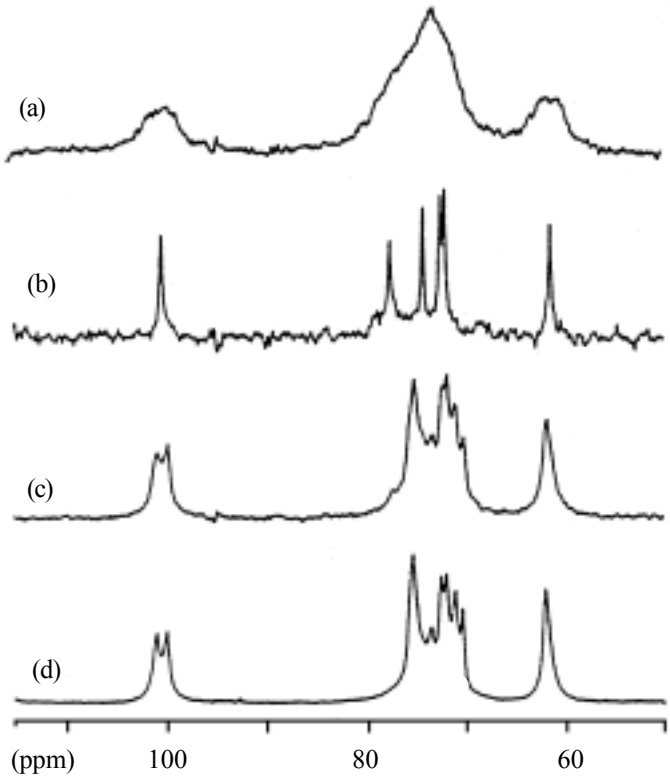

Figure 2.4 ^{13}C NMR spectra of a 10% amylose gel.
(a) single-pulse excitation without magic angle spinning,
(b) single-pulse excitation with magic angle spinning,
(c) cross polarisation with magic angle spinning (CP/MAS),
(d) CP/MAS on B-type crystalline solid amylose [34].

Other important information is given by measuring the spin lattice relaxation times T_1, the spin lattice relaxation times in the rotating frame $T_{1\rho}$ and the spin-spin relaxation times T_2 of ^1H and ^{13}C atoms. ^1H T_1 and $T_{1\rho}$ relaxation times, mostly detected indirectly via the ^{13}C resonances for a better resolution, provide information on the compatibility and miscibility in multi-component semi-crystalline polymeric systems. In general one can characterise the different phases due to their domain sizes and their mobility. ^{13}C $T_{1\rho}$ and T_2 provide additional information on the mobility of main chain or side chain atoms. ^{13}C T_1 and T_2 characterise fast motions in the MHz area, whereas ^{13}C $T_{1\rho}$ is sensitive to motions in the kHz area. Relaxation experiments can be used for characterising the influence of plasticisers added to starch.

Information on chemical structure, and especially on molecular order, mobility and the speed of molecular movements is obtained by two-dimensional solid state NMR, a rather advanced but time consuming technique. For example heterogeneity in solids is demonstrated by spin diffusion. A correlation between molecular structure and dynamics or between structure and order forms the basis of 2D NMR experiments as ^{1}H and ^{13}C nuclei are correlated.

The enormous freedom and flexibility of the NMR experiment have resulted in many different experimental approaches. Solid state NMR can give information on intramolecular conformation of the sample, like polymer stereoregularity, and on the intermolecular polymer chain packing in crystals. The chemical shifts give information on the extent of order in the material. Solid state NMR can give complementary information when detecting the less mobile sites by cross polarisation with magic angle spinning (CP/MAS) and the more mobile sites by single-pulse methods with high power decoupling (HP/DEC) [34]. Preference to the amorphous signal is given when a shorter time is taken in between the multiple scans, so that primarily the spins of the flexible parts are relaxed. Preference to the crystalline signal is given when CP contact is used, or spin-locking of the protons before CP. These techniques allow determination of the degree of molecular ordering, which can be compared with long-range ordering from, for example, X-ray diffraction. This can be related to the extent of retrogradation. Successful application is demonstrated by the characterisation of highly mobile hydrated biopolymers [35], primary plant cell walls [34] or starch gels [37-41].

Since 1985, starch has been subjected to solid state NMR spectroscopy, thereby identifying the different crystal types, their order and the proportion of each type [42-49]. Particularly the C-1 region in CP/MAS NMR experiments on starch is sensitive to the different crystal structures (Figure 2.5). The A-type starch structure shows three peaks in the C-1 region, due to three different glucose-units inside the crystal cell, whereas the B-type structure has two peaks for C-1, indicating two glucose-units in the crystal cell. The V-type structure can be identified by a broader C-1 resonance at 103-104 ppm, and a characteristic C-4 resonance at 82-83 ppm.

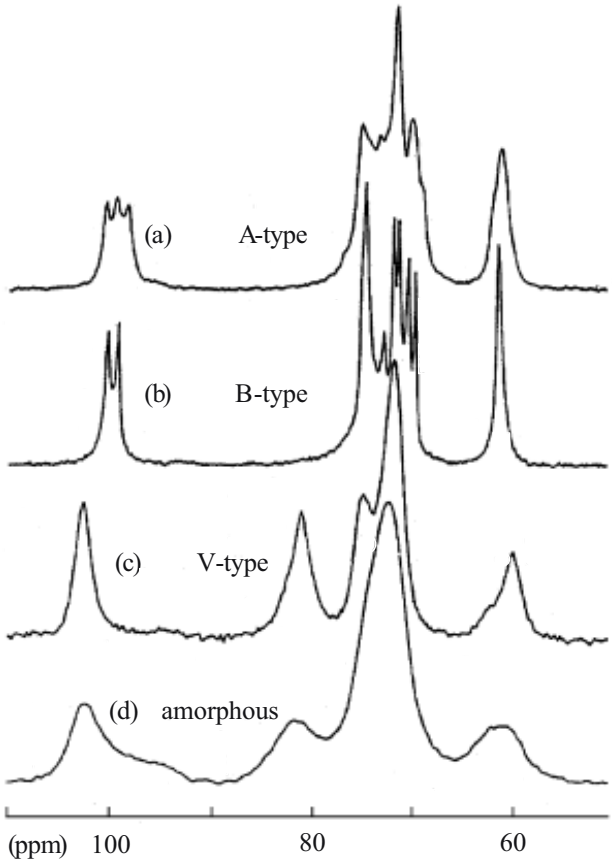

Figure 2.5 ^{13}C CP/MAS NMR spectra of double helical A-type (a) and B-type (b), and single helical V-type (c) crystalline starch, and amorphous starch (d) [34].

With the increasing knowledge on solid state NMR spectroscopy, many different NMR techniques have been used to learn more about starch. Molecular mobilities in starch gels, gel structures and water diffusion have been studied [7,39,50-53]. Two-dimensional solid state NMR techniques like the 2D Wideline Separation ^{1}H-^{13}C method (WISE) have been used to study the water organisation and molecular mobility in starch [54-57]. Other studies show the applicability of relaxation time experiments in starch based systems [38,44,57-61]. Fundamental studies concerning retrogradation of starch detected by solid state NMR, especially with relaxation time studies, are still limited. And the influence of different polyol plasticisers (including water) on retrogradation and the mobilities of plasticisers other than water have not been studied with NMR techniques.

Dielectric Relaxation Spectroscopy

Dielectric spectroscopy is a method to study molecular motions in polymers and is based on the measurement of the response of a material to an alternating electric field. Dielectric relaxation spectroscopy (DRS) is performed by placing a sample in a capacitor in the parallel plate geometry with a temperature control. The impedance is measured from which the dielectric permittivity ε', a measure of the polarisation in the sample, and the dielectric loss ε", a measure of the energy loss, are calculated. While the sample is subjected to a temperature program, frequency scans are taken at different temperatures. The dipoles and ions in the sample will try to follow the direction of the applied alternating current. At low frequencies the charges will move freely with the alternating current; the dielectric permittivity ε' is constant and the dielectric loss ε" is zero (Figure 2.6). At high frequencies the charges will not move, but are stuck in a position that does not have to be parallel with the field; the permittivity ε' is constant, but lower than in the low frequency situation, and the loss ε" is zero. During the frequency scan a transition between these two situations takes place; a smooth step in the permittivity ε' and a peak in the loss ε" is observed. The frequency at which such transition is found, depends on the characteristic relaxation time τ of the orientation process. Similarly, at low temperatures the charges are 'frozen' like at high frequencies. Upon increasing the temperature they become mobile and at high temperatures they move freely.

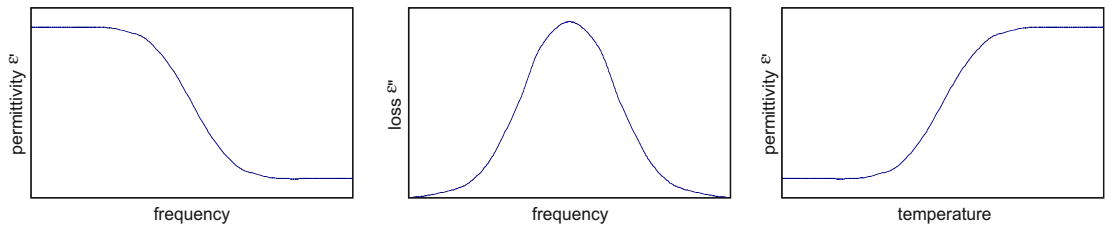

Figure 2.6 Changes in loss ε" and permittivity ε' during dielectric analysis.

For polymers more than one peak in loss ε" is found, because chain segments are more mobile than entire chains. At temperatures below the glass transition a ß-transition is found for the mobilisation of chain segments, and possibly at even lower temperatures a γ- or even a δ-transition are found for smaller segments. The relaxation times of these transitions follow Arrhenius law:

$$\tau = \tau_0 \exp (E_a / RT)$$

where τ_0 is the pre-exponent factor, denoting the relaxation time at infinite temperature, E_a is the thermal activation energy of the dipole rotation (J/mol), R is the gas constant (8.314 J/mol K) and T is the temperature (K).

The transition found at higher temperatures, due to mobilisation of whole chains (the glass transition), is an α-transition. It behaves according to Vogel-Fulcher-Tammann (VFT), which accounts for the fact that the dipole rotations are determined by the free volume in the polymer:

$$\tau = \tau_0 \exp (E_V / R(T-T_v))$$

where E_V is the VFT-activation energy and T_V is the VFT-temperature.

Dielectric spectroscopy is only recently applied to carbohydrates. In the past some studies of the dielectric properties of water in starch systems were reported [62,63]. Some saccharides and polysaccharides other than starch, such as cellulose and dextran have been analysed [64-68]. And recently different starch types, amylose-plasticiser systems and bread were studied [69-74].

References

1. A. Kawabata, N. Takase, E. Miyoshi, S. Sawayama, T. Kimura, K. Kudo, 'Microscopic observation and X-ray diffractometry of heat/moisture-treated starch granules', *Starch/ Stärke* **46** (1994), p 463-469,
2. S.H.D. Hulleman, F.H.P. Janssen, H. Feil, 'The role of water during plasticization of native starches', *Polymer* **39** (1998), p 2043-2048,
3. R.G. McIver, D.W.E. Axford, K.H. Colwell, G.A.H. Elton, 'Kinetic study of the retrogradation of gelatinised starch', *J. Sci. Food Agric.* **19** (1968), p 560-563,
4. Q. Liu, D.B. Thompson, 'Effects of moisture content and different gelatinization heating temperatures on retrogradation of waxy-type maize starches', *Carboh. Res.* **314** (1998), p 221-235,
5. J. Silverio, H. Fredriksson, R. Andersson, A.C. Eliasson, P. Åman, 'The effect of temperature cycling on the amylopectin retrogradation of starches with different amylopectin unit-chain length distribution', *Carboh. Polym.* **42** (2000), p 175-184,
6. V.M.F. Lai, S. Lu, C. Lii, 'Molecular characteristics influencing retrogradation kinetics of rice amylopectins', *Cereal Chem.* **77** (2000), p 272-278,
7. A.A. Karim, M.H. Norziak, C.C. Seow, 'Methods for the study of starch retrogradation', *Food Chem.* **71** (2000), p 9-36,
8. M.A. García, M.N. Martino, N.E. Zaritzky, 'Microstructural characterization of plasticized starch-based films', *Starch/Stärke* **52** (2000), p 118-124,
9. P.M. Forssell, J.M. Mikkilä, G.K. Moates, R. Parker, 'Phase and glass transition behaviour of concentrated barley starch-glycerol-water mixtures, a model for thermoplastic starch', *Carboh. Polym.* **34** (1997), p 275-282,
10. M.T. Kalichevsky, E.M. Jaroszkiewicz, A. Ablett, J.M.V. Blanshard, P.J. Lillford, 'The glass transition of amylopectin measured by DSC, DMTA and NMR', *Carboh. Polym.* **18** (1992), p 77-88,

11. H.J. Thiewes, P.A.M. Steeneken, 'The glass transition and the sub-T_g endotherm of amorphous and native potato starch at low moisture content', *Carboh. Polym.* **32** (1997), p 123-130,
12. R.L. Shogren, 'Effect of moisture-content on the melting and subsequent physical ageing of cornstarch', *Carboh. Polym.* **19** (1992), p 83-90,
13. A. Sarko, H.C.H. Wu, 'The crystal structures of A-, B-, and C-polymorphs of amylose and starch', *Starch/Stärke* **30** (1978), p 73-78,
14. A. Imberty, H. Chanzy, S. Pérez, A. Buléon, V. Tran, 'The double-helical nature of the crystalline part of A-starch', *J. Mol. Biol.* **201** (1988), p 365-378,
15. P.J. Jenskins, A.M. Donald, 'The influence of amylose on starch granule structure', *Int. J. Biol. Macromol.* **17** (1995), p 315-321,
16. J.J.G. van Soest, S.H.D. Hulleman, D. de Wit, J.F.G. Vliegenthart, 'Crystallinity in starch bioplastics', *Ind. Crops Prod.* **5** (1996), p 11-22,
17. J.J.G. van Soest, 'Starch plastics: structure-property relationships', Ph.D. thesis, Utrecht University (1996), Koninklijke Bibliotheek Den Haag,
18. N.W.H. Cheetham, L. Tao, 'Variation in crystalline type with amylose content in maize starch granules: an X-ray powder diffraction study', *Carboh. Polym.* **36** (1998), p 277-284,
19. A. Buléon, B. Pontoire, C. Riekel, H. Chanzy, W. Helbert, R. Vuong, 'Crystalline ultrastructure of starch granules revealed by synchroton radiation microdiffraction mapping', *Macromolecules* **30** (1997), p 3952-3954,
20. T.A. Waigh, A.M. Donald, F. Heidelbach, C. Riekel, M.J. Gidley, 'Analysis of the native structure of starch granules with small angle X-ray microfocus scattering', *Biopolymers* **49** (1999), p 91-105,
21. P.A. Perry, A.M. Donald, 'The effects of low temperatures on starch granule structure', *Polymer* **41** (2000), p 6361-6373,
22. R.D.L. Marsh, J.M.V. Blanshard, 'The application of polymer crystal growth theory to kinetics of formation of the B-amylose polymorph in a 50% wheat-starch gel', *Carboh. Polym.* **9** (1988), p 301-317,
23. B.J. Bulkin, Y. Kwak, I.C.M. Dea, 'Retrogradation kinetics of waxy-corn and potato starches; a rapid Raman-spectroscopic study', *Carboh. Res.* **160** (1987), p 95-112,
24. B.J. Goodfellow, R.H. Wilson, 'A Fourier transform IR study of the gelation of amylose and amylopectin', *Biopolymers* **30** (1990), p 1183-1189,
25. R.H. Wilson, B.J. Goodfellow, P.S. Belton, B.G. Osborne, G. Oliver, P.L. Russell, 'Comparison of Fourier transform mid infrared spectroscopy and near infrared reflectance spectroscopy with differential scanning calorimetry for the study of the staling of bread', *J. Sci. Food Agric.* **54** (1991), p 471-483,
26. Å. Rindlav, S.H.D. Hulleman, P. Gatenholm, 'Formation of starch films with varying crystallinity', *Carboh. Polym.* **34** (1997), p 25-30,
27. M. Kacuráková, R.H. Wilson, 'Developments in mid-infrared FT-IR spectroscopy of selected carbohydrates', *Carboh. Polym.* **44** (2001), p 291-303,
28. P. Bernazzani, C. Chapados, G. Delmas, 'Phase change in amylose-water mixtures as seen by FT-IR', *Biopolymers* **58** (2001), p 305-318,
29. J.J. Cael, J.L. Koenig, J. Blackwell, 'Infrared and Raman spectroscopy of carbohydrates', *Carboh. Res.* **29** (1973), p 123-134,
30. S.R. Delwiche, R.E. Pitt, K.H. Norris, 'Examination of starch-water and cellulose-water interactions with NIR diffuse reflectance spectroscopy', *Starch/Stärke* **43** (1991), p 85-92,
31. S.H.D. Hulleman, J.M. van Hazendonk, J.E.G. van Dam, 'Determination of crystallinity in native cellulose from higher plants with diffuse reflectance Fourier transform infrared spectroscopy', *Carboh. Res.* **261** (1994), 163-172,
32. N.A. Nikonenko, D.K. Buslov, N.I. Sushko, R.G. Zhbankov, 'Investigation of stretching vibrations of glycosidic linkages in disaccharides and polysaccharides with use of IR spectra deconvolution', *Biopolymers* **57** (2000), p 257-262,
33. J. Schaefer, E.O. Steijskal, 'Carbon-13 NMR of polymers spinning at the magic angle', *J. Am. Chem. Soc.* **98** (1976), p 1031-1032,

34. M.J. Gidley, 'High resolution solid state NMR of food materials', *Trends in Food Sci. & Tech.* **3**, (1992), p 231-236,
35. M.A. Ha, B.W. Evans, M.C. Jarvis, D.C. Apperley, A.M. Kenwright, 'CP/MAS NMR of highly mobile hydrated biopolymers: polysaccharides of Allium cell walls', *Carboh. Res.* **288** (1996), p 15-23,
36. T.J. Foster, S. Ablett, M.C. McCann, M.J. Gidley, 'Mobility-resolved ^{13}C-NMR spectroscopy of primary plant cell walls', *Biopolymers* **39** (1996), p 51-66,
37. P.S. Belton, 'NMR and the mobility of water in polysaccharide gels', *Int. J. Biol. Macromolecules* **21** (1997), p 81-88,
38. J.R. Garbow, J. Schaefer, 'Magic-angle ^{13}C-NMR study of wheat flours and doughs', *J. Agric. Food Chem.* **39** (1991), p 877-880,
39. A. Ohtsuka, T. Watanabe, T. Suzuki, 'Gel structure and water diffusion phenomena in starch gels studied by pulsed field gradient stimulated echo NMR', *Carboh. Polym.* **25** (1994), p 95-100,
40. J.Y. Wu, T.M. Eads, 'Evolution of polymer mobility during ageing of gelatinised waxy maize starch: A magnetisation transfer ^{1}H NMR study', *Carboh. Polym.* **20** (1993), p 51-60,
41. K.R. Morgan, R.H. Furneaux, R.A. Stanley, 'Observation by solid state ^{13}C CP/MAS NMR spectroscopy of the transformations of wheat starch associated with the melting and staling of bread', *Carboh. Res.* **235** (1992), p 15-22,
42. M.J. Gidley, S.M. Bociek, 'Molecular organisation in starches: a ^{13}C CP/MAS NMR study', *J. Am. Chem. Soc.* **107** (1985), p 7040-7044,
43. R.P. Veregin, C.A. Fyfe, R.H. Marchessault, 'Investigation of the crystalline V amylose complexes by ^{13}C CP/MAS NMR spectroscopy', *Macromolecules* **20** (1987), p 3007-3012,
44. F. Horii, H. Yamamoto, A. Hirai, R. Kitamaru, 'Structural study of amylose polymorphs by CP/MAS ^{13}C-NMR spectroscopy', *Carboh. Res.* **160** (1987), p 29-40,
45. V. Singh, S Zakiuddin Ali, S. Divakar, '^{13}C CP/MAS NMR spectroscopy of native and acid modified starches', *Starch/Stärke* **45** (1993), p 59-62,
46. K.R. Morgan, R.H. Furneaux, N.G. Larsen, 'Solid-state NMR studies on the structure of starch granules', *Carboh. Res.* **276** (1995), p 387-399,
47. C.E. Snape, W.R. Morrison, M. M. Maroto-Valer, J. Karkalas, R.A. Pethrick, 'Solid state ^{13}C NMR investigation of lipid ligands in V-amylose inclusion complexes', *Carboh. Polym.* **36** (1998), p 225-237,
48. N.W.H. Cheetham, L. Tao, 'Solid state NMR studies on the structural and conformational properties of natural maize starches', *Carboh. Polym.* **36** (1998), p 285-292,
49. P. Lebail, A. Buléon, D. Shiftan, R.H. Marchessault, 'Mobility of lipid in complexes of amylose-fatty acids by deuterium and ^{13}C solid state NMR', *Carboh. Polym.* **43** (2000), p 317-326,
50. S.J. Richardson, 'Molecular mobilities of instant starch gels determined by ^{17}O & ^{13}C NMR', *J. of Food Sci.* **53** (1988), p 1175-1180,
51. D. Le Botlan, P. Desbois, 'Starch retrogradation study in presence of sucrose by low-resolution NMR', *Cereal. Chem.* **72** (1995), p 191-193,
52. K.S. Lewen, I.H. McCormick, P. Molitor, S.J. Schmidt, T.M. Eads, 'Factors affecting the collection and fitting of nuclear magnetic cross-relaxation spectroscopy data with application to waxy corn starch', *J. Agric. Food Chem.* **48** (2000), p 4469-4476,
53. I. Hopkinson, R.A.L. Jones, P.J. McDonald, B. Newling, A. Lecat, S. Livings, 'Water ingress into starch and sucrose-starch systems', *Polymer* **42** (2001), p 4947-4956,
54. A.S. Kulik, J.R.C. de Costa, J. Haverkamp, 'Water organization and molecular mobility in maize starch investigated by two-dimensional solid state NMR', *J. Agric. Food Chem.* **42** (1994), p 2803-2807,
55. A.S. Kulik, J. Haverkamp, 'Molecular mobility of polysaccharide chains in starch investigated by two-dimensional solid state NMR spectroscopy', *Carboh. Polym.* **34** (1997), p 49-54,

56. J.P.M. van Duynhoven, A.S. Kulik, H.R.A. Jonker, J. Haverkamp, 'Solid-like components in carbohydrate gels probed by NMR spectroscopy', *Carboh. Polym.* **40** (1999), p 211-219,
57. P. Cornillon, L.C. Salim, 'Characterization of water mobility and distribution in low- and intermediate-moisture food systems', *Magn. Res. Imag.* **18** (2000), p 335-341,
58. S. Li, L.C. Dickinson, P. Chinachoti, 'Proton relaxation of starch and gluten by solid state NMR spectroscopy', *Cereal Chem.* **73** (1996), p 736-743,
59. S. Ratkovic, P. Pissis, 'Water binding to biopolymers in different cereals and legumes: proton NMR relaxation, dielectric and water imbibition studies', *J. Mat. Sci.* **32** (1997), p 3061-3068,
60. I.A. Farhat, J.M.V. Blanshard, J.R. Mitchell, 'The retrogradation of waxy maize starch extrudates: effect of storage temperature and water content', *Biopolymers* **53** (2000), p 411-422,
61. H.R. Tang, J. Godward, B. Hills, 'The distribution of water in native starch granules: a multinuclear NMR study', *Carboh. Polym.* **43** (2000), p 375-387,
62. A. Guilbot, R. Charbonniere, P. Abadie, P. Girard, 'L'eau de sorption de l'amidon: etude par spectrologie hertzienne', *Starch/Stärke* **11** (1960), p 327-332,
63. S. Ryynänen, P.O. Risman, T. Ohlsson, 'The dielectric properties of native starch solutions', *J. Microwave Power and Electromagnetic Energy* **31** (1996), p 50-53,
64. T.R. Noel, R. Parker, S.G. Ring, 'A comparative study of the dielectric relaxation behaviour of glucose, maltose and their mixtures with water in the liquid glassy state', *Carboh. Polym.* **282** (1996), p 193-206,
65. K. Fuchs, U. Kaatze, 'Molecular dynamics of carbohydrate aqueous solutions: dielectric relaxation as a function of glucose and fructose concentration', *J. Phys. Chem. B* **105** (2001), p 2036-2042,
66. H. Montès, J.Y. Cavaillé, 'Secondary dielectric relaxations in dried amorphous cellulose and dextran', *Polymer* **40** (1999), p 2649-2657,
67. L.H.M. da Silva, A.J.A. Meirelles, 'Phase equilibrium in polyethylene glycol/ maltodextrin aqueous two-phase systems', *Carboh. Polym.* **42** (2000), p 273-278,
68. A. de la Rosa, L. Heux, J.Y. Cavaillé, 'Secondary relaxations in PAA and PVA. II. Dielectric relaxations compared with dielectric behaviour of amorphous dried and hydrated cellulose and dextran', *Polymer* **42** (2001), p 5371-5379,
69. S. Ikeda, H. Kumagai, K. Nakamura, 'Dielectric analysis of food polysaccharides in aqueous solution', *Carboh. Res.* **301** (1997), p 51-59,
70. D. Lourdin, S.G. Ring, P. Colonna, 'Study of plasticizer-oligomer and plasticizer-polymer interactions by dielectric analysis: maltose-glycerol and amylose-glycerol-water systems', *Carboh. Res.* **306** (1998), p 551-558,
71. G. Roudaut, M. Maglione, D. van Dusschoten, M. Le Meste, 'Molecular mobility in glassy bread: a multispectroscopy approach', *Cereal Chem.* **76** (1999), p 70-77,
72. G. Roudaut, M. Maglione, M. Le Meste, 'Relaxations below glass transition temperature in bread and its components', *Cereal Chem.* **76** (1999), p 78-81,
73. M.F. Butler, R.E. Cameron, 'A study of the molecular relaxations in solid starch using dielectric spectroscopy', *Polymer* **41** (2000), p 2249-2263,
74. J. Einfeldt, A. Kwasniewski, D. Klemm, R. Dicke, L. Einfeldt, 'Analysis of side group motion in *O*-acetyl-starch using regioselective *2-O*-acetyl-starches by means of dielectric spectroscopy', *Polymer* **41** (2000), p 9273-9281.

Chapter 3

Ageing and Crystallisation of Completely Gelatinised and Compression Moulded Starch

A.L.M. Smits, F.C. Ruhnau, S.H.D. Hulleman, J.J.G. van Soest, J.F.G. Vliegenthart

[Published in part in *Starch/Stärke* **50** (1998), p 478-483,
and in *Polym. Adv. Technol.* **10** (1999), p 570-573]

Abstract

The retrogradation and physical ageing of completely gelatinised model starch systems with respect to their glass transition temperatures T_g have been investigated by infrared and solid state NMR spectroscopy. Diffuse reflectance Fourier transform infrared (DRIFT) spectra demonstrate the commencing retrogradation of starch materials stored above their T_g by changes in peak shapes and intensities in the characteristic area between 995 cm^{-1} and 1050 cm^{-1}. Solid state NMR proton relaxation times in the rotating frame (proton $T_{1\rho}$) of materials stored below T_g, at 30% RH, increase asymptotically in time due to physical ageing. When stored at 60% or 90% RH, T_g is below room temperature at equilibrium water content. The proton $T_{1\rho}$'s of these materials, increase until a moisture content is reached that rises them above T_g, decrease due to further water absorption and then increase due to recrystallisation (retrogradation).

Compression moulded starch systems containing glycerol and water as plasticisers at a ratio of 100:30:56 (w/w/w) were studied with respect to the effects of time and processing temperature on the B-type crystallinity, by using X-ray diffraction. Initial recrystallisation, developed during moulding, was investigated further on similar potato amylopectin and amorphous potato starch systems. The crystallinity prior to processing does not influence the initial recrystallisation. After moulding at high temperatures (>160°C), amylose is mainly responsible for initial recrystallisation into the B-type lattice. The observed degree of recrystallisation, however, cannot be due to amylose crystallisation alone. Amylose seems to serve as a nucleus for crystallisation of amylopectin or amylose-amylopectin co-crystallisation takes place.

Introduction

Starch is one of the main energy providers in the human diet and it is being used for many years as a natural food-thickener [1]. In the food industry plasticisers like water and sugars are used to improve the quality of food products like cakes, bread and frozen dough, and to delay the loss of moisture and ageing, causing staling which limits the shelf-life of bakery products [2,3].

Lately, there is much interest in biodegradable plastics to replace synthetic short-lifecycle products. Starch, for example, is a cheap biopolymer that is totally biodegradable forming carbon dioxide and water. Granular starch is mixed with suitable plasticisers to enable melting below the decomposition temperature, and moulded into biodegradable products, employing standard equipment as used for the processing of synthetic polymers, yielding thermoplastic starch (TPS) [4,5]. The produced starch plastics are complex systems because of the wide range of structures, which can occur due to variations in processing conditions, such as temperature and water content. Differences in composition of the starch source used, such as the water and lipid contents, and morphology are responsible for further variations [6-8]. Residual and time-induced double helical (B-type) crystallinity can be present, depending on the starch source and the plasticiser content [9]. Crystallinity of the produced viscoelastic semi-crystalline starch plastics strongly influences the mechanical properties. The limited knowledge of the relations between processing conditions and the structure and properties of starch-based plastics makes it difficult to predict and control the mechanical properties.

The time dependent behaviour of starch based materials during and after processing is of great importance in the food industry and for the development of bioplastics, since it causes staling and embrittlement, respectively [10-12]. Especially rheological and physico-chemical changes during storage (ageing) are important. Because the predominantly amorphous products are not at thermodynamic equilibrium, the systems will approach this equilibrium in time. This process involves starch molecular rearrangement and starch recrystallisation. In this matter, one should distinguish between physical ageing below the glass transition (sub T_g effects) [12] and ageing above T_g, i.e. retrogradation [13,14].

Recent research has demonstrated the applicability of advanced non-invasive solid state NMR [15-17] and infrared spectroscopic techniques [18-22], which have moved

forward the understanding of molecular phenomena in starch materials. With these techniques the molecular mobility and organisation in starch based systems can be directly determined and in combination with other analytical techniques, it is possible to obtain more information about the ageing of such systems.

By analogy with bakery products, model systems were prepared by gelatinising and freeze drying native potato starch. After preparation, the products were aged at specific conditions (humidity, temperature, time) with respect to their glass-transitions (T_g) [12,23]. We have monitored the physical ageing and retrogradation processes by solid state NMR spectroscopy, FT-IR spectroscopy and X-ray diffraction (XRD). To visualise both processes, we have correlated the proton relaxation times in the rotating frame (proton $T_{1\rho}$) with the storage time and the water content.

Structural changes in thermoplastic starch during processing and storage were investigated on compression moulded starch systems, using X-ray diffraction. Insight into the effect of starch composition, processing parameters, and time on the B-type crystallinity is essential for optimising and broadening the use of thermoplastic starch by controlling the molecular structure in the material.

Experimental

I Gelatinised sample preparation

Gelatinisation was performed in a Brabender viscometer. Native potato starch (42 g, moisture content 17%), PN (Avebe, NL), was mixed with 309 g de-ionised water to gain a 10% dry weight starch dispersion. Sodium azide (0.1 wt%), NaN_3 (Merck, NL), was added as a preservative against fungi growth. The mixture was poured into the Brabender and stirred at 75 rpm. The mixture was heated from room temperature to 90°C at 2°C/min and held at 90°C for 55 min, until the viscosity had reached a nearly constant value. Then, the mixture was frozen with liquid nitrogen and freeze-dried over two days. The dried mixtures were ground and stored at –22°C before conditioning. Samples were conditioned at 20°C and relative humidities (RH) of 30%, 60% and 90%, respectively. At 30% RH as the water content is about 11% no retrogradation is expected because the systems are below their glass transition temperature [24]. Sub T_g phenomena, however, can be investigated on these samples [23]. At 90% RH the systems are above their T_g and retrogradation can be

investigated on these samples [23]. Samples conditioned at 60% RH are stored at about their T_g and could exhibit either sub T_g or retrogradation phenomena.

II Compression moulded sample preparation

Thermoplastic starch samples were prepared by compression moulding of native potato starch, PN (Avebe, NL), with glycerol (Boom, NL) and de-ionised water at a dry matter: glycerol: water ratio of 100:30:56 (w/w/w) at different temperatures. Alternatively PN (Avebe), amorphous potato starch (Flocgel LV-W, Avebe) or potato amylopectin (Avebe) were compression moulded at various temperatures with glycerol and de-ionised water at a ratio of 100:30:30 (w/w/w). The ingredients were mixed and left to settle 24 h before processing. A PHI press, type 75U1209S-2JCS-J-Y2-S5-7, with a mould of 150×100×1 mm^3 (exterior dimensions 350×300 mm^2) containing 30 g premix was used. At 4 tons pressure (on the total mould surface) the temperature was increased to 100°C at 10°C/min. Then, the pressure was increased to 40 tons and the temperature increased further to the set cure temperature. After curing for 15 min, the samples were cooled to room temperature at 10-15°C/min for 8 min. The samples were stored at 20°C and 90% RH. At these controlled conditions, the water content remained 30 wt%.

Polarised light microscopy

A Zeiss Axioplan MC 100 polarised light microscope was used with a blue colour filter. Magnifications of 100×, 200× and 400× have been used. Samples were prepared by mixing a small amount of fine powder with a droplet of water.

X-ray diffraction

Wide Angle X-ray Scattering (WAXS) powder diffractograms were recorded on a Philips PC-APD diffractometer in the reflection geometry in the angular range 4-40 °(2θ). The CuK_α radiation from the anode operating at 40 kV and 50 mA was monochromised using a 15 μm Ni foil. The diffractometer parameters were: divergence slit 1°, receiving slit 0.2 mm and scatter slit 1°. A proportional detector was used to detect the scattered radiation. Diffractograms were baseline corrected by drawing a straight line between the intensities at 7 and 40°(2θ). The ratio of the height of the crystalline diffraction at 17.3°(2θ) and the height of the total diffraction at this

angle is defined as the crystallinity index, a measure for the amount of B-type crystallinity of the sample.

FT-IR spectroscopy

Diffuse reflectance Fourier transform infrared (DRIFT) spectra were recorded on a BioRad FTS-60A spectrometer with a liquid nitrogen cooled MCT detector using a Digilab diffuse reflectance accessory. DRIFT samples were prepared by mixing the fine powder starch sample with KBr (Uvasol®, Merck, <50 μm). The spectra obtained at resolution 4 cm^{-1} in the range 4000-550 cm^{-1} were averages of 256 scans. DRIFT spectra were recorded as Kubelka-Munk transformed spectra against a KBr background.

Solid state NMR spectroscopy

The ^{13}C NMR spectra were collected on a Bruker AMX 400 operating at 400 MHz for ^{1}H and 100.63 MHz for ^{13}C. Samples were spun at the magic angle (54.7°) with respect to the static magnetic field. Carbon and proton 90° pulse lengths were 5 μs in all experiments. Carbon chemical shifts relative to tetramethylsilane (TMS) were determined from the spectra, using solid glycine at room temperature as external reference. Samples were packed into 7 mm ceramic rotors and spun at 3-4 kHz. The ^{13}C spectra and proton $T_{1\rho}$ times were obtained with CP pulse sequence to enhance sensitivity. Variable delay times up to 20 ms have been used for the proton $T_{1\rho}$ experiments. In ^{13}C CP/MAS experiments, the cross polarisation time was set to 2 ms with a recycle delay of 2s.

Results and Discussion

I Ageing of completely gelatinised potato starch

X-ray diffraction and polarised light microscopy

X-ray diffraction has been used for a preliminary investigation of changes in crystallinity during processing and conditioning. The X-ray diffractograms of the freshly prepared freeze-dried gelatinised PN show the typical unstructured pattern of a completely amorphous material. This is in agreement with polarised light microscopy, from which it was concluded that the granular structure of PN is totally disrupted, because no characteristic Maltese crosses have been found.

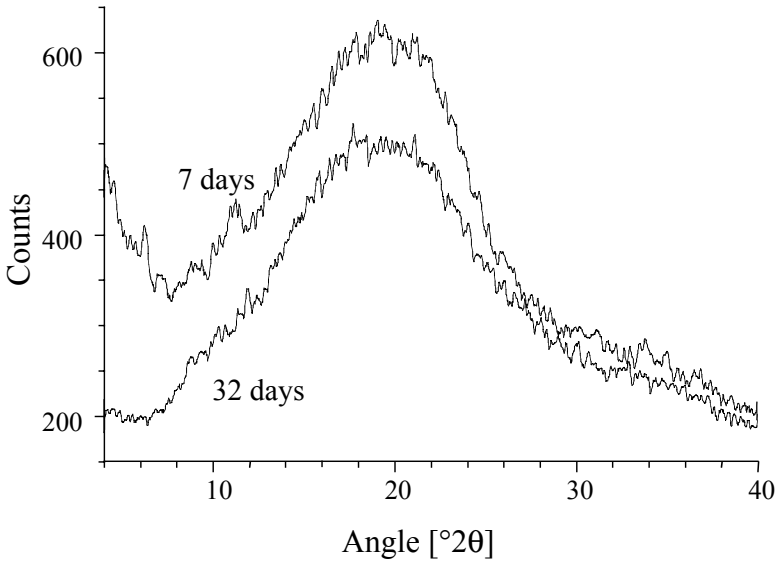

Figure 3.1 XRD diffractogram of freeze-dried gelatinised PN stored for 7 and 32 days at 20°C and 90% RH.

Storage up to 32 days at 20°C and at various humidities does not significantly increase the crystallinity of the prepared samples. This can be seen from Figure 3.1, wherein the X-ray diffractograms of freeze-dried gelatinised PN recorded after 7 and 32 days at 90% RH are presented. Powder XRD may be not sensitive enough to detect minor extents of recrystallisation or very small crystals.

Solid state NMR spectroscopy

The ^{13}C CP/MAS spectra of the freeze-dried samples are typical of completely amorphous PN. This is in agreement with polarised light microscopy, where no granules have been detected, and in agreement with X-ray diffraction from which only a broad, unstructured signal is detected. In the CP/MAS spectra, for carbon C-1 only one broad resonance without splitting is seen (Figure 3.2). The spectra of the conditioned samples show no significant changes in lineshapes or chemical shifts during storage at different humidities. Both CP/MAS and powder XRD experiments may be not sensitive enough to detect small variations in molecular structure, minor extents of recrystallisation or very small crystals.

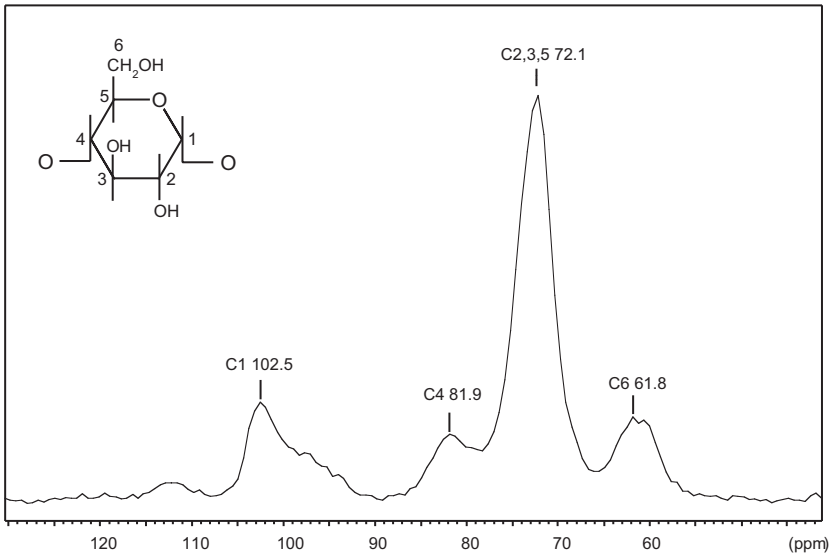

Figure 3.2 ^{13}C CP/MAS NMR spectrum of fresh freeze-dried gelatinised PN. Peak assignments with respect to the shown structure of the glucose ring.

FT-IR spectroscopy

Infrared spectroscopy has been used for investigating changes in starch structure on a short-range molecular level. Especially interesting are the peaks at 1047 cm^{-1} characteristic of the more organised part of starch, at 1022 cm^{-1} characteristic of amorphous starch, and at 995 cm^{-1} which is sensitive to water [5,25].

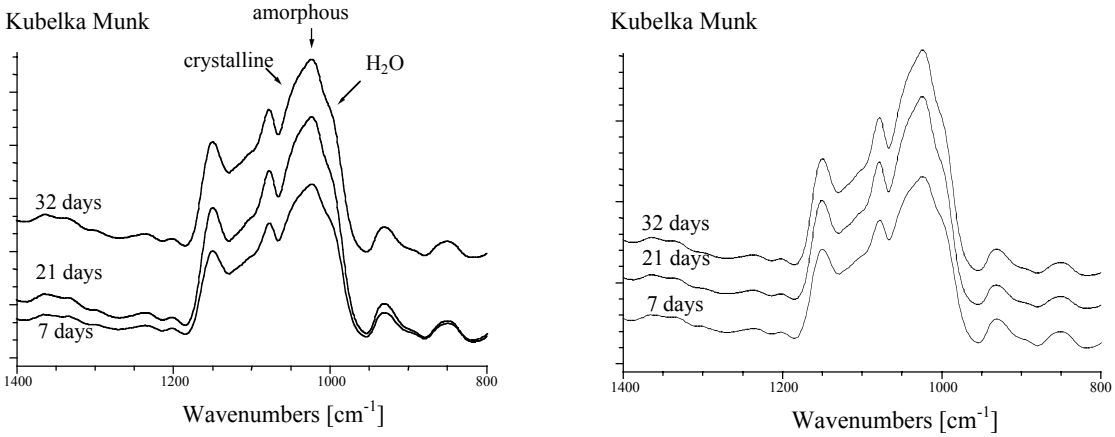

Figure 3.3 FT-IR spectra of freeze-dried gelatinised PN stored for 7, 21 and 32 days at 20°C and 30% RH (left) or 60% RH (right).

The infrared spectra of freeze-dried gelatinised PN conditioned at 20°C and 30% or 60% RH showed no major changes during 32 days (Figure 3.3). At 90% RH, depicted in Figure 3.4, the ratios of the peak intensities at 1047 cm^{-1} and 1022 cm^{-1} increased from 0.90 to 0.94, 0.98 and 0.99 after 7, 14, 21 and 32 days, respectively, implying a reducing amount of amorphous material, giving a more organised starch because retrogradation commenced. An increasing resemblance to native starch is observed during conditioning, for which this intensity ratio is 1.0.

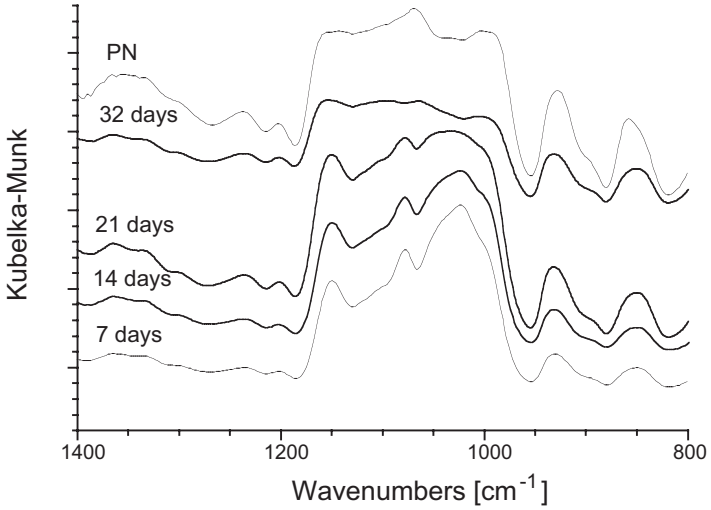

Figure 3.4 FT-IR spectra of freeze-dried gelatinised PN stored for 7 ,14, 21 and 32 days at 20°C and 90% RH, and of native potato starch PN.

Proton $T_{1\rho}$ measurements

The proton $T_{1\rho}$ relaxation times have been determined for the gelatinised and freeze-dried PN samples conditioned at 30%, 60% or 90% RH during storage for 32 days. In general, proton $T_{1\rho}$ relaxation times determine the rate of spin diffusion, which is governed by the strength of dipole-dipole interactions. Therefore, the rate of spin diffusion among the ^1H spins provides information about the domain sizes in polymer blends and about the molecular motion at the spin locking frequency of different phases in a homopolymer.

In Figure 3.5 the results are shown of the proton $T_{1\rho}$ measurements of the gelatinised PN samples conditioned at different humidities. The proton $T_{1\rho}$ values of the most intense signal at 72 ppm (glucose ring carbons 2, 3 and 5) have been used. Significant

differences are observed between starch samples conditioned at 30% relative humidity and the samples stored at 60% or 90% RH. After freeze drying the gelatinised samples have moisture contents of 11%. This fresh gelatinised and freeze-dried sub T_g material is expected to have a quite low proton $T_{1\rho}$ relaxation time, due to the low density (0.02 g/ml) of these materials after freeze drying and the completely amorphous character.

The initial moisture content of 11% is about the equilibrium moisture content at 30% relative humidity. For gelatinised freeze-dried PN samples conditioned at 30% RH, no retrogradation, but only sub T_g phenomena are expected to occur. During storage, at first an increase in proton $T_{1\rho}$ is detected and after one week the proton $T_{1\rho}$ value becomes constant. The increase in proton $T_{1\rho}$ relaxation time is caused by larger and better packed domains with stronger dipolar interactions of protons. This reorientation of the gelatinised PN is thought to be due to sub T_g physical ageing phenomena, which are related to a decrease in free volume or to an increase in water-starch (plasticiser-polymer) interactions, resulting in a stiffer material with a higher density [26,27].

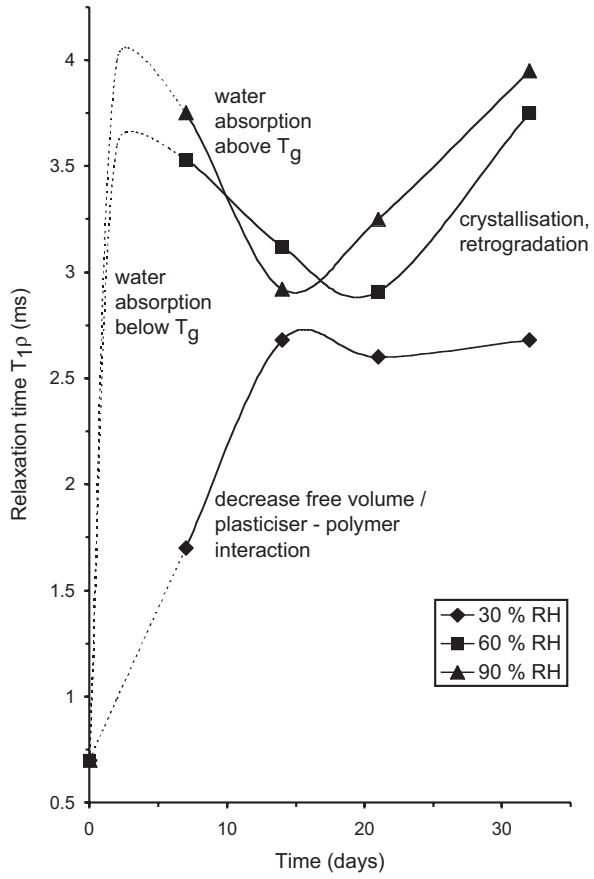

Figure 3.5 Proton $T_{1\rho}$ relaxation times for freeze-dried gelatinised PN conditioned at 20°C and 30%, 60% and 90% RH.

The gelatinised freeze-dried PN samples conditioned at 60% or 90% RH, show remarkable changes in the proton $T_{1\rho}$ after seven days of conditioning. To explain this behaviour, we have to consider again that two important factors are affecting the length of the proton $T_{1\rho}$. First, changes in the domain size influence the relaxation behaviour resulting in longer relaxation times for larger domains and secondly, the mobility of protons can result in a more effective relaxation resulting in a shorter proton $T_{1\rho}$ for an increased mobility. These factors can lead to opposing effects.

The samples stored at 60% or 90% RH are initially equal to the samples stored at 30% RH. They absorb water until their T_g is below room temperature. The interaction with this water causes a swelling of the starch network, resulting in bigger domains with a longer relaxation time $T_{1\rho}$, until the glass transition is reached. When enough water is absorbed, the glass transition temperature will be below room temperature and the mobility of the starch chains increases significantly. Therefore, we detect a decrease in relaxation time after seven days of storage. Reaching the equilibrium amount of water at these storage conditions, the T_g's of the samples are below room temperature and we can detect the retrogradation resulting in an increase in proton $T_{1\rho}$, because of recrystallisation (less mobility) and a growth of domains of recrystallised material.

The gelatinised freeze-dried PN samples conditioned at 60% or 90% RH, show a similar change in relaxation times during ageing. The changes are faster for the samples conditioned at 90% than for the samples stored at 60% RH, due to the higher water contents of the former, as seen by the fact that the minimum in $T_{1\rho}$ is observed at an earlier stage during ageing. For the freeze-dried gelatinised PN samples stored at 60% RH, which are close to their T_g, one can expect both retrogradation and sub T_g phenomena. But one can conclude that retrogradation is the governing process, because of the similar course of relaxation time compared to the gelatinised PN samples stored at 90% RH (Figure 3.5).

In general, the course of the proton $T_{1\rho}$ relaxation times during storage of potato starch can be determined in dependence of storage below or above T_g (Figure 3.5). Below T_g the sub T_g physical ageing process causes a sort of asymptotic rising course of the proton $T_{1\rho}$ due to free volume relaxation or increased polymer-plasticiser interactions [26,27]. The free volume decreases and the material becomes less flexible, resulting in slower movements and slower spin relaxation. Above T_g at first the absorption of water up to the equilibrium moisture content dominates the changes

in starch chain mobility. This results in the decrease of proton $T_{1\rho}$ because the material becomes more flexible. Above the glass rubber transition, the recrystallisation or retrogradation process starts. This process is the dominating factor after the equilibrium moisture content is reached, which is observed by an increase of proton $T_{1\rho}$ due to less flexibility.

II Ageing of compression moulded potato starch

Structural changes in thermoplastic starch during storage were investigated on compression moulded potato starch samples containing glycerol and water at a dry matter: glycerol: water ratio of 100:30:56 (w/w/w). With polarised light microscopy residual granular crystallinity was observed depending on the moulding temperature [8]. From X-ray diffraction it was concluded that during processing considerable initial (B-type) recrystallisation takes place followed by time-induced recrystallisation (retrogradation) during the first days of storage (Figure 3.6). The initial recrystallisation was determined directly after cooling the samples in the mould.

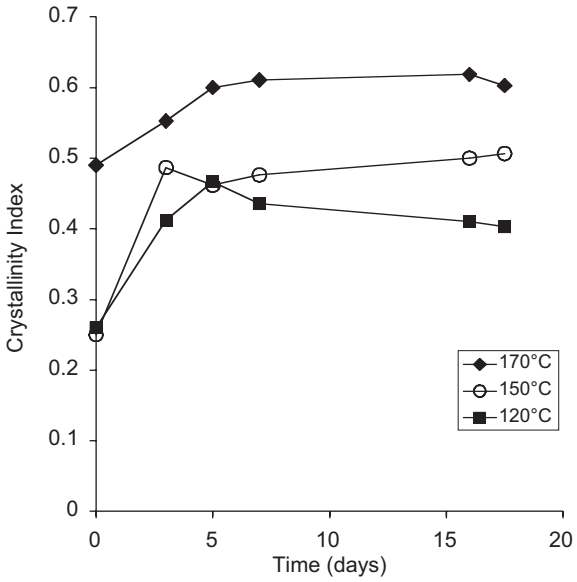

Figure 3.6 Recrystallisation in time as determined with XRD of PN, compression moulded at 120, 150 and 170°C, with glycerol and water at a ratio of 100:30:56 (w/w/w), conditioned at 20°C and 90% RH.

Since it was not expected to find a higher initial recrystallisation for samples cured at higher temperatures, this feature was investigated more thoroughly by compression moulding similar regular potato starch, amorphous potato starch, and potato

amylopectin mixtures with glycerol and water at a ratio of 100:30:30 (w/w/w) at various temperatures (Figure 3.7) [28]. It was found that initial recrystallisation takes place irrespective of the crystallinity before moulding, since it was also found for the amorphous potato starch samples. At higher moulding temperatures, more initial recrystallisation was observed for regular and amorphous potato starch, but for potato amylopectin a decrease in recrystallisation was found for increasing moulding temperatures. Amylose seemed to be necessary for initial recrystallisation into the B-type lattice after moulding at high temperatures. The observed recrystallisation of regular and amorphous potato starch was higher than could be attributed to amylose alone. Therefore it is suggested that amylose serves as a nucleus for amylopectin crystallisation or amylose-amylopectin co-crystallisation takes place.

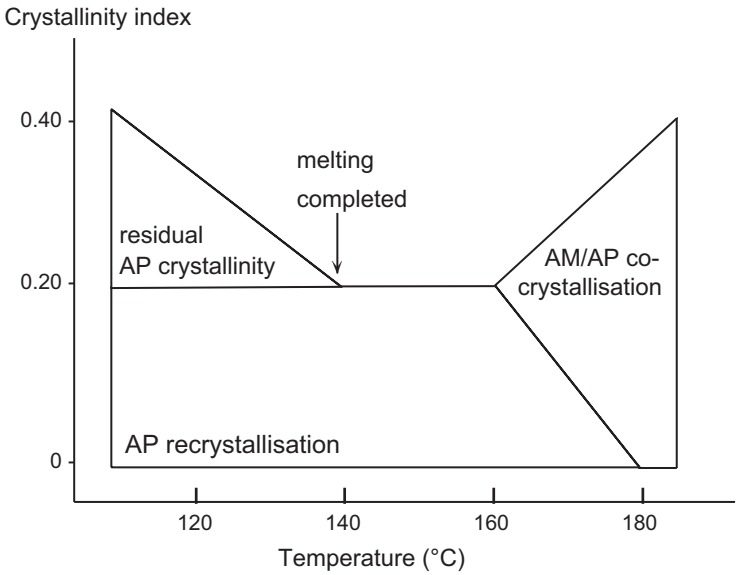

Figure 3.7 Schematic description of the contribution of the different starch components (AM = amylose, AP = amylopectin) to the crystallinity directly after compression moulding potato starch with glycerol and water at a ratio of 100:30:30 (w/w/w) at various temperatures.

Samples cured at temperatures above the melting-range of starch recrystallised more, when their cure temperature was higher. Since they all are amorphous, and all go through the same melting-range at equal speed upon cooling, equal recrystallisation was expected. We suggest that a decrease in molecular weight, due to degradation, causes an increase in recrystallisation, because shorter molecular chains crystallise more easily than long chains.

Conclusions

FT-IR and solid state NMR spectroscopy are good techniques for observing physical ageing and retrogradation by means of spectral changes in lineshapes and linewidths and by the determination of relaxation times. In FT-IR spectroscopy changes in the area of 1050 cm^{-1} and 995 cm^{-1} imply the retrogradation of starch based materials stored above T_g. Proton $T_{1\rho}$ relaxation times are very sensitive to changes in the degree of crystallinity, domain size, molecular arrangement and the moisture content during retrogradation. The influence of the storage humidity in relation to the T_g can be monitored via the relaxation times. Below the T_g the decrease in free volume results in an asymptotic increase in relaxation times. During water absorption the relaxation times are suggested to increase until the T_g is at about room temperature. Above the T_g further absorption of water increases the mobility of starch until the equilibrium moisture content has been reached. During and after this period retrogradation takes place and the relaxation times increase because of the development of crystallinity.

Insight into the recrystallisation of thermoplastic starch is obtained. It is shown that the control of starch recrystallisation and ordering is possible by means of variation of the processing temperature. A decrease in molecular weight due to degradation, causes an increase in recrystallisation. Amylose seems to serve as a nucleus for amylopectin crystallisation or amylose-amylopectin co-crystallisation takes place. Continuing research on the molecular structure in starch based systems will improve the control of the product mechanical properties, and therewith the use of various starches for different applications can be expanded.

References

1. G. Tegge, 'Stärke und Stärkederivate', in: *Behr's Verlag*, Hamburg (1984),
2. V.J. Morris, 'Starch gelation and retrogradation', *Trends in Food Sci. & Techn*. **1** (1990), p 2-6,
3. H.F. Zobel, 'The bread staling problem', *Cereal Chem.* **36** (1959), p 441-451,
4. I. Tomka, 'Thermoplastic starch', *Adv. in Exp. Medicine & Biology* **302** (1991), p 627-637,
5. J.J.G. van Soest, 'Starch plastics: structure-property relationships', Ph.D. thesis, Utrecht University (1996), Koninklijke Bibliotheek Den Haag,
6. M. Gudmundsson, 'Retrogradation of starch and the role of its components', *Thermochim. Acta*. **246** (1994), p 329-341,
7. J.J.G. van Soest and D.B. Borger, 'Structure and properties of compression-molded thermoplastic starch materials from normal and high-amylose maize starches', *J. Appl. Pol. Sci*. **64** (1997), p 631-644,

8. R.N. Tharanathan, 'Starch - the polysaccharide of high abundance and usefulness', *J. Sci. & Ind. Res*. **54** (1995), p 452-458,
9. J.J.G. van Soest and N. Knooren, 'Influence of glycerol and water content on the structure and properties of extruded starch plastic sheets during aging', *J. Appl. Pol. Sci*. **64** (1997), p 1411-1422,
10. J.J.G. van Soest, J.F.G. Vliegenthart, 'Crystallinity in starch plastics', *Trends in Biotechn*. **15** (1997), p 208-213,
11. J.J.G. van Soest, S.H.D. Hulleman, D. de Wit and J.F.G. Vliegenthart, 'Changes in the mechanical properties of thermoplastic potato starch in relation with changes in B-type crystallinity', *Carboh. Polym*. **29** (1996), p 225-232,
12. H.J. Thiewes, P.A.M. Steeneken, 'The glass transition and the sub-T_g endotherm of amorphous and native potato starch at low moisture content', *Carboh. Polym*. **32** (1997), p 123-130,
13. T.J. Lu, J.L. Jane, P.L. Keeling, 'Temperature effect on retrogradation rate and crystalline structure of amylose', *Carboh. Polym.* **33** (1997), p 19-26,
14. S.S. Stivala, V. Crescenzi, I.C.M. Dea, 'Small angle neutron and X-ray scattering', in: *Industrial Polysaccharides*, S.S. Stivala, V. Crescenzi, I.C.M. Dea, eds., Gordon & Breach Science Publishers, New York (1987),
15. J.R. Garbow, J. Schaefer, 'Magic-angle ^{13}C-NMR study of wheat flours and doughs', *J. of Agric. Food Chem.* **39** (1991), p 877-880,
16. F. Horii, H. Yamamoto, A. Hirai, R. Kitamaru, 'Structural study of amylose polymorphs by CP/MAS ^{13}C-NMR spectroscopy', *Carboh. Res*. **160** (1987), p 29-40,
17. A.S. Kulik, J.R.C. de Costa, J. Haverkamp, 'Water organization and molecular mobility in maize starch investigated by two-dimensional solid state NMR', *J. of Agric. Food Chem.* **42**, (1994), p 2803-2807,
18. B.J. Goodfellow, R.H. Wilson, 'A Fourier transform IR study of the gelation of amylose and amylopectin', *Biopolym.* **30** (1990), p 1183-1189,
19. R.H. Wilson, B.J. Goodfellow, P.S. Belton, B.G. Osborne, G. Oliver, P.L. Russell, 'Comparison of Fourier transform mid infrared spectroscopy and near infrared reflectance spectroscopy with differential scanning calorimetry for the study of the staling of bread', *J. Sci. Food Agric.* **54** (1991), p 471-483,
20. B.J. Bulkin, Y. Kwak, I.C.M. Dea, 'Retrogradation kinetics of waxy-corn and potato starches; a rapid Raman-spectroscopic study', *Carboh. Res*. **160** (1987), p 95-112,
21. J.J. Cael, J.L. Koenig, J. Blackwell, 'Infrared and Raman spectroscopy of carbohydrates', *Carboh. Res*. **29** (1973), p 123-134,
22. S.H.D. Hulleman, J.M. van Hazendonk, J.E.G. van Dam, 'Determination of crystallinity in native cellulose from higher plants with diffuse reflectance Fourier transform infrared spectroscopy', *Carboh. Res*. **261** (1994), p 163-172,
23. H. Bizot, P. Le Bail, B. Leroux, J. Davy, P. Roger, A. Buleon, 'Calorimetric evaluation of the glass transition in hydrated, linear and branched polyanhydroglucose compounds', *Carboh. Polym.* **32** (1997), p 33-50,
24. H. Bizot, A. Buleon, N. Mouhous-Riou, J.L. Multon, 'Some facts concerning water vapour sorption hysteresis on potato starch', in: *Properties of water in foods*, D. Simatos, J.L. Multon, eds., Martinus Nijhoff Publishers, Dordrecht (1985), p 83-93,
25. S.R. Delwiche, K.H. Norris, 'Examination of starch-water and cellulose-water interactions with near infrared (NIR) diffuse reflectance spectroscopy', *Starch/Stärke* **43** (1990), p 85-92,
26. I.A.M. Appelqvist, D. Cooke, M.J. Gidley, S.J. Lane, 'Thermal properties of polysaccharides at low moisture, an endothermic melting process and water-carbohydrate interactions', *Carboh. Polym*. **4** (1993), p 291-299,
27. R.L. Shogren, 'Effect of moisture content on the melting and subsequent physical ageing of cornstarch', *Carboh. Polym*. **2** (1992), p 83-90,
28. S.H.D. Hulleman, M.G. Kalisvaart, F.H.P. Janssen, H. Feil and J.F.G. Vliegenthart, 'Origins of B-type crystallinity in glycerol-plasticised, compression-moulded potato starches', *Carboh. Polym*. **39** (1999), p 351-360.

Chapter 4

Interaction between Dry Starch and Plasticisers Glycerol or Ethylene Glycol, Measured by Differential Scanning Calorimetry and Solid State NMR Spectroscopy

A.L.M. Smits, P.H. Kruiskamp, J.J.G. van Soest, J.F.G. Vliegenthart

[Submitted for publication]

Abstract

The interaction of crystalline amylose and of crystalline and amorphous amylopectin with the plasticisers glycerol or ethylene glycol in the absence of water was studied, by using DSC and solid state NMR spectroscopy. Upon heating starch freshly mixed with plasticisers, a strong exothermal interaction enthalpy of $\Delta H \sim -35$ J/g was detected by DSC. At room temperature glycerol interacts mainly with the amorphous starch regions, the interaction taking 8 days to reach equilibrium. For ethylene glycol the interaction is faster, taking 4 days to reach equilibrium, and the rate is not affected by crystallinity. Ethylene glycol interacts in a more ordered manner with amorphous than with crystalline material, resulting in a narrower ethylene glycol CP/MAS signal when equilibrium is reached at room temperature. Upon heating, more glycerol or ethylene glycol is immobilised, but in a less ordered manner than upon storage at room temperature. This results in a more intense, but broader plasticiser CP/MAS signal upon heating. Interaction in a more ordered manner probably implies interaction with more of the hydroxy groups of the plasticiser. The polysaccharide mobility is increased more when the plasticiser interacts in a more ordered manner, as observed by small starch signals in HP/DEC spectra.

Introduction

Starch is a cheap biopolymer that is totally biodegradable, ultimately up to carbon dioxide and water. Starch is used as a natural food-ingredient and is a main energy provider in the human diet. Thermoplastic starch (TPS) materials are obtained from granular starch mixed with plasticisers to enable melting below the decomposition temperature. TPS is a complex system, since the structure depends mainly on variations in processing conditions [1-3]. The ageing of starch based systems causes the embrittlement of starch plastics and the staling of bakery products [4,5], leading to deterioration of the product. Plasticisers can be used to influence this ageing induced by retrogradation. For instance, in bread the degree of retrogradation is strongly reduced by the addition of monoglycerides, which interact with the initially amorphous amylopectin [6]. Van Soest *et al.* [7] showed that an increasing glycerol concentration in a waxy maize starch gel reduces the rate of retrogradation. The inhibiting effect of various saccharides on retrogradation has also repeatedly been reported [8-11].

However, specific interactions between plasticiser and starch chains are difficult to elucidate. It is generally accepted that plasticisers lower the number of physical cross-links between starch chains, and consequently retard the rate of retrogradation [12]. Recently, the interaction of glycerol and starch was investigated on a molecular level in the absence of water [13-15]. By using differential scanning calorimetry (DSC), a strong exothermal transition was found between 50°C and 150°C. Heat treatment gave rise to a strong starch-glycerol interaction. In the present study the interaction of the plasticisers glycerol and ethylene glycol with each of the starch polysaccharides is investigated. Solid state nuclear magnetic resonance spectroscopy (NMR) is used to investigate the material before and after heating above the exothermal transition. The time- and temperature-dependence of the interaction was studied by using DSC and solid state NMR spectroscopy.

Experimental

Sample preparation

Amylopectin obtained from granular potato starch, with a remainder of 5% amylose (Amylopectin-UG), and amylose (Amylose-V) were provided by Avebe (Foxhol, the

Netherlands). Glycerol (≤0.1% H_2O) was obtained from Fluka (Neu-Ulm, Germany) and ethylene glycol (≤0.05% H_2O) from Acros (Geel, Belgium).

The originally crystalline amylopectin was fully gelatinised by stirring and heating to 90°C a 10% dry weight amylopectin dispersion in de-ionised water for 1 h. Even though some crystallinity (~8%) is present, the gelatinised amylopectin will be referred to as amorphous amylopectin. Amylopectin (either crystalline or amorphous) and amylose were dried under reduced pressure in a vacuum-oven at 70°C. The dried material (<3% H_2O) was mixed manually under a nitrogen gas flow with glycerol or ethylene glycol. The plasticiser concentration was 4.3 mmol/g amylopectin for glycerol (corresponding to 29 wt%) and an equal molar amount for ethylene glycol (21 wt%). The samples were stored airtight. Samples exposed to heat treatment for the NMR analyses were heated for 30 min at 165°C in a small, airtight container.

Analyses

The crystallinity of the starch samples at atmospheric humidity was examined with wide-angle X-ray scattering, using a Philips PC-APD diffractometer. The crystallinity index X_H is defined as the height of the crystalline diffraction at 17.3° relative to the total height of that peak measured from the baseline [16]. For comparison, native potato starch (X_H = 0.60) has a crystallinity of approximately 25%.

DSC was performed on a Perkin-Elmer DSC7 robotic system. Samples were prepared in stainless steel 80 µl DSC cups. They were heated with 10°C/min from 20°C to 180°C.

Solid state NMR spectra were collected on a Bruker AMX 400 spectrometer operating at 100.63 MHz for ^{13}C. Samples were spun at the magic angle (54.7°) with respect to the static magnetic field. Carbon chemical shifts relative to tetramethylsilane (TMS) were determined from the spectra, using solid glycine at room temperature as external reference. Samples were packed into 7-mm ceramic rotors and spun at 4 kHz. In ^{13}C cross-polarisation magic angle spinning (CP/MAS) experiments the cross polarisation time was set to 500 µs and in both ^{13}C CP/MAS and ^{13}C high power decoupling (HP/DEC) experiments the recycle delay was set to 4 s [17].

Results

Differential scanning calorimetry

When the mixtures of amylose or amylopectin, either crystalline or amorphous, with glycerol or ethylene glycol were heated, a strong exothermal interaction enthalpy (ΔH ~ –35 J/g) could be detected by DSC [13,14]. The transition enthalpy is proportional to the amounts of glycerol or ethylene glycol added, suggesting that the plasticiser is responsible for the observed exothermic event. The process is irreversible, since reheating of the samples showed no exothermal enthalpy peak. Heat treatment gives rise to a strong starch-plasticiser interaction, most probably caused by H-bond formation. The peak temperature range was 95-110°C for the amylopectin/glycerol mixtures, 95-105°C for the amylose/glycerol mixtures, 70-85°C for the amylopectin/ethylene glycol mixtures, and 65-75°C for the amylose/ethylene glycol mixtures. In all cases the exothermal transition started well above room temperature. However, when stored for several days at room temperature, the transition enthalpy measured by DSC, decreased (Figure 4.1). The decrease in enthalpy for the various mixtures is not accompanied by a significant shift in the interaction temperature.

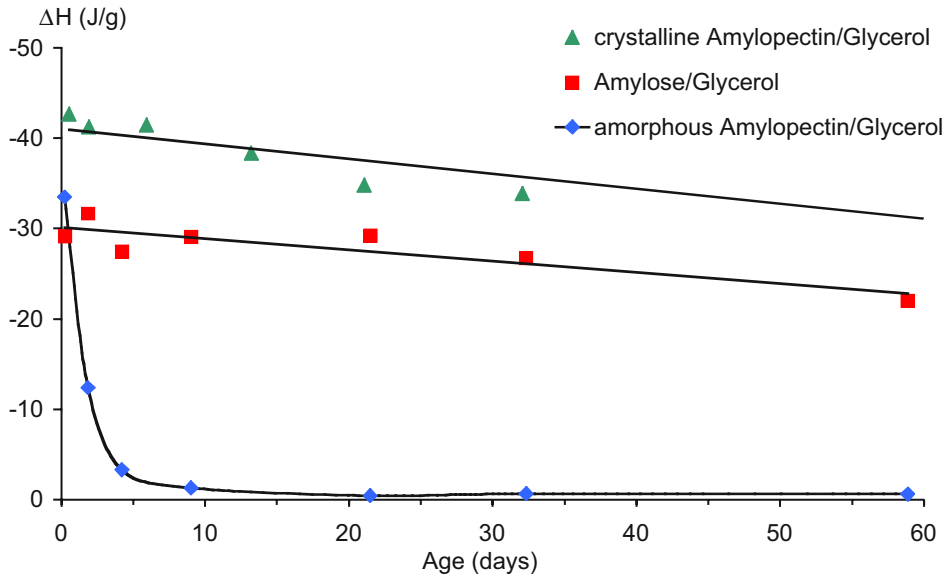

Figure 4.1 Enthalpy of the exothermal interaction of dry mixtures of amylopectin (crystalline or amorphous) or crystalline amylose with glycerol, as a function of storage time at room temperature.

The mixture of crystalline amylopectin (X_H = 0.40) with glycerol proved to be fairly stable in the sense that the interaction enthalpy decreased only gradually during storage at room temperature. After 30 days, a reduction of only 20-25% was observed. For amylose, which is also crystalline (X_H = 0.35), results are similar to crystalline amylopectin. After 30 days at room temperature, a reduction in the enthalpy of only 15-20% is found. For amorphous amylopectin (X_H = 0.20) the interaction enthalpy decreased to less than 5% of its initial value after 8 days of storage at room temperature. This indicates that the interaction is a kinetically controlled process.

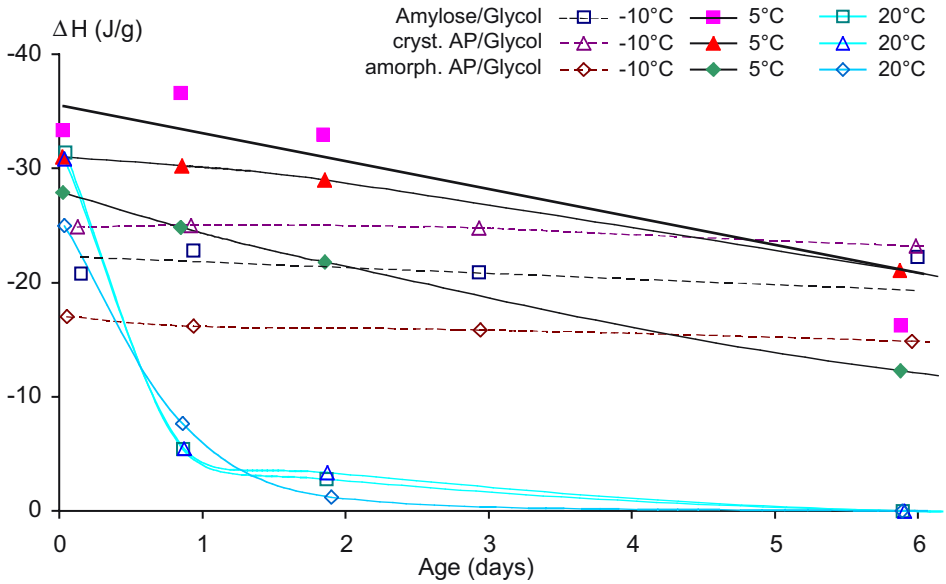

Figure 4.2 Enthalpy of interaction between dry amylopectin (crystalline or amorphous) or crystalline amylose and ethylene glycol, as a function of storage time at –10°C, 5°C or room temperature (20°C).

For amylose and amylopectin (amorphous and crystalline) with ethylene glycol, the interaction enthalpy reduced to less than 5% of its initial value already after 4 days of storage at room temperature (Figure 4.2). In contrast to glycerol, overall it appeared that the interaction at room temperature between starch and ethylene glycol was independent of the crystallinity of amylopectin. The decrease of interaction enthalpy during storage follows almost identical patterns for all mixtures. When comparing this interaction with that between amorphous amylopectin and glycerol, the interaction enthalpy decreases about twice as fast for ethylene glycol. Because of the smaller size of glycol, it is able to penetrate the starch chains more easily. And the crystallinity does not obstruct this penetration.

Directly after preparation of the mixtures there was a clear difference in behaviour between the amorphous and the crystalline mixtures. Ethylene glycol was readily absorbed, but the rate of this process appeared to be higher for amorphous amylopectin than for crystalline amylopectin or amylose. These different mixing characteristics may explain why the initial exothermal-enthalpy, measured directly after mixing, was higher for crystalline amylopectin than for amorphous amylopectin. The interaction probably started during the mixing period due to mechanical energy input, and the crystalline material is less penetrable. On exploring the influence of mixing on the interaction between crystalline amylopectin and ethylene glycol, it was observed that smaller sample sizes and longer mixing times resulted in a faster interaction. But for the results reported here, similar sample sizes and mixing times were used, in order to largely eliminate this effect.

The kinetic involvement of the starch-ethylene glycol interaction was explored by varying the temperature at which the samples were conditioned. At low temperatures, ethylene glycol molecules become less mobile, and behaviour similar to glycerol at room temperature is expected. In Figure 4.2 the course of the interaction enthalpy during storage is shown at conditioning temperatures of –10°C, 5°C and 20°C. When conditioned at 20°C, the interaction takes place very quickly. After 4 days almost no interaction enthalpy was observed by DSC, implying that the interaction has mainly reached equilibrium. At 5°C the interaction is much slower, taking approximately 17 days to reach equilibrium. The decrease in enthalpy per day of storage (slope in Figure 4.2) is similar for the three mixtures, though. The variation in initial enthalpy value is probably caused by different energy input during sample mixing. When stored at –10°C, almost no decrease in interaction enthalpy is observed. It takes approximately 90 days of storage for amylose and amorphous amylopectin/ethylene glycol mixtures before the interaction has reached equilibrium. Because the initial enthalpy value was larger for crystalline amylopectin, the interaction process took longer to reach equilibrium. Also, at low temperatures no differences in the interaction processes between amylose and amylopectin, and between amorphous and crystalline amylopectin can be detected. The crystalline regions do not obstruct the ethylene glycol molecules from penetration.

Solid state nuclear magnetic resonance spectroscopy

For dry potato amylose or amylopectin mixed with glycerol, sharp peaks appeared in the HP/DEC spectrum, as depicted in Figure 4.3a for amorphous amylopectin. Since mobile structures dominate the HP/DEC spectrum it was concluded that the glycerol was highly mobile. After heat treatment of the mixtures, the glycerol peaks in the HP/DEC spectrum became less intense and broader (Figure 4.3b), the intensity diminishing to less than 5% of that of the fresh mixtures (Figure 4.3a), indicating a decrease in glycerol mobility.

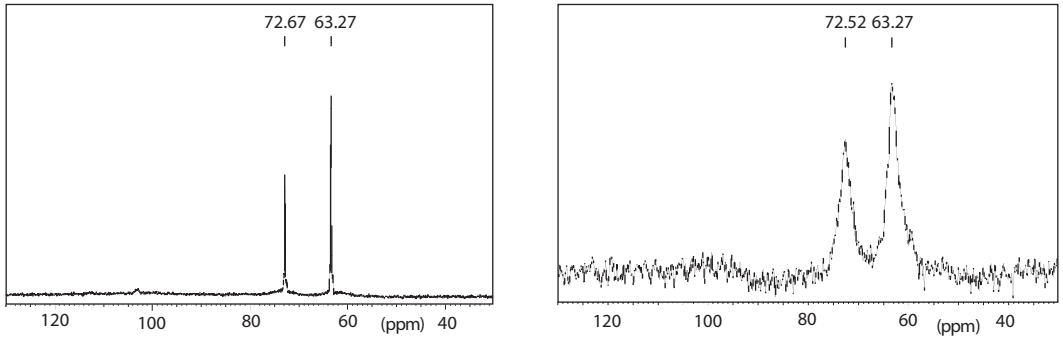

3a **3b**

Figure 4.3 ^{13}C HP/DEC NMR spectra of dry amorphous potato amylopectin with 29 wt% glycerol, freshly mixed (3a), and after heating for 30 min at 165°C (3b).

Weak starch signals are detectable in HP/DEC after heat treatment, which may indicate that the starch chains have become somewhat more mobile. In the CP/MAS spectrum, which displays more solid-like material, the glycerol peaks appeared alongside the starch signals after heat treatment (e.g. at δ = 63.4 ppm), indicating the immobilisation of glycerol (Figure 4.4) [13-15]. A molecular interaction was realised between glycerol and starch.

From the DSC results it was concluded that the interaction also takes place upon storage at room temperature. Crystalline amylopectin and amylose showed similar behaviour, interacting more slowly than amorphous amylopectin. The plasticisers do not seem to discriminate between the two starch polysaccharides. Therefore, the NMR investigation is limited to crystalline and amorphous amylopectin. For crystalline amylopectin with glycerol, no changes in the NMR spectra were observed after several days of storage at room temperature. However, as in agreement with the DSC results, for amorphous amylopectin with glycerol, a significant change was found in the NMR spectra after 8 days of storage at room temperature (Figure 4.5).

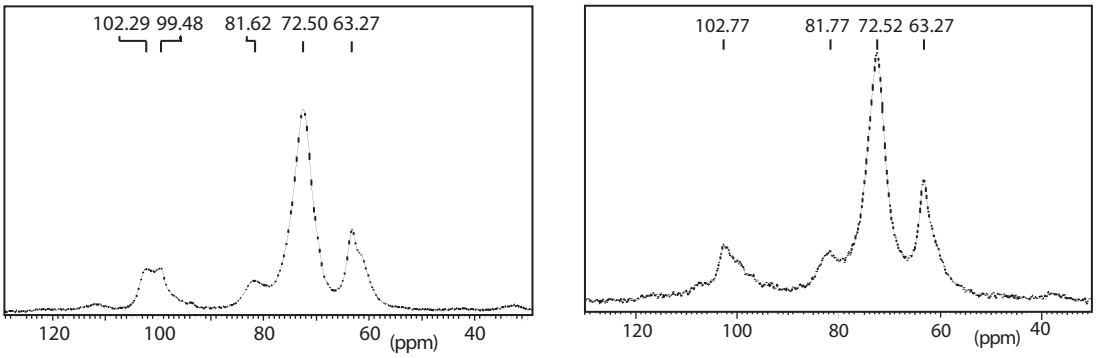

4a **4b**

Figure 4.4 ^{13}C CP/MAS NMR spectra of dry crystalline (4a), and amorphous (4b) amylopectin with 29 wt% glycerol, after heating for 30 minutes at 165°C.

The HP/DEC spectrum showed a considerable broadening and decrease in intensity of the glycerol peaks, as compared with freshly mixed material (Figure 4.3a). Also, the glycerol signals appeared in the CP/MAS spectrum. Especially the glycerol signal at 63.3 ppm was prominent, since the signal at 72.7 ppm overlapped largely with the amylopectin C2/C3/C5 signals. Comparing the spectra to those after heat treatment (Figure 4.4), the intensity-decrease and broadening of the glycerol signals in the HP/DEC spectrum was relatively small. Moreover, the glycerol signals in the CP/MAS spectrum were less intense but sharper after 8 days of conditioning at room temperature. After 8 days at room temperature, a smaller portion of the glycerol molecules is bound to amorphous amylopectin, explaining the less intense signals, but they are bound in a more ordered fashion than after heat treatment, explaining the sharper signals.

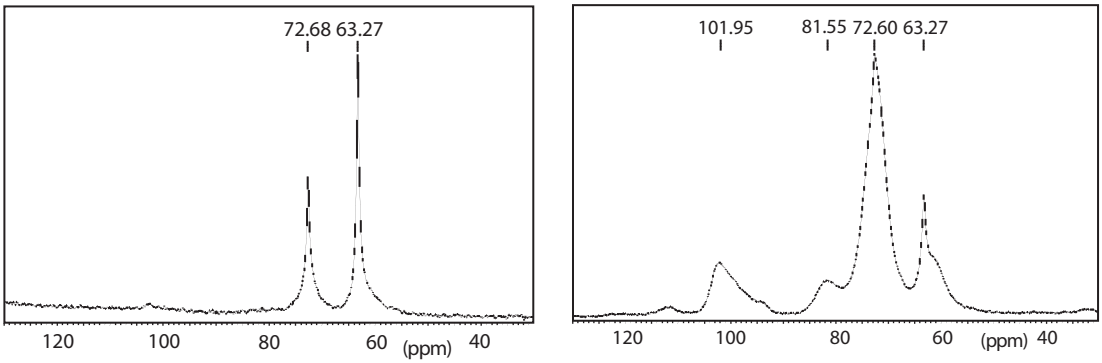

5a **5b**

Figure 4.5 ^{13}C HP/DEC (5a) and CP/MAS (5b) NMR spectra of dry amorphous amylopectin with glycerol (29 wt%), after 8 days of storage at room temperature.

According to the DSC results, ethylene glycol interacts rapidly with amylose as well as with crystalline or amorphous amylopectin. For mixtures of amylopectin (crystalline or amorphous) with ethylene glycol, in analogy with glycerol, the ethylene glycol signal appeared in the CP/MAS spectra after heat treatment (Figure 4.6).

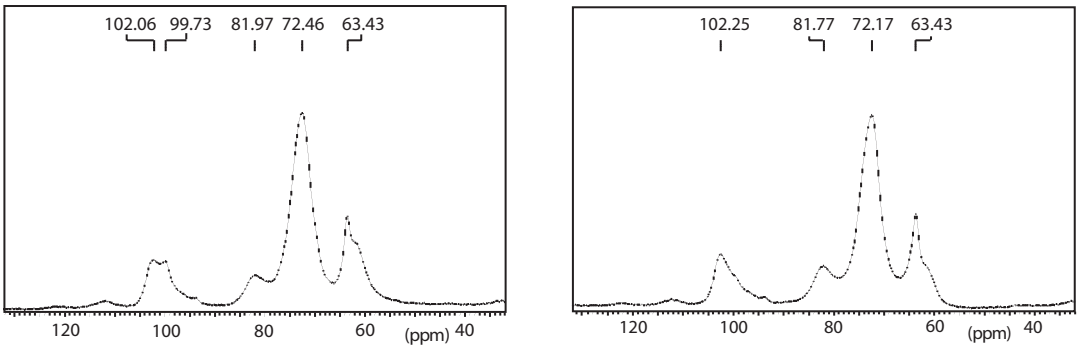

6a **6b**

Figure 4.6 ^{13}C CP/MAS NMR spectra of dry crystalline (6a) and amorphous (6b) amylopectin with ethylene glycol (21 wt%), after heating for 30 min at 165°C.

Also, after 5 days of storage at room temperature the CP/MAS spectrum showed an immobilisation of ethylene glycol (Figure 4.7). The linewidths of the ethylene glycol signal (63.4 ppm) were about 1½ times larger in the crystalline amylopectin mixture than in the amorphous amylopectin mixture. This may indicate that in crystalline amylopectin ethylene glycol is bound in a less ordered manner than in amorphous amylopectin. The ethylene glycol signal was considerably larger (~1½ times higher) and about 2 times broader after heat treatment compared to storage at room temperature. The HP/DEC spectra supported this immobilisation of ethylene glycol, both after storage at room temperature and after heat treatment. In the HP/DEC spectra weak amylopectin signals are detected, which are ~10% stronger for amorphous than for crystalline amylopectin. Apparently a more ordered distribution of the plasticiser results in an increased mobility of the starch chains.

In order to probe the flexibility of the polysaccharide and the plasticiser in the mixtures, the CP/MAS contact time is varied. A different response of signal intensity to the contact time within a system, demonstrates that the components do not share a common relaxation pathway (^1H $T_{1\rho}$) [18]. A series of CP/MAS experiments is performed on dry amorphous amylopectin with glycerol after heat treatment, with a contact time of 100-3500 μs. The glycerol peak intensity, relative to the amylopectin

C1 peak, is found to be linearly related to the contact time. It is possible that the intensities are averages of heterogeneous relaxation environments for the two components.

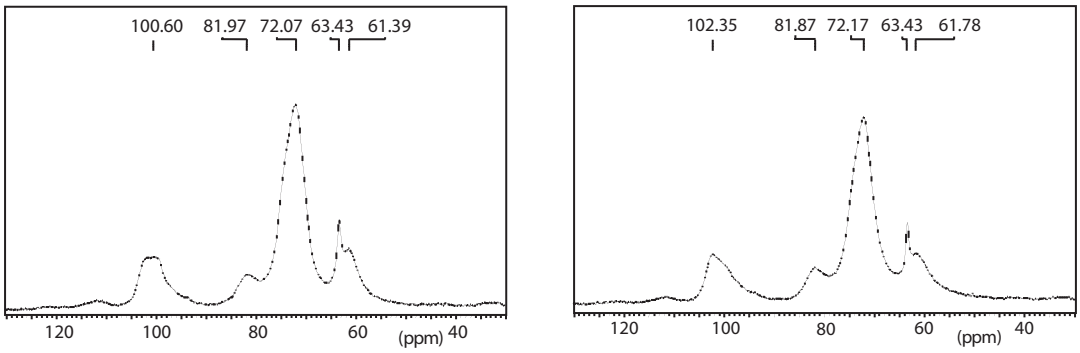

7a **7b**

Figure 4.7 ^{13}C CP/MAS NMR spectra of dry crystalline (7a) and amorphous (7b) amylopectin with ethylene glycol (21 wt%), after 5 days of storage at room temperature.

Discussion

These results showed that upon heating and upon storage at room temperature for several days, the plasticisers glycerol and ethylene glycol interact with crystalline amylose and crystalline and amorphous amylopectin. At room temperature, ethylene glycol interacts at a similar rate with crystalline amylose and crystalline and amorphous amylopectin. However, glycerol interacts slower with crystalline amylose and amylopectin, than with amorphous amylopectin. The interaction is similar for crystalline amylose and crystalline amylopectin, implying that the plasticiser does not discriminate between the two polysaccharides. This suggests that the interaction with amorphous amylose would be similar to the interaction with amorphous amylopectin. Because of the different rates of interaction of the mixtures at room temperature, this kinetically controlled interaction is mainly effective in the amorphous regions of starch polysaccharides, which allow glycerol to interact with the polymer chains more easily. According to DSC, the interaction between amorphous amylopectin and glycerol or ethylene glycol has reached equilibrium after 8, respectively 4 days of storage at room temperature. At room temperature, the crystalline structure largely prevents glycerol from interacting and obstructs ethylene glycol to interact in an ordered manner.

Heat treatment clearly immobilised the plasticisers more than storage at room temperature, although in a less ordered manner. At room temperature the interaction develops more gradually, which explains the difference in order. It may be, that at room temperature less plasticiser molecules are bound to the polysaccharide, but with more of the hydroxy groups of the plasticiser. Therefore, the plasticiser is bound in a more ordered fashion, but in total the plasticiser is immobilised less because less plasticiser molecules are bound. Weak amylopectin signals are detected in the HP/DEC spectra, that are stronger when the plasticiser is bound in a more ordered fashion. The plasticiser is better capable of mobilising polysaccharide chains when it interacts in a more ordered fashion. When interacting with more hydroxy groups per plasticiser molecule, locally it prevents hydrogen bonding between starch chains in a region of the size of the plasticiser molecule.

Solid state NMR CP/MAS contact time variation experiments showed that the glycerol signal relative to the amylopectin C1 peak is linearly related to the contact time. Highly mobile glycerol would not be detected with CP/MAS. When glycerol were tightly bound to the amylopectin chains, one would expect similar relaxation behaviour for both glycerol and amylopectin. This is not the case, which suggests that the amylopectin/glycerol interaction is relatively weak, or that the average of heterogeneous relaxation environments of glycerol is measured. The appearance of the plasticiser in the CP/MAS spectrum suggests that the interaction is strong enough to immobilise plasticiser molecules. The amylopectin/glycerol interaction may be involved in some sort of chemical exchange mechanism, in which the glycerol is continuously moving through the mixture and interacting alternately with different sites, as is common for plasticisers.

When processing starch, the ingredients are often premixed. The time dependent interaction with plasticisers affects the molecular mobility and therewith the material properties. In freshly mixed material, starch chains are less flexible and the material may even be glassy or brittle by lack of plasticisation. Due to the interaction with plasticisers starch mobility increases, viscosity reduces, and the material behaves like a rubber. Variation in the time between premixing and processing may influence for example flow properties or resistance to shear, thereby influencing processing conditions.

Recently, Perry *et al*. reported SAXS and WAXS X-ray diffraction results on mixtures of granular potato or waxy maize starch and high concentrations (55-75%)

of glycerol, ethylene glycol or 1,4-butanediol [19]. They suggest that the exothermal transition that has been reported previously [13,14,20], results from crystallinity development, comparable with the side by side alignment of helices during annealing [21]. The results in this paper, show that the exothermal transition results from interaction development between starch and plasticiser. Because this interaction occurs, the polysaccharide is plasticised and the helices are enabled to align. Crystal lattice perfection thus is a secondary process. Previously, based on dielectric relaxation spectroscopy results, it was suggested that crystallinity developed, but at the plasticiser concentrations used in this paper (21-29%), crystallinity could not be observed with WAXS [15].

Conclusions

It has been previously reported, that upon heating granular or recrystallised starch with glycerol or ethylene glycol in the absence of water, an exothermal transition could be detected by DSC [20]. This was suggested to be caused by an interaction between starch and the plasticisers. The present study shows that upon heating this interaction takes place between glycerol or ethylene glycol with amylose as well as with amylopectin, and that it is independent of the presence of crystallinity of the polysaccharide.

Furthermore, it was found that a similar interaction takes place during storage at room temperature for several days. This affects the molecular mobility and may influence for example flow properties and resistance to shear when premixing ingredients prior to processing starch. At room temperature, the plasticiser glycerol mainly interacts with the amorphous regions of dry amylopectin or amylose. Ethylene glycol, a smaller molecule, interacts more easily with dry starch polysaccharides than glycerol. This interaction is regardless of the presence of crystallinity. Partial immobilisation of the plasticisers is the result of these interactions. NMR results showed that heat treatment of the starch/plasticiser mixtures generally causes further immobilisation of both glycerol and ethylene glycol. Heat treatment also causes broadening of the plasticiser signal, as compared with storage at room temperature. It may be that upon heating, more plasticiser molecules interact, but with less of the hydroxy groups of the plasticiser, than upon storage at room temperature. Starch chains are mobilised more when the plasticiser interacts in a more ordered manner, which occurs when the interaction develops at room temperature. Therefore, when ingredients are premixed,

this may facilitate processing. The fact that crystal lattice perfection may result from the mobilisation of starch chains, however, may aggravate processing when the premixed ingredients are stored at room temperature for some days. Premixing is generally accepted as a tool for mixing ingredients without further implications. The present study yet shows that the time between premixing and processing can influence material properties and processing conditions.

References

1. M. Gudmundsson, 'Retrogradation of starch and the role of its components', *Thermochim. Acta* **246** (1994), p 329-341,
2. J.J.G. van Soest and D.B. Borger, 'Structure and properties of compression molded thermoplastic starch materials from normal and high amylose maize starches', *J. Appl. Polym. Sci.* **64** (1997), p 631-644,
3. R.N. Tharanathan, 'Starch - the polysaccharide of high abundance and usefulness', *J. Sci. & Ind. Res.* **54** (1995), p 452-458,
4. J.J.G. van Soest, S.H.D. Hulleman, D. de Wit and J.F.G. Vliegenthart, 'Changes in the mechanical properties of thermoplastic potato starch in relation with changes in B-type crystallinity', *Carboh. Polym*. **29** (1996), p 225-232,
5. H.J. Thiewes and P.A.M. Steeneken, 'The glass transition and the sub T_g endotherm of amorphous and native potato starch at low moisture content', *Carboh. Polym*. **32** (1997), p 123-130,
6. N. Krog, S.K. Oleson, H. Toernaes and T. Joensson, 'Retrogradation of the starch fraction in wheat bread', *Cereal Foods World* **34** (1989), p 281-285,
7. J.J.G. van Soest, D. de Wit, H. Tournois and J.F.G. Vliegenthart, 'The influence of glycerol on structural changes in waxy maize starch as studied by Fourier transform infra-red spectroscopy', *Polymer* **35** (1994), p 4722-4727,
8. L.A. Bello-Pérez and O. Parades-López, 'Effects of solutes on retrogradation of stored starches and amylopectins: a calorimetric study', *Starch/Stärke* **47** (1995), p 83-86,
9. K. Katsuta, M. Miura and A. Nishimura, 'Kinetic treatment for rheological properties and effects of saccharides on retrogradation of rice starch gels', *Food Hydrocoll*. **6** (1992), p 187-198,
10. K. Katsuta, A. Nishimura and M. Miura, 'Effects of saccharides on stabilities of rice starch gels: 1. Monosaccharides and disaccharides', *Food Hydrocoll*. **6** (1992), p 387-398,
11. K. Kohyama and K. Nishinari, 'Effect of soluble sugars on gelatinization and retrogradation of sweet potato starch', *J. Agric. Food Chem*. **39** (1991), p 1406-1410,
12. J.H. Jagannath, K.S. Jayaraman, S.S. Arya and R. Somashekar, 'Differential scanning calorimetry and wide-angle X-ray scattering studies of bread staling', *J. Appl. Polym. Sci*. **67** (1998), p 1597-1603,
13. A.L.M. Smits, S.H.D. Hulleman, J.J.G. van Soest, H. Feil and J.F.G. Vliegenthart, 'The influence of polyols on the molecular organisation in starch-based plastics', *Polym. Adv. Technol.* **10** (1999), p 570-573,
14. P.H. Kruiskamp, A.L.M. Smits, J.J.G. van Soest, J.F.G. Vliegenthart, 'The influence of plasticiser on the molecular organisation in dry amylopectin measured by differential scanning calorimetry and solid state nuclear magnetic resonance spectroscopy', *J. Ind. Microbiol. Biotech.* **26** (2001), p 90-93,
15. A.L.M. Smits, M. Wübbenhorst, P.H. Kruiskamp, J.J.G. van Soest, J.F.G. Vliegenthart, J. van Turnhout, 'Structure evolution in amylopectin/ethylene glycol mixtures by H-bond formation and phase separation studied with dielectric relaxation spectroscopy', *J. Phys. Chem. B* **105** (2001), p 5630-5636,

16. J.J.G. van Soest, H. Tournois, D. de Wit and J.F.G. Vliegenthart, 'Short-range structure in (partially) crystalline potato starch determined with attenuated total reflectance Fourier-transform IR spectroscopy', *Carboh. Res*. **279** (1995), p 201-214,
17. M.J. Gidley, 'High-resolution solid-state NMR of food materials', *Trends in Food Sci. & Tech.* **3** (1992), p 231-236,
18. T.J. Foster, S. Ablett, M.C. McCann and M.J. Gidley, 'Mobility-resolved ^{13}C NMR spectroscopy of primary plant cell walls', *Biopolymers* **39** (1996), p 51-66,
19. P.A. Perry and A.M. Donald, 'The role of plasticization in starch granule assembly', *Biomacromolecules* **1** (2000), p 424-432,
20. J.J.G. van Soest, R.C. Bezemer, D. de Wit and J.F.G. Vliegenthart, 'Influence of glycerol on the melting of potato starch', *Ind. Crops Prod.* **5** (1996), p 1-9,
21. R.F. Tester, S.J.J. Debon, 'Annealing of starch: a review', *Int. J. Biol. Macromol.* **27** (2000), p 1-12.

Chapter 5

Structure Evolution in Amylopectin/Ethylene Glycol mixtures by H-Bond Formation and Phase Separation studied with Dielectric Relaxation Spectroscopy

A.L.M. Smits, M. Wübbenhorst, P.H. Kruiskamp,
J.J.G. van Soest, J.F.G. Vliegenthart, J. van Turnhout
[Published in *J. Phys. Chem. B* **105** (2001), p 5630-5636]

Abstract

The interaction between amylopectin, a starch polysaccharide, and ethylene glycol (EG) was investigated using broad-band dielectric relaxation spectroscopy. Water-free amylopectin (AP) was mixed with 21 wt% ethylene glycol. This resulted in a continuous ethylene glycol phase, as well as a molecularly mixed AP/EG fraction. After storage at room temperature or annealing, the mixture shows dynamic properties typical of a polymer with weak intermolecular interactions, suggesting that EG binds preferentially to AP and forms intra-chain H-bridges leading to increased chain stiffness and thus an increased glass transition temperature. This structure evolution is accompanied by a sharp reduction in the size of the ethylene glycol droplets to a few nanometres, as revealed by pronounced confinement effects in the α-relaxation of the dispersed EG.

Introduction

Starch is used as a natural food ingredient and is, amongst other carbohydrates, one of the main energy providers in the human diet. Furthermore, starch-based polymeric materials are playing an increasing role as biodegradable material, which can easily be processed by moulding techniques widely used for synthetic polymers. One can obtain thermoplastic starch products with a broad range of material properties, owing to the diversity of natural starch itself [1-3], which is usually combined with a low molecular plasticiser. It is known that these properties also depend strongly on the processing conditions, such as temperature and water content. The limited knowledge about the relations between processing conditions and the resulting molecular structure and properties of starch plastics makes it difficult to predict and control their physical properties.

Ageing induced by starch retrogradation causes staling of bakery products and embrittlement of starch plastics, which deteriorate the properties of these materials [4,5]. These ageing processes can be influenced in particular by plasticisers, since they strongly affect the molecular organisation and hence the viscoelastic properties of the thermoplastic, semi-crystalline starch plastics in time. For example, in bread the degree of retrogradation is reduced markedly by the addition of monoglycerides, which interact with amylopectin [6]. The inhibiting effect of various saccharides on retrogradation has often been reported [7-10], and glycerol e.g. has been reported to reduce the rate of retrogradation in a waxy maize starch gel [11].

Insight into the plasticiser-macromolecule interaction is essential for the optimisation of the material properties of thermoplastic starch by controlling the molecular structure. Recently, the interactions of glycerol and ethylene glycol with dry starch polysaccharides (amylose and amylopectin) were investigated using DSC and solid state NMR spectroscopy, showing that for both plasticisers a strong interaction is induced by heat and time [12,13]. The interaction of starch with ethylene glycol develops more rapidly than with glycerol.

Dielectric relaxation spectroscopy (DRS) has established itself as a powerful technique for the study of molecular dynamics in polymers in the past decade, ever since automated spectrometers covering a broad frequency range (10^{-3}-10^{9} Hz) became available. Although DRS is well introduced in the field of synthetic polymers, only a few dielectric studies on bioplastics have been published as yet, mainly

involving carbohydrate systems. Besides the molecular assignment of dielectric relaxation processes of ionic carbohydrates, cellulose, dextran and various starches [14-16], changes in dielectric relaxation processes in carbohydrate systems upon addition of glycerol and water have been described [17]. Here we report on the dielectric analysis of the interaction between dry amylopectin and ethylene glycol.

Experimental

Dry amylopectin/ethylene glycol samples were prepared by mixing ethylene glycol (≤0.05% H_2O, Acros, B) with dried potato amylopectin (Amylopectin UG, Avebe, NL). The potato amylopectin was examined with X-ray diffraction, its crystallinity being similar to that of native potato starch (~25%). Amylopectin was dried for 48 h under reduced pressure in a vacuum-oven at 70°C. The dried material (<3% H_2O) was mixed manually under a nitrogen gas flow with 21 wt% ethylene glycol (corresponding to 4.3 mmol ethylene glycol per gram amylopectin). For the dielectric experiments disk-shaped samples were prepared by pressing the sample material between circular brass electrodes (diameter 20 mm), which resulted in 300-600 μm thick samples. Preparation took place under flowing gaseous nitrogen.

Dielectric experiments on the AP/EG mixtures were performed using a combination of two dielectric measurement systems covering a frequency range from 10^{-2} to 10^{6} Hz: 1) a frequency response analyser (Schlumberger 1260) equipped with a custom-made dielectric interface (developed by TNO) for frequencies between 10^{-2} and 10^{3} Hz, and 2) a Hewlett-Packard 4284A precision LCR-meter for frequencies between 10^{3} and 10^{6} Hz. The sample was placed in a nitrogen flushed cryostat (Novocontrol), the temperature of which was controlled with a stability of better than ±50 mK. More details about the experimental set-up can be found in Reference 18.

Dielectric measurements were performed on three different samples, the thermal histories of which are indicated in Table 5.1. The temperatures given in Table 5.1 have the meaning of either the highest temperature (25°C) or the temperature at which the sample was annealed just prior to a subsequent cooling run to –120°C by steps of 5°C. Such a cooling program was chosen to ensure that kinetic changes, if present, were restricted to the upper (start) temperature interval. The average cooling rate was about 1°C/min.

Table 5.1 Sample history and VFT-parameters of α_{AP} and α_{EG} for AP/EG mixtures

sample	annealing temp [°C]	α_{AP}					α_{EG}		
		T_g* [K]	T_V [K]	E_V [kJ/mol]	log (τ_∞ [s])	m	T_V [K]	E_V [kJ/mol]	log (τ_∞ [s])
1	25	200	96.6	29.0	-12.7	28.3	131	13.5	-12.8
1	40	220	114	27.5	-11.5	28.1	110.3	25.2	-15.5
2	60	222	81.2	39.7	-12.7	23.2	133	15.4	-12.8
2	80	226	112	29.5	-11.5	26.8	74.5	36.6	-16.8
2	100	249	89	43.0	-12.0	21.8	7.3	54.5	-17.7
2	120	251	93.6	39.4	-11.1	20.9	0**	57.9	-18.2
3	100	224	105	30.4	-11.4	25.3	132	13.4	-12.0
3	120	249	74	45.0	-11.4	19.0	0**	57.1	-18.0

*An operationally defined T_g was derived from the VFT-parameters using eq. 2 with the assumption that $\tau(T_g) = 100$s

**Fit with $T_V = 0$ (Arrhenius fit)

Results and Discussion

Overview of the relaxations and analysis of the dielectric relaxation data

A typical three-dimensional loss spectrum of sample (1), which was cooled from room temperature to –120°C immediately after sample preparation, is shown in Figure 5.1. Since strong Ohmic conduction dominated the measured dielectric loss ε", we have calculated the alternative loss $\varepsilon"_{deriv}$ from the permittivity ε' according to

$$\varepsilon''_{deriv} = -\frac{\pi}{2}\frac{\partial \varepsilon'(\omega)}{\partial \ln \omega} \approx \varepsilon'' \qquad (1)$$

This yields a fair approximation of the 'conduction-free' loss ε" for distributed relaxation peaks like those of the α-transition and the secondary relaxations [19,20].

By using this derivative technique, two strong and well resolved relaxation processes are revealed (cf. Figures 5.1 and 5.2), which were assigned to the dynamic glass-transitions of phase separated ethylene glycol (α_{EG}) –the fast or low-temperature process– and of 'plasticised' amylopectin (α_{AP}), respectively. Such α-relaxation processes can be identified by their temperature dependence of the relaxation time

$\tau(T)$, which typically obeys the Vogel-Fulcher-Tammann law (eq. 2), rather than the well-known Arrhenius equation:

$$\tau(T) = \tau_\infty \exp\left[\frac{E_V}{R(T - T_V)}\right] \tag{2}$$

Here the parameters R, E_V, T_V, and τ_∞ denote the gas constant, the 'Vogel activation energy', the 'Vogel scaling temperature' and the pre-exponential factor.

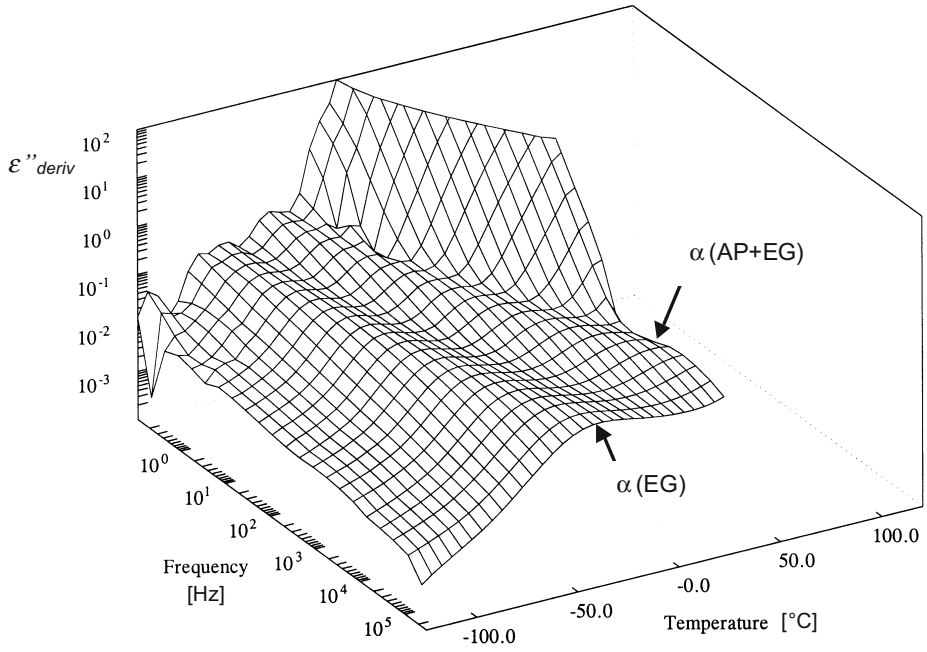

Figure 5.1 Three-dimensional representation of the 'conduction-free' loss $\varepsilon''_{deriv}(f, T)$ for a freshly mixed AP/EG sample (sample (1) in Table 5.1), showing two distinct non-Arrhenius α-relaxation processes.

In order to determine the relaxation time $\tau(T)$ from the dielectric loss curves we have fitted the loss spectra $\varepsilon''(\omega)$ by a set of two Havriliak-Negami (HN) relaxation functions (eq. 3), using the Levenberg-Marquardt algorithm:

$$\varepsilon'' = -\sum_{k=1}^{2} \mathrm{Im}\left\{\frac{\Delta\varepsilon_k}{\left(1+(i\omega\tau_k)^{a_k}\right)^{b_k}}\right\} + \frac{\sigma}{\varepsilon_0\omega} \tag{3}$$

where $\Delta\varepsilon_k$ and τ_k correspond to the relaxation strength and the mean relaxation time of the k^{th} process. The two shape parameters a_k and b_k, which determine the slope

dε''/dlnω of the low-frequency loss tail a and the high-frequency loss tail $-a \cdot b$, are determined by the underlying distribution in relaxation times. The 2nd term in eq. 3 accounts for pure Ohmic conduction.

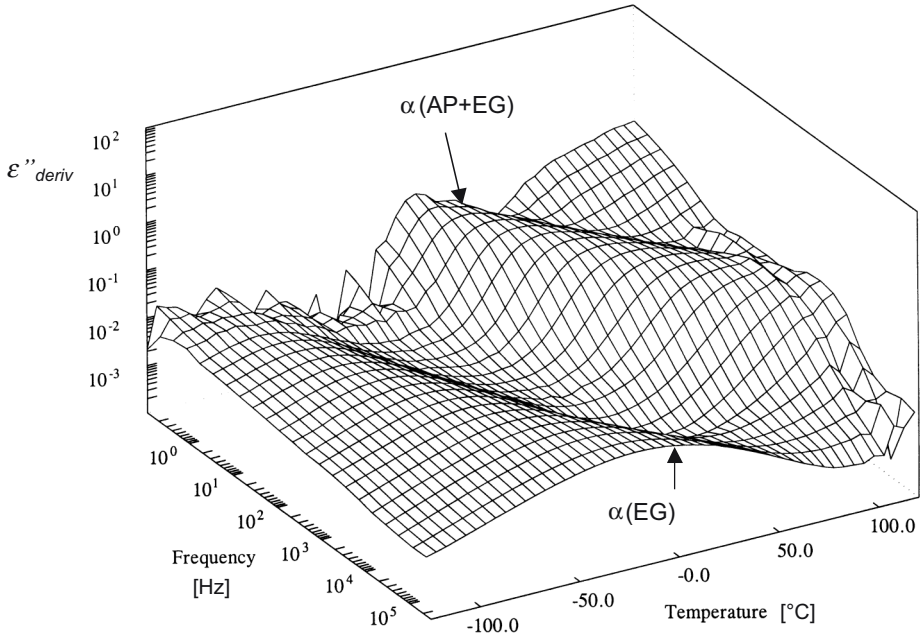

Figure 5.2 Three-dimensional representation of $\varepsilon''_{\mathrm{deriv}}(f, T)$ of AP/EG sample (2) after annealing at 120°C.

Alternatively, we have fitted the derivative-based loss spectra $\varepsilon''_{deriv}(\omega)$ to the analytical derivative of the Havriliak-Negami function $\partial\varepsilon'_{HN}/\partial\ln\omega$:

$$\frac{\partial\varepsilon'_{HN}}{\partial\ln\omega} = -\frac{ab\Delta\varepsilon(\omega\tau)^a\cos\left[a\pi/2-(1+b)\theta_{HN}\right]}{\left[1+2(\omega\tau)^a\cos(\pi a/2)+(\omega\tau)^{2a}\right]^{\frac{1+b}{2}}} \tag{4}$$

with

$$\theta_{HN} = \arctan\left[\sin(\pi a/2)\Big/\left((\omega\tau)^{-a}+\cos(\pi a/2)\right)\right] \tag{5}$$

In particular, we have used the fit function $\partial\varepsilon'_{HN}/\partial\ln\omega$ in order to find reliable (start) parameters for the two HN-functions (1st term of eq. 3) in cases where the loss ε'' did not reveal any peak or shoulder of the slow relaxation process due to dominating Ohmic conduction. In these cases, the fit of $\varepsilon''_{deriv}(\omega)$ yielded a first (good) approximation of the HN-parameters, which were then used as start parameters for a subsequent fit of the original $\varepsilon''(\omega)$ spectra resulting in 'refined' fit-parameters.

The relaxation times obtained by the HN-fit procedures are presented in a relaxation map (Figure 5.3) and have been fitted with the VFT-equation. One clearly sees that indeed most of the relaxation processes show a curvature according to the VFT-law as a characteristic feature of cooperative α-relaxation processes. The VFT-parameters are summarised in Table 5.1.

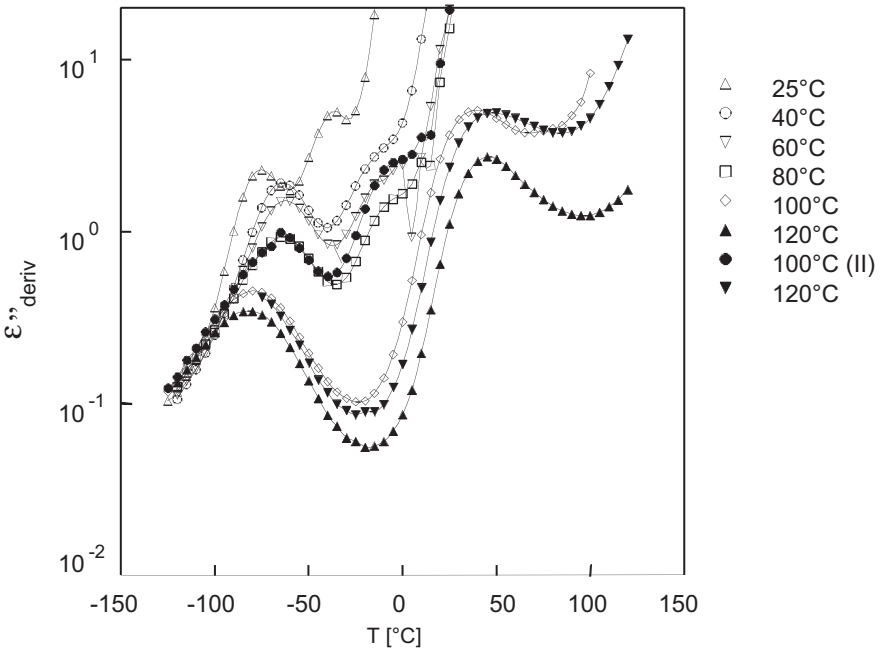

Figure 5.3 Temperature-dependent $\varepsilon''_{deriv}(f, T)$ at f = 14 Hz for AP/EG annealed at different temperatures.

Effect of annealing on the glass transitions and relaxation strengths

A first impression of the influence of annealing on the dynamic properties of AP/EG mixtures can be obtained by comparing Figures 5.1 and 5.2, which show the two relaxation processes α_{EG} and α_{AP} for the two extreme cases of a freshly prepared sample (Figure 5.1) and a sample (2) that was stepwise annealed up to 120°C (Figure 5.2). Although both relaxation processes are still present after annealing, in particular the loss peak of amylopectin undergoes a dramatic up-shift by 50-80°C, depending on the frequency.

In order to elucidate the role of the thermal history on the relaxation properties, a series of stepwise annealing experiments on three different samples was performed (cf. Table 5.1). For a fair comparison of the dielectric results we have presented both

the loss ε''_{deriv}(f = 14 Hz) and the dielectric constant ε'(f = 28 kHz) as a function of the temperature for all eight cooling runs (Figures 5.3 and 5.4).

The first two cooling runs were made on sample (1), one immediately after preparation (25°C), the second after subsequent annealing at 40°C for 400 min. According to Figures 5.3 and 5.4, this treatment already causes a slight shift of the α_{EG} peak accompanied by a strong increase in the α_{AP} peak temperature by approximately 40°C.

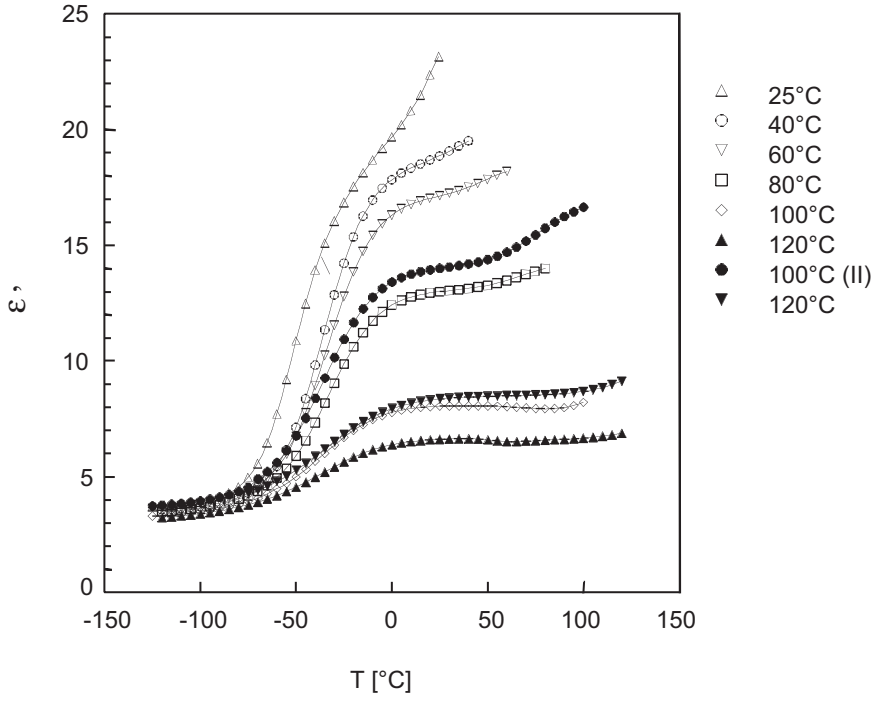

Figure 5.4 Temperature-dependent permittivity $\varepsilon'(T)$ at f = 28 kHz for AP/EG annealed at different temperatures.

A second fresh sample was treated as follows: annealing at 60°C for 400 min, measurement during cooling to –120°C, annealing at 80°C for 300 min, again cooling and measuring and finally storage at room temperature for one week under dry conditions in a desiccator. After this period the sample was further annealed at 100°C for 300 min, measured upon cooling to –120°C, and subsequently subjected to 120°C for 300 min and again measured during cooling.

In contrast to the first annealing step (at 40°C), the treatments at 60 and 80°C only result in marginal shifts of the peak positions of both the α_{EG} and the α_{AP} relaxation. Concurrently, the relaxation strengths $\Delta\varepsilon$ of both processes decrease by a factor of two as can be seen in Figure 5.4 ($\Delta\varepsilon \sim \varepsilon''$ peak maximum) or in Figure 5.5 ($\Delta\varepsilon_{EG}$ given

by the step in ε'). A plausible explanation for the weakening of the α_{EG} peak process is the reduction of the volume fraction of phase-separated EG by diffusion into the molecularly mixed AP/EG phase. On the other hand, the reduction of the α_{AP} relaxation strength is not obvious with respect to a virtually unchanged glass transition temperature of AP (cf. Figure 5.3 and the Arrhenius presentation in Figure 5.5). Most likely, to some extent short-range ordering (e.g. helix formation) or crystallisation of AP/EG took place at 60 and 80°C, temperatures far above (~100°C) the estimated glass transition temperature of AP. Explicit evidence for such slow crystallisation requires additional studies.

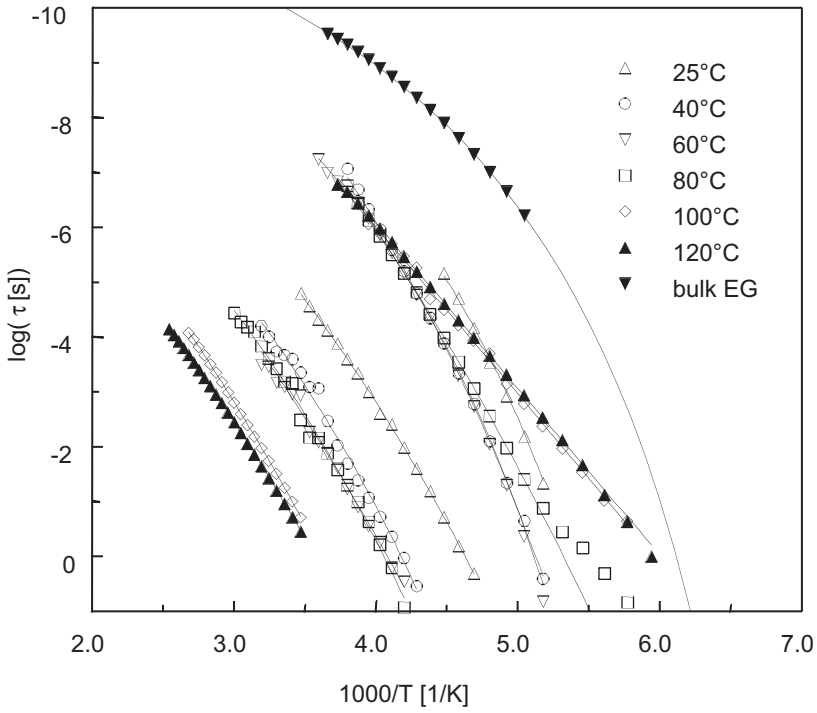

Figure 5.5 Relaxation map of samples (1) and (2): sample (1) fresh (25°C), and after annealing at 40°C, and sample (2) after annealing at 60, 80, 100, and 120°C. For comparison, the relaxation data of bulk ethylene glycol are given as well.

Continued annealing at 100 and 120°C leads to a further reduction of the free ethylene glycol fraction to about 20% of its initial value, which is again accompanied by a significant increase of the glass transition temperature T_g(AP). Obviously, high-temperature annealing results in an almost complete incorporation of EG in a semi-crystalline structure consisting of branched amylopectin macromolecules and H-bonded low-molecular ethylene glycol. Although the details of the molecular organisation of such a structure, like the conformation of AP or preferential

H-bonding sites, are not known yet, it is obvious that the formation and optimisation of the AP/EG structure is a time-consuming process.

An important question is the validity of the time-temperature equivalence for the structure formation, which typically holds for thermally activated processes and the glass transition of simple systems. To check this equivalence we tried a different route to obtain a fully cured sample by starting annealing experiments directly at 100 and 120°C with another freshly prepared sample (3). Interestingly, the dielectric results of sample (3) measured after annealing at 100 and 120°C strongly resemble those of sample (2) measured at 80 and 100°C. This 'delaying' behaviour is plausible due to the shorter thermal/time history of sample (3) and supports the validity of the time-temperature equivalence. However, comparison of the 80°C curve with the 100°C (II) curve in Figures 5.3 and 5.4, shows that almost identical α_{EG} peak positions and intensities correspond to markedly different intensities of the α_{AP} relaxation. We suggest that the higher α_{AP} relaxation strength of sample (3) can be attributed to a lower degree of short-range order or crystallinity in the AP/EG phase, which points to a melting temperature of helices or AP/EG crystallites between 80 and 100°C.

So far we have not specified the nature of H-bonding of EG to AP chains in annealed AP/EG mixtures. In principle, the increase in the glass transition temperature of AP by more than 50°C can be rationalised by different ways of hydrogen bond formation between AP chains and EG molecules. The two main options are chain stiffening by single or double hydrogen bonding of EG molecules or the formation of a physical network by *interchain* EG bridges. Explicit evidence for the existence or non-existence of *intermolecular* physical cross-links can be obtained from the temperature dependence of the relaxation time of the α_{AP} process, which is shown in Figure 5.3 and quantified by the VFT-fit parameters listed in Table 5.1.

Compared to the VFT-curves of the α_{EG} process at 40 and 60°C, the α_{AP} relaxation time shows only slightly curved VFT-lines, i.e. the α_{AP} process resembles a simple Arrhenius behaviour. The degree of curvature of the VFT-dependence has been proposed by Angell as a powerful criterion to classify low molecular and polymeric glass formers into fragile glasses (high curvature) and strong glass formers (weak curvature of VFT-curve) [21]. For polymers, fragility, which can be defined in various ways, is a measure of the degree of intermolecular coupling of polymer chains. Factors that contribute to intermolecular coupling are, for example, sterical hindrance

by bulky side groups, covalent cross-links, or other specific *interchain* interactions. A useful quantification of fragility is given by the steepness index *m*, which was defined by Böhmer *et al.* [22]

$$m = \left. \frac{d \log\langle \tau \rangle}{d\left(T_g / T\right)} \right|_{T=T_g} \tag{6}$$

m is linked to the VFT-parameters by eq. 7:

$$m = \frac{E_V}{2.303R} \frac{T_g}{\left(T_g - T_V\right)^2} \tag{7}$$

Using eq. 7, we have calculated *m* for the α_{AP} relaxation, and the results are listed in Table 5.1. According to reference data [23], our *m*-values are at the lower limit, which qualify AP/EG as a very strong glass former, corresponding to a low degree of *interchain* coupling. Upon annealing, this coupling merely decreases, which makes the idea of a H-bonded AP network created by intermolecular EG bridges unlikely.
This finding rather favours the assumption of *intrachain* EG bridges. In this way, EG is able to occupy H-bonding sites in the AP chain, which inhibits the formation of interchain H-bonds between different AP branches or molecules.

Molecular dispersion of ethylene glycol: effects of confinement and anchoring on inner surfaces

While the α-relaxation process of the AP structure continuously slows down with increasing annealing temperature (25-120°C), the (low-temperature) α-process of the EG phase shows a more complex behaviour (cf. Figure 5.6). At low annealing temperatures (40 and 60°C), an initial slowing down of the α_{EG} dynamics can be observed. Heat treatment at higher temperatures then causes a qualitative change of the relaxation time-temperature characteristics from initially VFT behaviour to a genuine Arrhenius behaviour (100 and 120°C), which is accompanied by an acceleration of the α-process.
This discontinuous shift of the α-relaxation time with ageing is qualitatively in line with results from EG and other glass forming liquids that are confined to small (nm) pores or cages [24,25]. The molecular dynamics of such confined systems is

determined by the balance between surface- and confinement-effects: while interactions with the inner surfaces will delay the molecular dynamics, the reduction in pore size (increase of confinement) will speed-up the glass-transition dynamics.

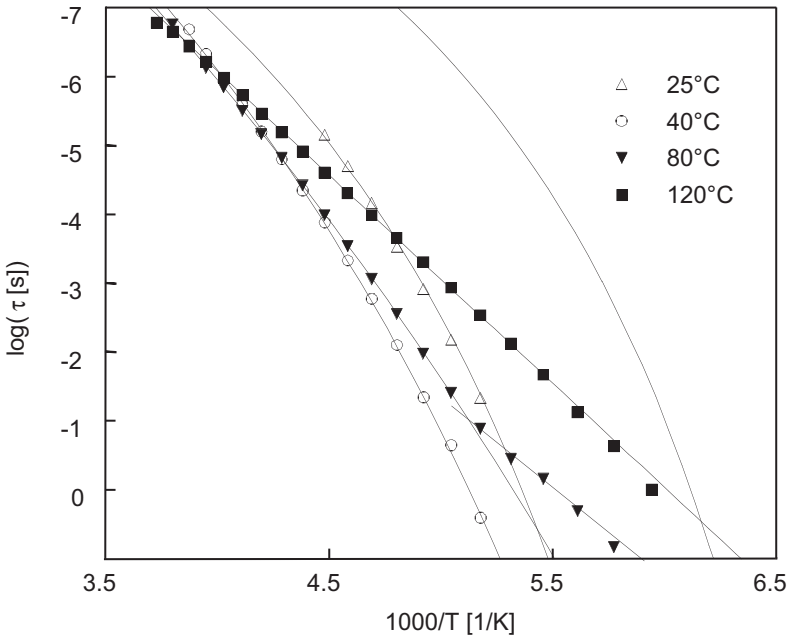

Figure 5.6 Relaxation time τ of the fast α-process (α_{EG}) in AP/EG after different thermal treatments. For comparison, the relaxation data of bulk ethylene glycol are shown as a line on the far right.

In this sense, the initial slowdown of the α_{EG} relaxation process in the AP/EG system compared to bulk-EG points to a larger amount of less mobile EG located near the inner surfaces of EG droplets after annealing. However, the drastic difference in the dynamics between bulk-EG and dispersed EG by 2-3 decades cannot be explained by surface anchoring alone, in particular not in the initial coarse morphology (cf. Figure 5.9a). We therefore hypothesise that the overall delay of the EG dynamics in AP/EG hints to the existence of a dispersed phase constituted by EG with partially dissolved AP molecules and chain sequences. Such a dilute solution of AP in EG provides a natural explanation for the delayed glass transition of EG without loosing its cooperativity for establishing the VFT-dynamics of a bulk liquid.

After annealing at 80°C, the $\tau(T)$ dependence (Figure 5.6) becomes flatter and shows a clear deviation from its VFT behaviour at lower frequencies. This change in dynamics marks the point at which the size (geometrical confinement) of the glass forming molecular ensemble starts to influence its cooperative dynamics. Whereas in

the bulk the characteristic length of cooperativity ξ increases with decreasing temperature leading to a curved VFT-dependence, one intuitively expects a qualitative change of the $\tau(T)$ dependence in the case that ξ becomes restricted by the geometrical limits of the molecular ensemble. Hence, the departure of $\tau(T)$ from a VFT-curve implies that the droplet size after annealing at 80°C has reached the length of cooperativity, which is typically 2-3 nm near the glass transition temperature [26].

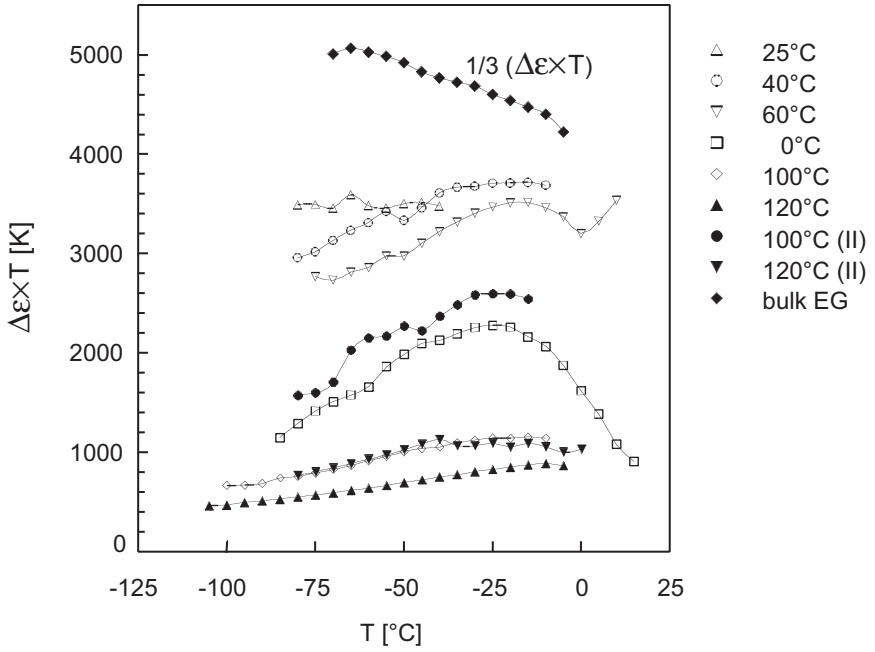

Figure 5.7 Relaxation strength $\Delta\varepsilon$ times temperature T vs temperature T for the α_{EG} process in bulk-EG and in AP/EG after different thermal treatments. For an easier comparison, the $\Delta\varepsilon \times T$ data for bulk-EG have been reduced to one-third of their original values.

Further annealing at 100 and 120°C completely alters the dynamics from VFT to a genuine Arrhenius behaviour, even for short relaxation times (Figures 5.3 and 5.6). In other words, the dynamics of EG has changed from cooperative liquid dynamics to thermally activated, single molecule dynamics. Such a behaviour has been previously reported for ethylene glycol that was confined to a variety of zeolitic host systems characterised by different sizes of their pores or cages [25].

Additional evidence for our molecular picture comes from the relaxation strength $\Delta\varepsilon$ and the shape parameter a_{HN} of the α_{EG} relaxation process. Figure 5.7 displays the temperature dependence of the quantity $\Delta\varepsilon \times T$ for bulk-EG as well as for all the

AP/EG samples with different thermal history (cf. Table 5.1). Besides the gradual decrease of the (average) relaxation strength with increasing annealing temperature, a marked change in the temperature dependence of $\Delta\varepsilon \times T$, viz. from a *decrease* (for bulk-EG) to an *increase* with increasing temperature can be recognised. Whereas the decrease in $\Delta\varepsilon \times T$ with increasing T is a known property of glass forming liquids, due to gradual loss in cooperativity of the α-relaxation [27], the opposite behaviour is usually found for secondary relaxations and other thermally activated relaxation processes [28]. Consequently, the qualitative change in the slope $\mathrm{d}(\Delta\varepsilon \times T)/\mathrm{d}T$, according to Figure 5.7, is in agreement with the change from VFT to Arrhenius behaviour, caused by increased confinement of the dispersed EG phase.

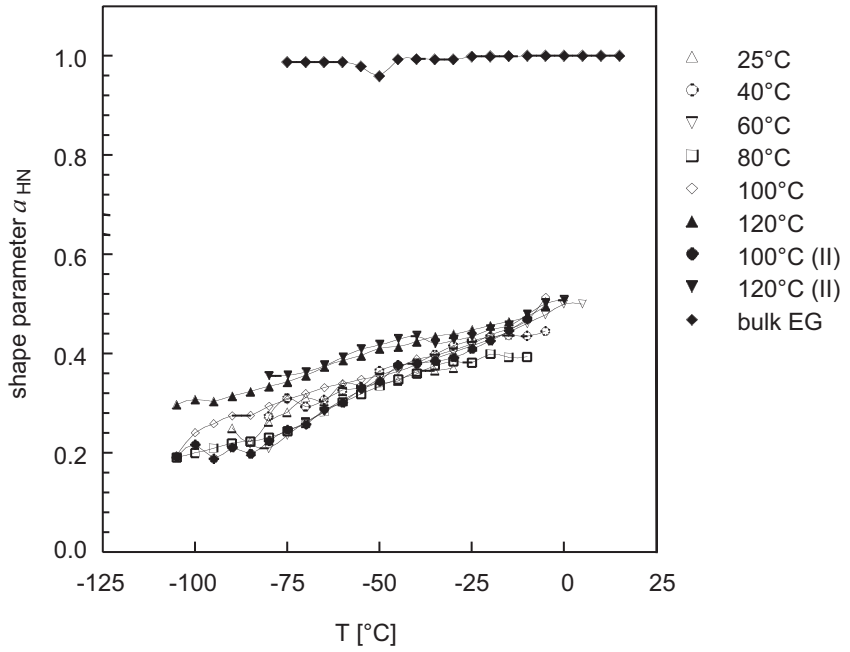

Figure 5.8 Shape parameter a_{HN} vs temperature for the α_{EG} process in bulk-EG and in AP/EG after different thermal treatments.

In contrast to the relaxation strength, the shape of the loss peak of the α_{EG} process is quite different between AP/EG samples and bulk-EG. This is expressed by the shape parameter a_{HN}, describing the low-frequency slope of the spectra $\log(\varepsilon'')$ vs $\log(f)$ (cf. Figure 5.8). However, a_{HN} appears to be insensitive to the thermal history and thus the morphology of the AP/EG samples. Obviously, the degree of confinement, as manifested in the mean relaxation times $\tau(T)$ (cf. Figures 5.5 and 5.6), plays a minor role in the broadening of the α_{EG} peak. Therefore, it is suggested that the tremendous

broadening reflects the (bulk) dynamics of the dispersed EG fraction modified by dissolved AP molecules or chain segments, rather than the influence of surface anchoring of EG molecules as studied by other authors [29].

The reduction of the final droplet size to far below the µm-range was also clear from the optical appearance of the AP/EG samples, which changed from white (light scattering) to transparent upon annealing. This finding was corroborated by results from scanning electron microscopy (SEM) experiments, shown in Figure 5.9a,b.

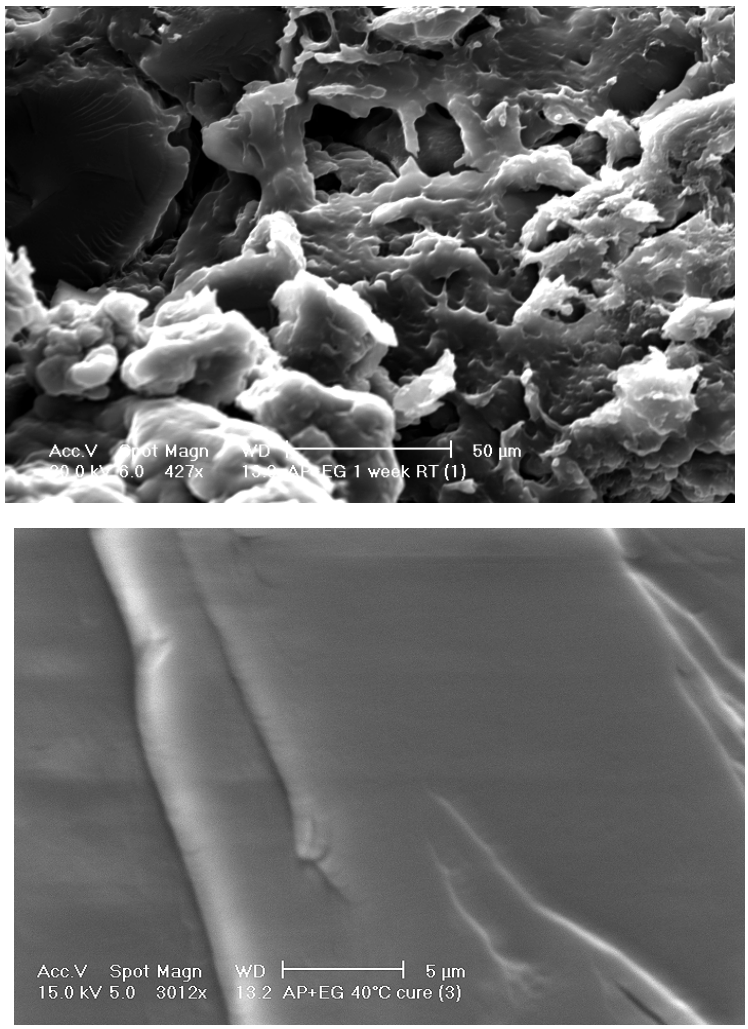

9a

9b

Figure 5.9 SEM photographs of two AP/EG samples with different thermal histories: (9a) after storage at room temperature for 1 week, and (9b) after 40°C annealing and subsequent storage at room temperature for 4 weeks.

Whereas a microporous morphology with a characteristic size of a few µm remains present after short storage at room temperature, no structural details could be detected anymore in a sample that was exposed to 40°C and subsequently stored for 4 weeks.

Breaking the latter resulted in very smooth fracture surfaces as is demonstrated in Figure 5.9b. A strong hint that EG is still present in a dispersed phase at a size inaccessible to SEM was noticed by the observation that higher e-beam radiation power resulted in strong plastic deformation and finally bursting of the heated area, most likely caused by the evaporation of EG.

Conclusions

The structure evolution of amylopectin/ethylene glycol mixtures was studied with dielectric relaxation spectroscopy. Both long-time storage at room temperature and annealing at elevated temperatures provoked a significant rise of the dynamic glass transition (T_g increase) of the initially 'plasticised' AP phase. Results from samples with a different thermal history imply the validity of the time-temperature equivalence for structure formation kinetics.

A detailed analysis of the VFT temperature dependence of the relaxation time of the dynamic glass transition process of AP (α_{AP}) indicated that AP/EG mixtures behave like strong glasses, which points to a low degree of dynamic coupling between different AP chains. From this finding we conclude that upon time/temperature treatment chain stiffening and *interchain* decoupling of AP chain segments is promoted by H-bonded EG molecules.

The increase in T_g of AP was accompanied by a continuous reduction of the EG droplet size, resulting in nanometer size droplets in which about 20% of the initial amount of EG concentrates. In such a small geometry ethylene glycol becomes dynamically confined, which results in a transition of the α_{EG} dynamics from VFT towards a genuine Arrhenius behaviour. This confinement effect is accompanied by a general delay in the dynamics of dispersed EG, due to interaction of EG molecules with partially dissolved AP chains in the EG-rich phase. These results are in agreement with previously reported data on the interaction between starch polysaccharides and glycerol or ethylene glycol, which showed that time as well as heat strongly immobilise the plasticiser [12,13].

Confinement effects on the glass transition dynamics of EG in polymer dispersed nanodroplets have not been reported previously. Furthermore, the results lead to new insights in the influence of polyols on the molecular organisation in starch. Interactions between starch and glycerol, ethylene glycol, or other plasticisers, and especially the formation of a structure preventing *interchain* H-bonding between AP-

chain segments, reduces starch recrystallisation/retrogradation. This may improve the control of the mechanical properties of the products and expand the use of starches for various applications.

References

1. M. Gudmundsson, 'Retrogradation of starch and the role of its components', *Thermochim. Acta*. **246** (1994), p 329-341,
2. J.J.G. van Soest and D.B. Borger, 'Structure and properties of compression molded thermoplastic starch materials from normal and high amylose maize starches', *J. Appl. Polym. Sci*. **64** (1997), p 631-644,
3. R.N. Tharanathan, 'Starch - the polysaccharide of high abundance and usefulness', *J. Sci. Ind. Res*. **54** (1995), p 452-458,
4. J.J.G. van Soest, S.H.D. Hulleman, D. de Wit and J.F.G. Vliegenthart, 'Changes in the mechanical properties of thermoplastic potato starch in relation with changes in B-type crystallinity', *Carboh. Polym*. **29** (1996), p 225-232,
5. H.J. Thiewes, P.A.M. Steeneken, 'The glass transition and the sub-T_g endotherm of amorphous and native potato starch at low moisture content', *Carboh. Polym.* **32** (1997), p 123-130.
6. N. Krog, S.K. Oleson, H. Toernaes, T. Joensson, 'Retrogradation of the starch fraction in wheat bread', *Cereal Foods World* **34** (1989), p 281-285,
7. K. Kohyama, K. Nishinari, 'Effect of soluble sugars on gelatinization and retrogradation of sweet potato starch', *J. Agric. Food. Chem.* **39** (1991), p 1406-1410,
8. K. Katsuta, M. Miura, A. Nishimura, 'Kinetic treatment for rheological properties and effects of saccharides on retrogradation of rice starch gels', *Food Hydrocoll.* **6** (1992), p 187-198,
9. K. Katsuta, A. Nishimura, M. Miura, 'Effects of saccharides on stabilities of rice starch gels: 1. Monosaccharides and disaccharides', *Food Hydrocoll.* **6** (1992), p 387-398,
10. L.A. Bello-Pérez, O. Parades-López, 'Effects of solutes on retrogradation of stored starches and amylopectins: a calorimetric study', *Starch/Stärke* **47** (1995), p 83-86,
11. J.J.G. van Soest, D. de Wit, H. Tournois, J.F.G. Vliegenthart, 'The influence of glycerol on structural changes in waxy maize starch as studied by FT-IR spectroscopy', *Polymer* **35** (1994), p 4722-4727,
12. A.L.M. Smits, S.H.D. Hulleman, J.J.G. van Soest, H. Feil, J.F.G. Vliegenthart, 'The influence of polyols on the molecular organisation in starch-based plastics', *Polym. Adv. Technol.* **10** (1999), p 570-573,
13. P.H. Kruiskamp, A.L.M. Smits, J.J.G. van Soest, J.F.G. Vliegenthart, 'The influence of plasticiser on the molecular organisation in dry amylopectin measured by DSC and solid state NMR spectroscopy', *Ind. Microbiol. & Biotechn.* **26** (2001), p 90-93,
14. S. Ikeda, H. Kumagai, K. Nakamura, 'Dielectric analysis of food polysaccharides in aqueous solution', *Carboh. Res.* **301** (1997), p 51-59,
15. H. Montès, J.Y. Cavaillé, 'Secondary dielectric relaxations in dried amorphous cellulose and dextran', *Polymer* **40** (1999), p 2649-2657,
16. M.F. Butler, R.E. Cameron, 'A study of the molecular relaxations in solid starch using dielectric spectroscopy', *Polymer* **41** (2000), p 2249-2263,
17. D. Lourdin, S.G. Ring, P. Colonna, 'Study of plasticizer-oligomer and plasticizer-polymer interactions by dielectric analysis: maltose-glycerol and amylose-glycerol-water systems', *Carboh. Res.* **306** (1998), p 551-558,
18. I.J.A. Mertens, M. Wübbenhorst, W.D. Oosterbaan, L.W. Jenneskens, J. van Turnhout, 'Novel polymer electrolytes based on amorphous poly(ether-ester)s containing 1,4,7-trioxanonyl main chain units. Ionic conductivity versus polymer chain mobility', *Macromolecules* **32** (1999), p 3314-3324,

19. M. Wübbenhorst, E. van Koten, J. Jansen, W. Mijs, J. van Turnhout, 'Dielectric relaxation spectroscopy of amorphous and liquid-crystalline side-chain polycarbonates', *Macromol. Rapid Commun.* **18** (1997), p 139-147,
20. M. Wübbenhorst, J. van Turnhout, ' "Conduction-free" dielectric loss – A powerful tool for the analysis of strong (ion) conducting dielectric materials', *Dielectrics Newsletter*, Novocontrol GmbH, **14** (2000), p 1-3,
21. C.A. Angell, 'Spectroscopy, simulation, and the medium range order problem in glass', *J. Non-Cryst. Solids* **73**, (1985), p 1,
22. R. Böhmer, K.L. Ngai, C.A. Angell, D.J. Plazek, 'Nonexponential relaxations in strong and fragile glass formers', *J. Chem. Phys.* **99** (1993), p 4201-4209,
23. R. Richert, C.A. Angell, 'Dynamics of glass forming liquids. V. On the link between molecular dynamics and configurational entropy', *J. Chem. Phys.* **108** (1998), p 9016-9026,
24. M. Arndt, R. Stannarius, H. Groothues, E. Hempel, F. Kremer, 'Length scale of cooperativity in the dynamic glass transition', *Phys. Rev. Lett.* **79** (1997), p 2077-2080,
25. A. Huwe, F. Kremer, P. Behrens, W. Schwieger, 'Molecular dynamics in confining space: from the single molecule to the liquid state', *Phys. Rev. Lett.* **82** (1999), p 2338-2341,
26. E. Donth, 'The size of cooperatively rearranging regions at the glass transition', *J. Non-Cryst. Solids* **53** (1982), p 325-330,
27. A. Schönhals, F. Kremer, A. Hofmann, E.W. Fischer, E. Schlosser, 'Anomalies in the scaling of the dielectric alpha-relaxation', *Phys. Rev. Lett.* **70** (1993), p 3459-3462,
28. E. Schlosser, A. Schönhals, H.E. Carius, H. Goering, 'Evaluation method of temperature-dependent relaxation behavior of polymers', *Macromolecules* **26** (1993), p 6027-6032,
29. W. Gorbatschow, M. Arndt, R. Stannarius, F. Kremer, 'Dynamics of H-bonded liquids confined to nanopores', *Europhys. Lett.* **35** (1996), p 719-724.

Chapter 6

Interaction between Dry Amylopectin and Ethylene Glycol or Glycerol, Measured by ^{13}C Inverse Recovery Cross Polarisation NMR Spectroscopy

A.L.M. Smits, P.H. Kruiskamp, J.J.G. van Soest, J.F.G. Vliegenthart

[Submitted to be published]

Abstract

The interaction between dry amylopectin and ethylene glycol or glycerol is studied with Inverse Recover Cross Polarisation solid state NMR spectroscopy, for examining the mobility within the system. Upon storage at room temperature for a period of days up to months, the interaction developed. The plasticiser mobility decreased, for ethylene glycol as well as for glycerol, and the amylopectin carbon C6 mobility increased. The mobility of the other amylopectin carbons generally did not change, which means that the interaction mainly occurs at carbon C6. This is a new insight on how starch-plasticiser interactions take place on a molecular level.

Upon heating, the interaction develops fast, after which crystal perfection is suggested to take place during storage at room temperature. Ethylene glycol as well as glycerol mobilise the amylopectin chains. For ethylene glycol, the amylopectin mobility remains even 16 months after heat treatment. For glycerol, however, 16 months after heat treatment amylopectin has immobilised again. It is proposed that the small ethylene glycol molecules, which can easily penetrate the ordered amylopectin chains, prevent the amylopectin chains from becoming immobilised. The larger glycerol molecules are hindered in penetrating the crystal structure of amylopectin and primarily interact at the edges of the crystalline lamellae. Therefore, they are unable to prevent immobilisation of the amylopectin chains.

Introduction

Biopolymers such as starch have been studied as replacements of synthetic polymers, for environmental and cost-related reasons. Starch can be processed into thermoplastic materials using thermal and mechanical forces. Water and polyol plasticisers, such as glycerol or ethylene glycol, are added to enable melting below the decomposition temperature. During storage of these thermoplastic materials, retrogradation and recrystallisation occur. Some plasticisers are known to reduce these ageing processes. To understand this influence of plasticisers, it is important to investigate their interactions with starch.

Previously, it was reported that the interaction between dry starch polysaccharides and the plasticisers ethylene glycol or glycerol could be observed with ^{13}C solid state CP/MAS and HP/DEC NMR spectroscopy [1-3]. Upon heating, a fast interaction took place. During storage at room temperature the interaction proceeded dependent on starch crystallinity and plasticiser mobility. The plasticiser was partly immobilised by the interaction and appeared in the CP/MAS spectra, while the HP/DEC signal decreased and broadened.

In the present study, the interactions between dry amylopectin and the plasticisers ethylene glycol or glycerol are further investigated, using ^{13}C solid state Inverse Recovery Cross Polarisation (IRCP) NMR spectroscopy. With this method it is fairly straightforward to visualise differences in the dynamics of the carbon atoms. It is a relatively simple technique that proves to be valuable for investigating starch-plasticiser interactions.

Experimental

Sample preparation

Amylopectin obtained from granular potato starch, with a remainder of 5% amylose (Amylopectin-UG) was provided by Avebe (Foxhol, the Netherlands). Glycerol (≤0.1% H_2O) was obtained by Fluka (Neu-Ulm, Germany) and ethylene glycol (≤0.05% H_2O) by Acros (Geel, Belgium).

The crystalline amylopectin was dried under reduced pressure in a vacuum-oven at 70°C. The dried material (<3% H_2O) was mixed manually under a nitrogen gas flow with glycerol or ethylene glycol. The plasticiser concentration was 4.3 mmol plasticiser/g amylopectin, corresponding to 28.6 wt% for glycerol and 21.3 wt% for

ethylene glycol. The samples were stored airtight. The samples are analysed directly after mixing, and during storage at room temperature, while the interaction develops. Alternatively, the interaction is enforced by heat treatment, after which the samples are examined. Samples exposed to heat treatment were heated for 30 min at 165°C in a small, airtight container.

Analyses

Solid state ^{13}C NMR spectra were collected on a Bruker AMX 400 spectrometer operating at 100.63 MHz. Samples were spun at the magic angle (54.7°) with respect to the static magnetic field. Carbon chemical shifts relative to tetramethylsilane (TMS) were determined from the spectra, using solid glycine at room temperature as external reference. Samples were packed into 7-mm ceramic rotors and spun at 4 kHz. In ^{13}C cross-polarisation magic angle spinning (CP/MAS) experiments the cross polarisation time was set to 500 μs.

In the IRCP pulse sequence [4], a relatively long cross polarisation period of 5 ms is used, in order to maximise the polarisation of the ^{13}C nuclei, followed by a phase inversion pulse. The dynamics of inversion is similar to the polarisation dynamics in a standard CP sequence, and is therefore strongly dependent on the ^{13}C-^{1}H dipolar coupling. Consequently, the inversion recovery sequence is very sensitive to the local proton environment and to molecular motion [5]. By using a variable inversion time of 10 μs-10 ms, the evolution of magnetisation of the CH_n groups is obtained. The magnetisation starts with an optimum value, and decreases with increasing inversion time.

Two different models can be used to describe the spin dynamics associated with the IRCP method [6-9]. The first model is used for systems with a small dipolar coupling such as non-protonated groups or systems with an important molecular motion (type I magnetisation). In this model the magnetisation can be described by a single exponential decrease. The second model describes systems with a strong heteronuclear dipolar coupling, like rigid CH_n groups (type II magnetisation). The magnetisation can be described, at least for the first ms of inversion time, by a more complex equation. The cross polarisation is not a single exponential process, but involves two processes with different time scales. The magnetisation decreases

rapidly in the first tens of microseconds (up to ~50 µs), and then reaches the minimum value more slowly. The IRCP method is widely used for spectral editing, in which signals are subsequently nulled using different inversion times [6,7,9-11]. Another application is to distinguish between mobile and immobile domains or functional groups in solids [12-14], and to explore local intra- and intermolecular dipolar interactions [4,8].

In all NMR experiments, ^{13}C CP/MAS, high power decoupling (HP/DEC), and IRCP, the recycle delay was set to 4 s [15].

Results and Discussion

Ethylene glycol interaction during storage at room temperature

IRCP NMR experiments are performed on freshly mixed amylopectin and ethylene glycol. The integral values of the ^{13}C peaks as a function of the phase inversion time at day 1 are shown in Figure 6.1.

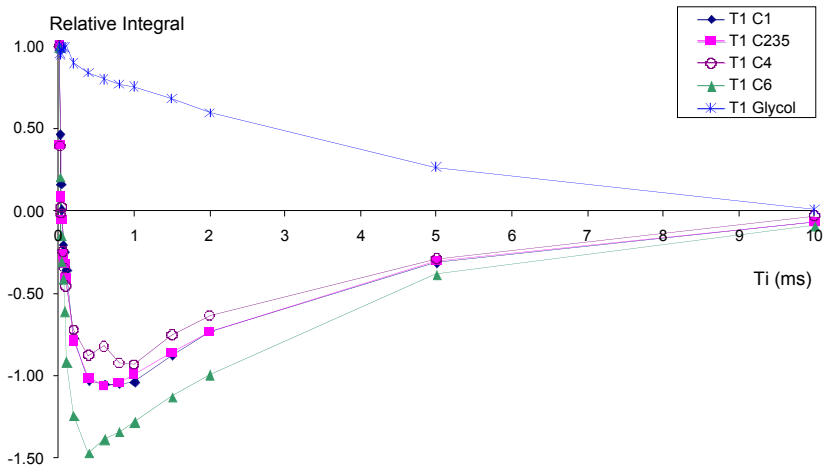

Figure 6.1 Relative integral values of the ^{13}C IRCP NMR signals of freshly mixed amylopectin with ethylene glycol as a function of the phase inversion time.

The behaviour of the magnetisation of ethylene glycol with increasing inversion time is very different from amylopectin. The ethylene glycol carbon shows a behaviour consistent with a model exhibiting a small dipolar coupling, like systems with an important molecular motion (type I). The amylopectin carbons show a behaviour consistent with a model of strong heteronuclear coupling, like rigid CH_n groups (type II). This has to be expected, since ethylene glycol is highly mobile in the fresh

mixture, while the solid amylopectin is rigid. Since carbon C6 has two directly bound protons, in contrast to the other amylopectin carbons that only have one proton, the C6 curve is steeper and has a deeper minimum value (in agreement with Bonhomme *et al.* [11]).

The mixture is followed with IRCP for 14 days. Within this period, the ethylene glycol-amylopectin interaction has reached equilibrium. Differential Scanning Calorimetry (DSC) measurements previously showed that less than 10% of the interaction enthalpy is observed after one day of storage, and less than 5% after four days [1]. The integral values of the signals of the ring carbons of amylopectin (C1, C2/C3/C5 and C4) show no significant change in 14 days. For ethylene glycol and amylopectin C6 the development of the curves during storage is depicted in Figure 6.2. The ethylene glycol curve, although still showing behaviour of a mobile system, has changed gradually during the 14 days of storage. It appears that the curve has become a mixture of type I and type II magnetisation. This can be explained by considering that ethylene glycol is immobilised during the interaction with amylopectin, as was previously observed with ^{13}C CP/MAS and HP/DEC NMR spectroscopy [1-3]. The amylopectin C6 curve has also changed considerably, its minimum value being increased from –1.5 to –0.8. This demonstrates that C6 is involved in the interaction process. While the change of the ethylene glycol curve is rather gradual, for C6 the change mainly takes place within 1 day.

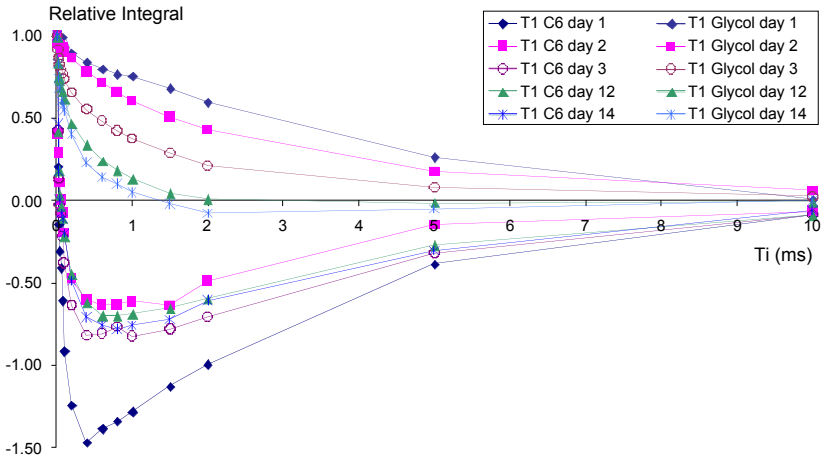

Figure 6.2 Development of the IRCP curves during storage, for amylopectin carbon C6 and for ethylene glycol.

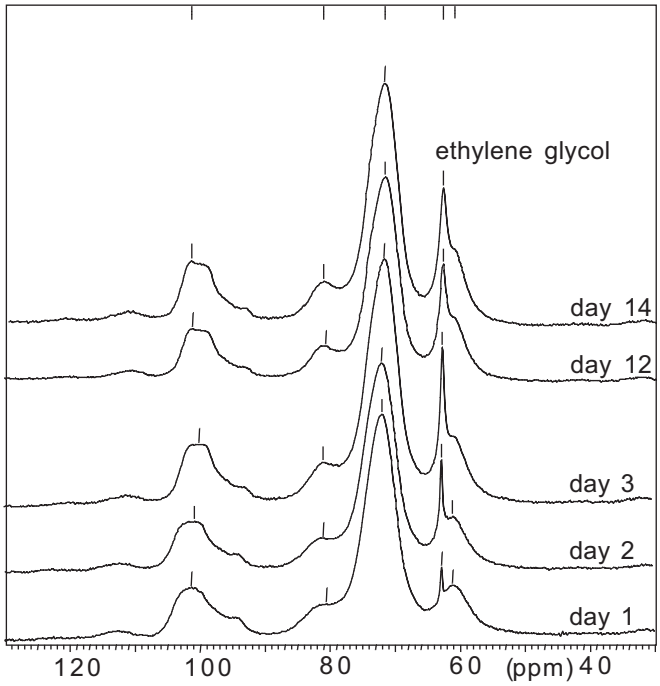

Figure 6.3 CP/MAS NMR spectra of amylopectin with ethylene glycol during storage at room temperature at days 1, 2, 3, 12, and 14.

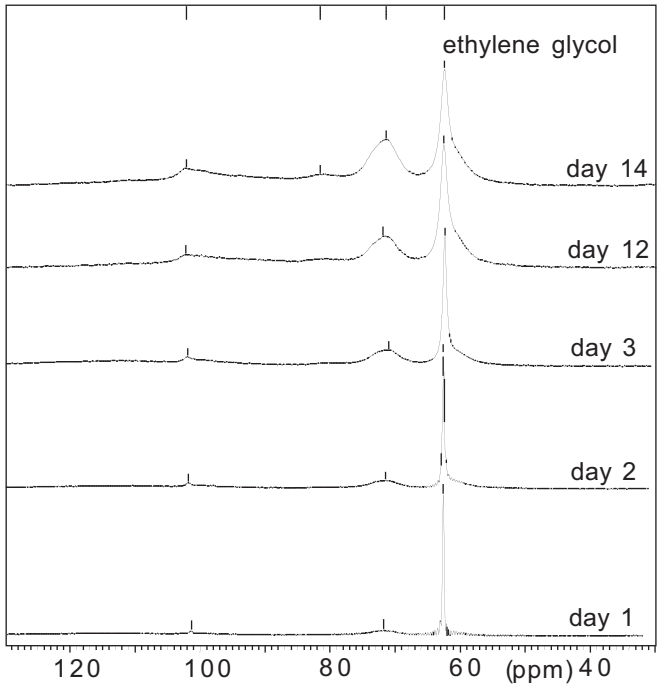

Figure 6.4 HP/DEC NMR spectra of amylopectin with ethylene glycol during storage at room temperature at days 1, 2, 3, 12, and 14.

CP/MAS and HP/DEC spectra were also recorded of these samples during storage at room temperature (Figures 6.3 and 6.4). The CP/MAS spectra show that ethylene glycol is immobilised during the first 3 days. After 12 days, the signal has broadened, indicating that the interaction has become less ordered. In the HP/DEC spectra, the ethylene glycol signal has become broader during storage. An increase of the amylopectin signals is observed during storage, indicating a mobilisation of amylopectin caused by the interaction with ethylene glycol. Although the interaction between ethylene glycol and amylopectin has reached equilibrium in a few days, some molecular rearrangements (crystal perfection) proceed in a secondary process, as was shown earlier [1].

Glycerol interaction during storage at room temperature

For freshly mixed glycerol and amylopectin the IRCP curves of the amylopectin carbons are similar to those of freshly mixed ethylene glycol and amylopectin (Figure 6.5). The signal at 71 ppm of the central carbon of glycerol overlaps largely with the amylopectin C2/C3/C5 signal, making it impossible to integrate this peak. The IRCP curve of the glycerol signal at 63.3 ppm is a little steeper than that of ethylene glycol in the previous paragraph, indicating that glycerol is somewhat less mobile. As was found for the interaction of amylopectin with ethylene glycol, the curves of amylopectin C1, C2/C3/C5 and C4 do not change during storage.

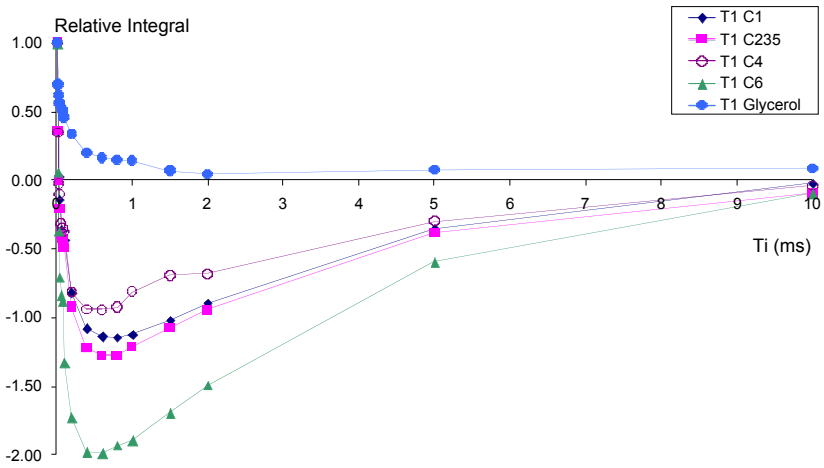

Figure 6.5 Relative integral values of the ^{13}C IRCP NMR signals of freshly mixed amylopectin and glycerol as a function of the phase inversion time. For glycerol, the signal of the terminal carbon atoms is depicted.

The development of the curves of amylopectin C6 and of the terminal glycerol carbon atoms during storage at room temperature is depicted in Figure 6.6. There is hardly any change in the glycerol curve during 25 days of storage. It seems that the mobility is slightly increased at day 2, after which it remains stable. It may be that glycerol was temporarily somewhat restrained during the physical mixing process. The curve of the amylopectin C6 does change significantly during storage, but not as quickly as with ethylene glycol. Its minimum value increased gradually from –2.0 to –1.4 during the first 25 days. This more gradual change is in agreement with the fact that glycerol does not interact with amylopectin as fast as ethylene glycol does, in line with previous findings [1-3].

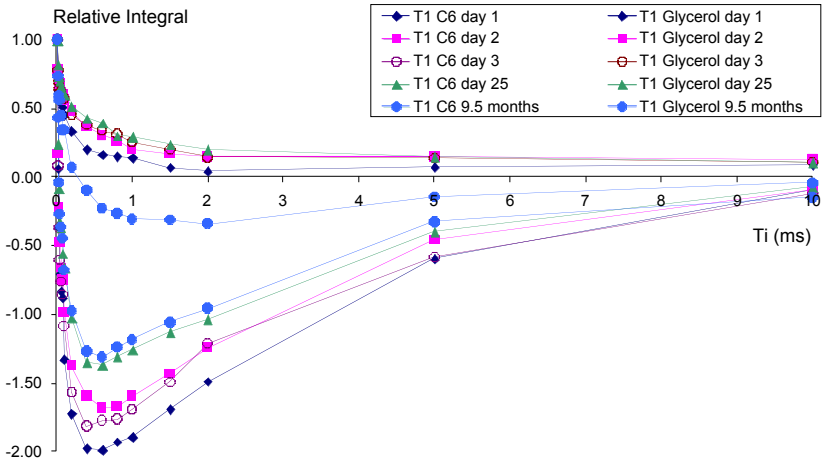

Figure 6.6 Development of the IRCP curves during storage, for amylopectin carbon C6 and for the terminal glycerol carbon atoms.

After 25 days of storage, the HP/DEC and CP/MAS spectra show that only a small part of the glycerol has interacted with amylopectin (Figure 6.7). Just a small glycerol signal is observed in CP/MAS, and in HP/DEC there is a slight broadening of the glycerol signals. After several months, the IRCP experiment shows a considerable immobilisation of glycerol, while the C6 curve does not change remarkably. The HP/DEC spectrum after 9 months of storage at room temperature confirms the immobilisation of glycerol as observed with IRCP.

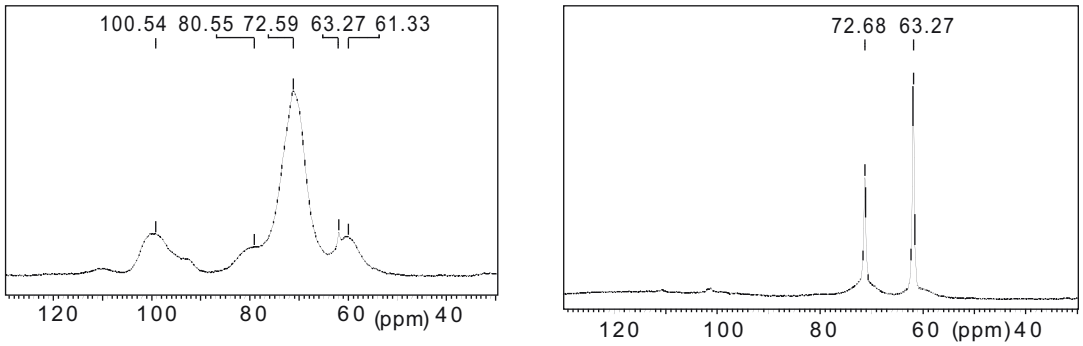

Figure 6.7 Solid state CP/MAS (left) and HP/DEC (right) NMR spectra of amylopectin with glycerol, after storing 25 days at room temperature.

Ethylene glycol interaction after heat treatment

Samples were heated to accomplish the interaction between amylopectin and ethylene glycol. The integral values of the ^{13}C peaks as a function of the phase inversion time of the amylopectin/ethylene glycol samples, measured a few hours after heat treatment, are given in Figure 6.8. The amylopectin curves are much shallower than those observed for the mixtures stored at room temperature, with a minimum value of about –0.25.

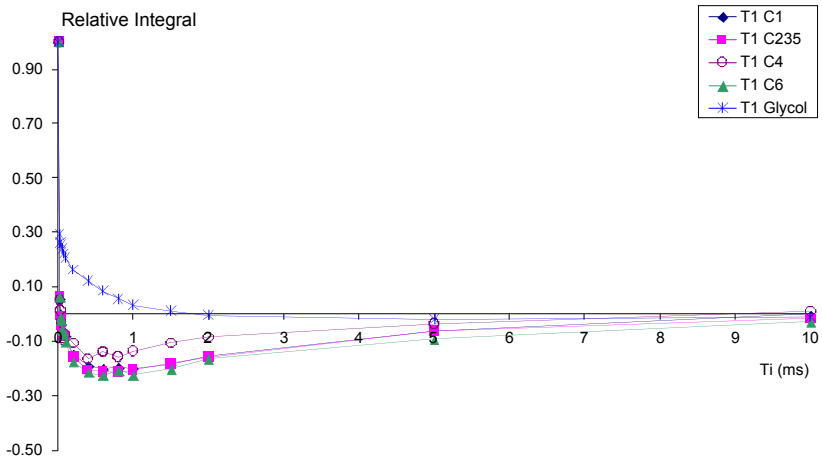

Figure 6.8 Relative integral of the ^{13}C IRCP NMR signals of amylopectin and ethylene glycol as a function of the phase inversion time, several hours after heating for 30 min at 165°C.

The HP/DEC spectra of the heated amylopectin/ethylene glycol samples are depicted in Figure 6.9. A few hours after heat treatment the ethylene glycol signal is less intense and broader than that of a sample before heating. The mobility of amylopectin as detected with HP/DEC is similar to that of the sample stored for 12 days at room temperature. The IRCP curves of these samples are not similar at all, though. Because the IRCP measurements are done with a large cross polarisation time, in order to obtain maximum magnetisation, only the mobility of relatively rigid regions is measured. It might be that during heat treatment a dislocation of the CH_n groups of amylopectin has taken place due to the interaction with ethylene glycol.

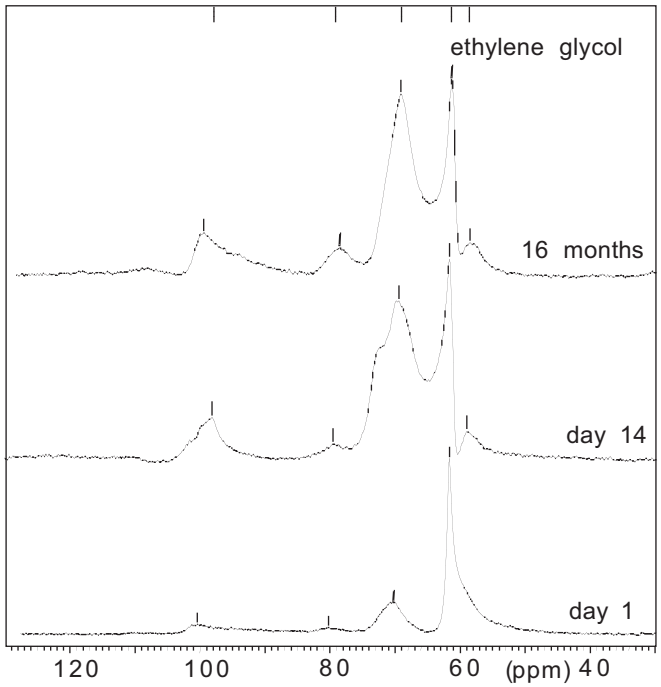

Figure 6.9 HP/DEC NMR spectra of amylopectin with ethylene glycol after heating for 30 min at 165°C, after a few hours (day 1), 13 days, and 16 months.

The IRCP curves of the integral values measured 14 days after heat treatment (Figure 6.10), are similar to those after 14 days of storage at room temperature. At day 14 after heat treatment the amylopectin HP/DEC signals have become eminent, implying that amylopectin has become significantly mobile. After 16 months, no significant changes in the IRCP curves are detected compared to the measurement at day 14 after heat treatment. Apparently the process caused by heating the sample is not finished directly after heating, but takes up to 14 days. Since the interaction between amylopectin and ethylene glycol has reached equilibrium during the heating

process [1], another process appears to take place afterwards. This may very well be crystal perfection leading to alignment of the amylopectin helices, as proposed by Perry *et al.* [16], that is enabled because the interaction causes mobilisation of the amylopectin chains [1]. The amylopectin mobility as observed with HP/DEC remains even 16 months after heat treatment. This remaining mobility after the suggested crystal perfection might be explained, considering that the small ethylene glycol molecules can easily penetrate the amylopectin structure, even if the chains are highly ordered [1]. Possibly these ethylene glycol molecules prevent the amylopectin chains from becoming immobilised, due to ageing.

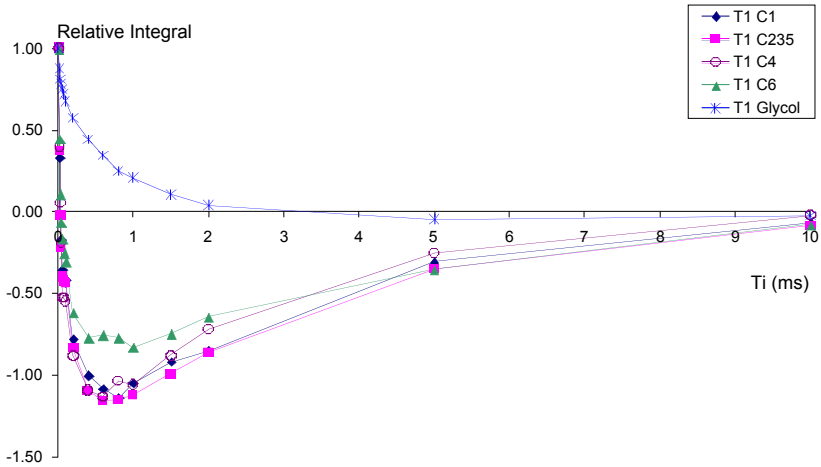

Figure 6.10 Relative integral of the ^{13}C IRCP NMR signals of amylopectin and ethylene glycol as a function of the phase inversion time, 14 days after heating for 30 min at 165°C.

Glycerol interaction after heat treatment

Mixtures of amylopectin and glycerol were subjected to heat treatment in order to accomplish the interaction between amylopectin and glycerol. The IRCP curves, measured one day after heating the sample are given in Figure 6.11. The results are similar to the IRCP curves of amylopectin with ethylene glycol, measured directly after heating, although the amylopectin curves are even shallower. The minimum value of the amylopectin curves is about –0.1. The HP/DEC spectra of the heated amylopectin/glycerol samples are depicted in Figure 6.12. Due to the heat treatment, the intensity of the signal of the terminal glycerol carbon atoms is reduced and glycerol is immobilised considerably.

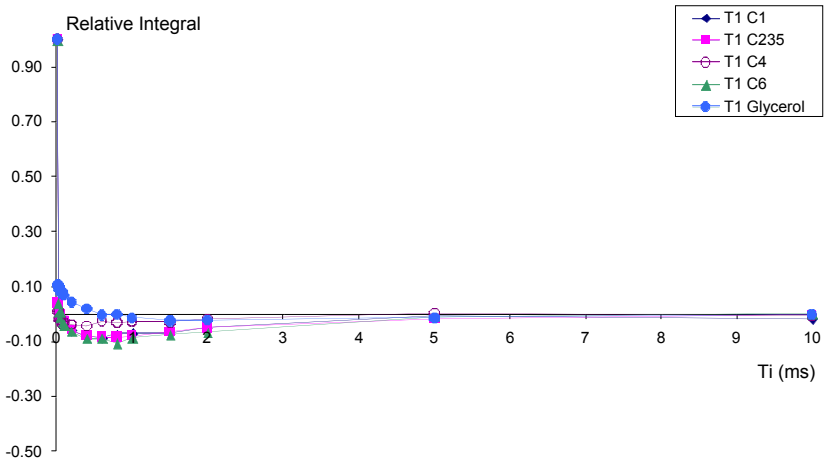

Figure 6.11 Relative integral of the ^{13}C IRCP NMR signals of amylopectin and glycerol as a function of the phase inversion time, 1 day after heating for 30 min at 165°C.

At day 15 after heat treatment (Figure 6.13), the IRCP curves of amylopectin are less shallow, but still not as deep as was observed during storage at room temperature. Apparently, due to glycerol, the process of crystal perfection [1,16], induced by heat treatment, is slower than with ethylene glycol as plasticiser. The IRCP curve of the signal of the terminal glycerol carbon atoms does show significant immobilisation. At day 15 after heat treatment, the HP/DEC signals of amylopectin are clearly visible, indicating that amylopectin has become mobile.

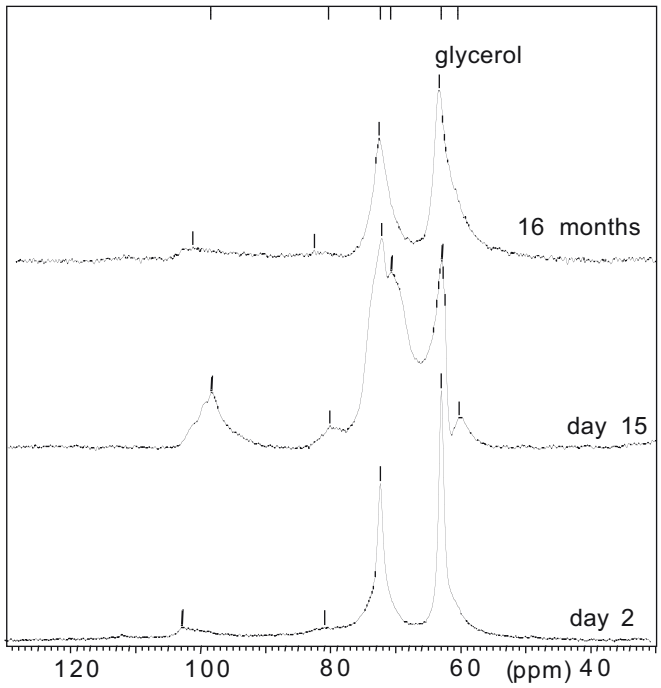

Figure 6.12 HP/DEC NMR spectra of amylopectin with glycerol after heating for 30 min at 165°C, after 1 day, 14 days, and 16 months.

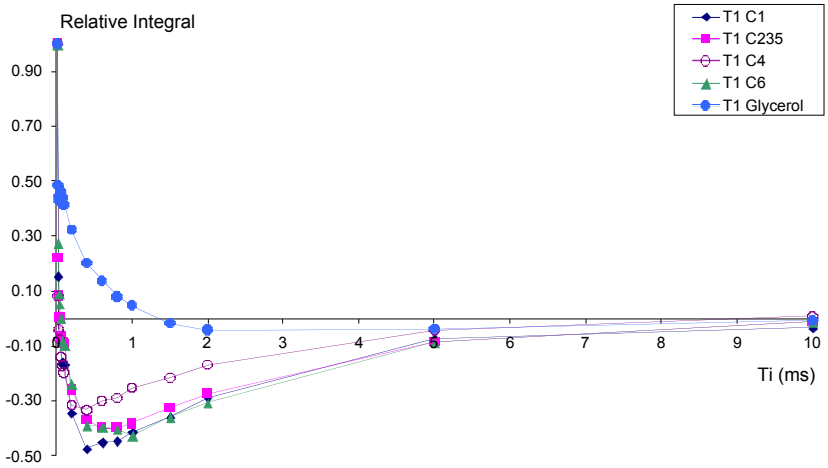

Figure 6.13 Relative integral of the ^{13}C IRCP NMR signals of amylopectin and the terminal glycerol carbon atoms as a function of the phase inversion time, at day 15 after heating for 30 min at 165°C.

In Figure 6.14 the IRCP measurement 16 months after heating is depicted, which shows that the C6 curve has become relatively shallow compared to the other amylopectin curves, similar to C6 of the amylopectin/ethylene glycol mixture after storage or heat treatment. However, the C4 curve has also undergone a significant change. Its minimum has changed from –1.0 before heat treatment to –2.1 at 16 months after heat treatment. In contrast to the mixture of amylopectin with ethylene glycol, the HP/DEC spectrum 16 months after heat treatment shows that the mobility of amylopectin has practically disappeared, while glycerol has regained mobility. Interestingly, now that amylopectin is again immobilised, IRCP results show that C6 still appears to be more mobile than the other amylopectin carbons, while C4 seems to be more rigid.

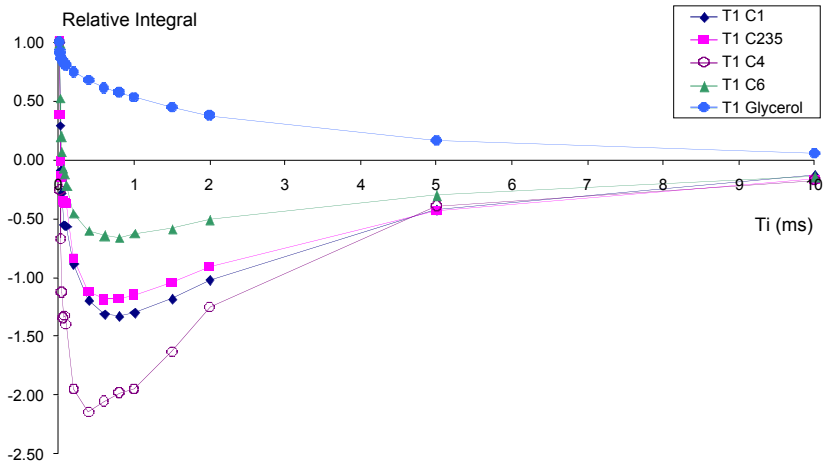

Figure 6.14 Relative integral of the ^{13}C IRCP NMR signals of amylopectin and the terminal glycerol carbon atoms as a function of the phase inversion time, 16 months after heating for 30 min at 165°C.

The CP/MAS spectra show that the immobilisation of glycerol gradually increased during storage (Figure 6.15). The CP/MAS signal became narrower 16 months after heat treatment, suggesting that the glycerol molecules that interact with amylopectin, do so in a more ordered way.

Amylopectin is initially mobilised by the interaction with glycerol, while glycerol is partly immobilised by this interaction. During continued storage after heat treatment, amylopectin is immobilised again. This is probably caused by the continuation of the process of crystal perfection [16]. Unlike ethylene glycol the larger glycerol molecules are hindered in penetrating the crystals [1]. They primarily interact at the edges of the crystalline lamellae, and are therefore unable to prevent immobilisation of the amylopectin chains.

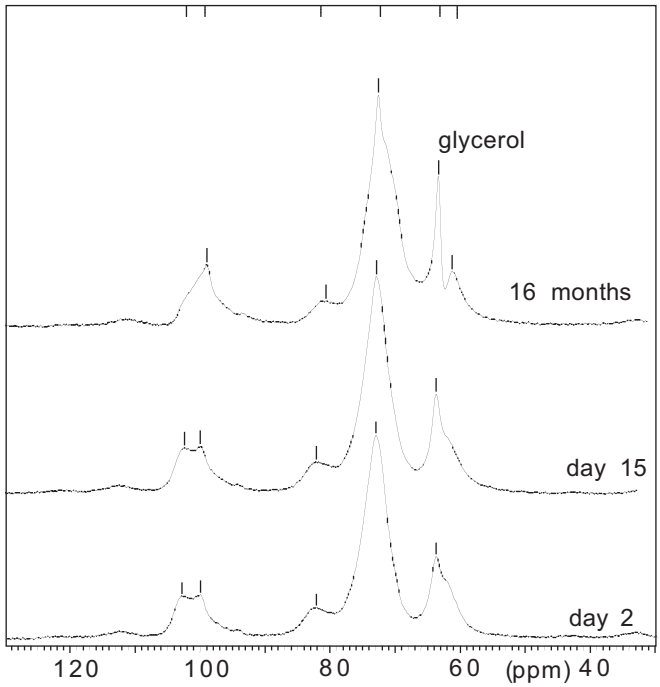

Figure 6.15 CP/MAS NMR spectra of amylopectin with glycerol after heating for 30 min at 165°C, after 1 day, 14 days, and 16 months.

Conclusions

These results show that Inverse Recovery Cross Polarisation solid state NMR spectroscopy is a useful technique for examining changes in the molecular mobility in starch systems. New insights were gained on how starch-plasticiser interactions take place on a molecular level. When the interaction between dry amylopectin and ethylene glycol or glycerol develops, the plasticiser mobility decreases and the amylopectin carbon C6 mobility increases. The mobilities of the other amylopectin carbons do not change significantly, showing that the interaction mainly occurs at

carbon C6. Chemical modification at the amylopectin carbon C6 can be used to increase the affinity to plasticiser molecules, in order to reduce starch retrogradation. Upon heating, the interaction develops fast, after which crystal perfection is suggested to take place due to this interaction. The process of crystal perfection is slower for glycerol than for ethylene glycol. Whereas the ethylene glycol molecules penetrate the crystalline structure, the larger glycerol molecules are hindered in penetrating the crystals.

When ingredients are premixed prior to processing, the resulting increase in molecular mobility of amylopectin may influence conditions such as flow properties and resistance to shear. After processing, the occurrence of crystal perfection gives the product more strength. The interactions between starch and ethylene glycol or glycerol may reduce starch retrogradation or recrystallisation, which would improve the control of the mechanical properties of the product.

References

1. A.L.M. Smits, P.H. Kruiskamp, J.J.G. van Soest, J.F.G. Vliegenthart, 'Interaction between dry starch and plasticisers glycerol or ethylene glycol, measured by DSC and solid state NMR spectroscopy', Chapter 4, to be published,
2. A.L.M. Smits, S.H.D. Hulleman, J.J.G. van Soest, H. Feil and J.F.G. Vliegenthart, 'The influence of polyols on the molecular organisation in starch-based plastics', *Polym. Adv. Technol.* **10** (1999), p 570-573,
3. P.H. Kruiskamp, A.L.M. Smits, J.J.G. van Soest, J.F.G. Vliegenthart, 'The influence of plasticiser on the molecular organisation in dry amylopectin measured by differential scanning calorimetry and solid state nuclear magnetic resonance spectroscopy', *J. Ind. Microbiol. Biotech.* **26** (2001), p 90-93,
4. F. Babonneau, J. Maquet, C. Bonhomme, R. Richter, G. Roewer, D. Bahloul, '^{29}Si and ^{13}C NMR investigation of the polysilane-to-poly(carbosilane) conversion of poly(methylchlorosilanes) using Cross-Polarization and Inversion-Recovery Cross-Polarization techniques', *Chem. Mater.* **8** (1996), p 1415-1428,
5. X. Wu, S. Zhang, 'Selective polarization inversion and depolarization of ^{13}C in cross relaxation in NMR', *Chem. Phys. Lett.* **156** (1989), p 79-81,
6. X. Wu, K.W. Zilm, 'Complete spectral editing in CP/MAS NMR', *J. Magn. Reson. A* **102** (1993), p 205-213,
7. R. Sangill, N. Rastrup-Andersen, H. Bildsøe, H.J. Jakobsen, N.C. Nielsen, 'Optimized spectral editing of ^{13}C MAS NMR spectra of rigid solids using Cross-Polarization methods', *J. Magn. Reson. A.* **107** (1994), p 67-78,
8. J. Hirschinger, M. Hervé, 'Cross-polarization dynamics and spin diffusion in some aromatic compounds', *Solid State NMR* **3** (1994), p 121-135,
9. C.Gervais, F. Babonneau, J. Maquet, C. Bonhomme, D. Massiot, E. Framery M. Vaultier, '^{15}N Cross-Polarization using the Inversion-Recovery Cross-Polarization technique and ^{11}B Magic Angle Spinning NMR studies of reference compounds containing B-N Bonds', *Magn. Reson. Chem.* **36** (1998), p 407-414,
10. X. Wu, S.T. Burns, K.W. Zilm, 'Spectral editing in CP/MAS NMR. Generating subspectra based on proton multiplicities', *J. Magn. Reson. A* **111** (1994), p 29-36,

11. C. Bonhomme, P. Tolédano, J. Maquet, J. Livage, L. Bonhomme-Coury, 'Studies of octameric vinylsilasesquioxane by carbon-13 and silicon-29 cross polarization nuclear magnetic resonance spectroscopy', *J. Chem. Soc. Dalton Trans.***7** (1997), p 1617-1626,
12. P. Tekely, J.J. Delpuech, 'Mobility and hydrogen distribution in coal as revealed by polarization inversion in high-resolution solid state ^{13}C CP/MAS NMR', *Fuel* **68** (1989), p 947-949,
13. D.G. Cory, W.M. Ritchey, 'Inversion Recovery Cross-Polarization NMR in solid semicrystalline polymers', *Macromolecules* **22** (1989), p 1611-1615,
14. C. Bonhomme, F. Babonneau, J. Maquet, J. Livage, M. Vaultier, E. Framery, 'Studies of model organic and inorganic compounds by ^{15}N CP/MAS NMR using Inversion Recovery Cross Polarization', *J. Chim. Phys.* **92** (1995), p 1881-1884,
15. M.J. Gidley, 'High-resolution solid-state NMR of food materials', *Trends in Food Sci. & Tech.* **3** (1992), p 231-236,
16. P.A. Perry and A.M. Donald, 'The role of plasticization in starch granule assembly', *Biomacromolecules* **1** (2000), p 424-432.

Chapter 7

The Influence of Various Plasticisers on the Retrogradation of (partly) Gelatinised Starch

A.L.M. Smits, P.H. Kruiskamp, J.J.G. van Soest, J.F.G. Vliegenthart

[Submitted to be published]

Abstract

Ageing of gelatinised and partly gelatinised potato starch and wheat starch were investigated in the presence of plasticisers with increasing size and number of OH groups (ethylene glycol, glycerol, threitol, xylitol, glucose, and for potato starch also maltose). The influences of these plasticisers and of granular remnants (ghosts) on recrystallisation were determined by using X-ray diffraction. Recrystallisation of potato starch samples in the presence of plasticisers resulted in crystallinity indices of ~0.5. The largest reduction in potato starch recrystallisation is found for threitol (4 OH) and xylitol (5 OH). In the plasticiser range examined, the crystallisation inducing effect of granular potato starch remnants is reduced better when the plasticiser contains more OH groups. Wheat starch recrystallises to a lesser extent than potato starch, resulting in crystallinity indices of ~0.4. The results for wheat starch do not show clear trends for the influences of plasticiser size and of ghosts. The difference in behaviour of the two starches is probably caused by wheat starch having shorter amylopectin chains. Resulting from these shorter amylopectin chains, the remaining structure in wheat starch ghosts may resemble A-type crystallinity, making it more difficult to form B-type crystals. Alternatively, the trends as found for potato starch may occur, but are less manifest for wheat starch, due to the lower total extent of recrystallisation. Solid state CP/MAS NMR spectra were obtained of the wheat starch samples containing ethylene glycol, in order to compare completely and partly gelatinised systems. The spectra were identical, confirming that the ghost structures do not influence wheat starch recrystallisation. Apparently, wheat starch ghosts do not act as nuclei for crystallisation.

Introduction

Starch based foods are processed at high water contents, leading to (partial) starch gelatinisation, and low water content products. Starch is transformed from a crystalline granular material into a system containing granular remnants, or to an amorphous paste with no structure at all. During gelatinisation, starch granules swell, while losing their crystallinity, until starch is completely dissolved. At some point, non-crystalline swollen granule-shaped structures remain, named ghosts [1]. Sugars, lipids, flavours, salt and other additives are used to improve the product perception and sometimes to control the staling process. This reduction of the retrogradation process is mainly empirical and therefore often ineffective. Plasticisers such as water and sugars are needed to enable starch destructuring during processing. Plasticisers lower the glass transition temperature of starch, which may cause the material to be above T_g at room temperature. Unfortunately, in that state retrogradation can occur, which reduces the products shelf-life. Some plasticisers reduce retrogradation as compared with equal amounts of other plasticisers, such as water. Therefore, the influence of plasticisers such as water and sugars on the recrystallisation of gelatinised starch is important for the processing and the shelf-life of starch-based foods [2-7]. Especially for new products, e.g. low-fat baked foods, insufficient insight is available into the retrogradation process. Like in foods, retrogradation influences the processing and final product properties in non-food starch based products. Starch based coatings, adhesives and plastics become brittle in the course of time because of starch retrogradation. Water and other plasticisers influence this process, glycerol for example is reducing it [8].

Changes in the molecular organisation in low water content starch-plasticiser systems during ageing, and the inhibiting effect of polyol plasticisers on the ageing process were investigated. Plasticisers were used with increasing size and number of OH groups (ethylene glycol, glycerol, threitol, xylitol, glucose, and for potato starch also maltose). Potato starch and wheat starch were fully or partly gelatinised in order to examine the influence of granular remnants on ageing.

Experimental

Sample preparation

Gelatinisation is performed in a Brabender viscometer. 41.86 g native potato starch, PN (Avebe), or 40.49 g wheat starch, WN (Amidon Haussy, Avebe), were mixed with de-ionised water to gain 350 g of a 10% dry weight starch dispersion. The 350 g mixture was poured into the Brabender and stirred at a frequency of 75 rpm, while heating from room temperature to 90°C with 2°C/min. The completely gelatinised mixture was obtained by keeping it at 90°C for 55 min. The partly gelatinised sample was prepared by stopping at the peak viscosity, which was reached for PN at 65°C and for WN after keeping it for 4 min at 90°C. The partly gelatinised samples were inspected with polarised light microscopy for the presence of ghost structures, and for the absence of granules. Granules would appear as Maltese crosses.

The gelatinised mixtures were dried under reduced pressure in a vacuum-oven for 24 h at 50°C. Plasticisers were added to the PN and WN samples in a ratio dry starch / plasticiser of 100:30 w/w. Solid plasticisers were dissolved in a small amount of water and mixed with the gel, when it was still humid. Liquid plasticisers were mixed in after drying, in order to prevent evaporation during drying. Plasticisers used were dry glycerol (Fluka), dry ethylene glycol (Acros), threitol and xylitol (Aldrich), glucose (Sigma), and maltose (Merck). Equal plasticiser weight ratios imply similar total numbers of hydroxy groups in the plasticiser. The samples were ground after freezing with liquid nitrogen and conditioned at 20°C and 90% RH. Their crystallinity was measured using X-ray diffraction.

Results for erythritol (Aldrich) are not considered, because that plasticiser did not dissolve completely. In XRD intense sharp peaks were found characteristic of crystalline sugars (linewidth <0.5°(2θ)), implying a phase-separated character. Only the dissolved part of erythritol acts as a plasticiser.

Analyses

Wide angle X-ray powder diffraction (XRD) was performed on a Philips PC-APD diffractometer in the reflection geometry in the angular range 4-40°(2θ). The CuK radiation from the anode operating at 40 kV and 50 mA was monochromised using a 15 µm Ni foil, filtering off the $CuK_{ß}$ radiation (1.39 Å) and letting through CuK_{α}

radiation (1.54 Å). The diffractometer parameters were: divergence slit 1°, receiving slit 0.2 mm and scatter slit 1°. A proportional detector was used to detect the scattered radiation. Diffractograms were baseline corrected by drawing a straight line between the intensities at 7 and 40°(2θ). The ratio of the height of the crystalline diffraction at 17.3°(2θ) and the height of the total diffraction at this angle was defined as the crystallinity index, a measure for the B-type crystallinity of the sample.

Solid state cross-polarisation magic angle spinning (CP/MAS) NMR spectra were collected on a Bruker AMX 400 spectrometer operating at 100.63 MHz for ^{13}C. Samples were spun at the magic angle (54.7°) with respect to the static magnetic field. Carbon chemical shifts relative to tetramethylsilane (TMS) were determined from the spectra, using solid glycine at room temperature as external reference. Samples were packed into 7-mm ceramic rotors and spun at 4 kHz. The cross polarisation time was set to 500 µs and the recycle delay was set to 4 s.

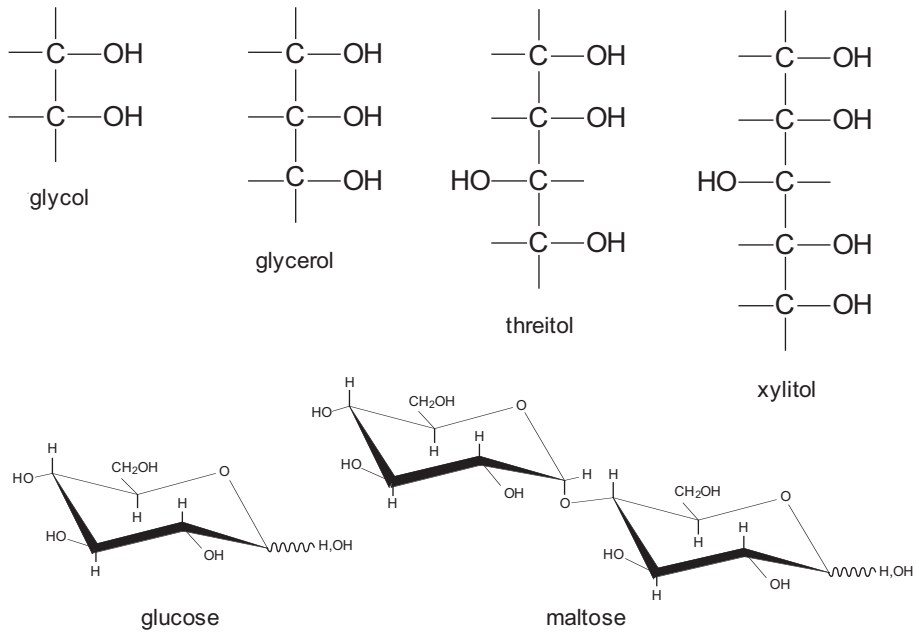

Figure 7.1 Plasticisers varying in size and in the number of OH groups.

Results and Discussion

Retrogradation was examined on fully and partly gelatinised potato and wheat starch, using a range of plasticisers with increasing size and number of OH groups (Figure 7.1) at a dry starch / plasticiser weight ratio of 100:30. Within two days of conditioning at 90% RH and 20°C, the samples are at equilibrium moisture content.

By that time most of the recrystallisation as measured by X-ray diffraction has already taken place. Therefore, focus is on the final recrystallisation. Experiments are well reproducible with a spread of ±0.01 in crystallinity index.

Less recrystallisation takes place when no plasticiser is added. This is due to the lower amount of plasticiser (including water). By consequence, the samples have a different condition with respect to their glass transition temperature. Therefore, it is only possible to compare the influence of plasticisers other than water.

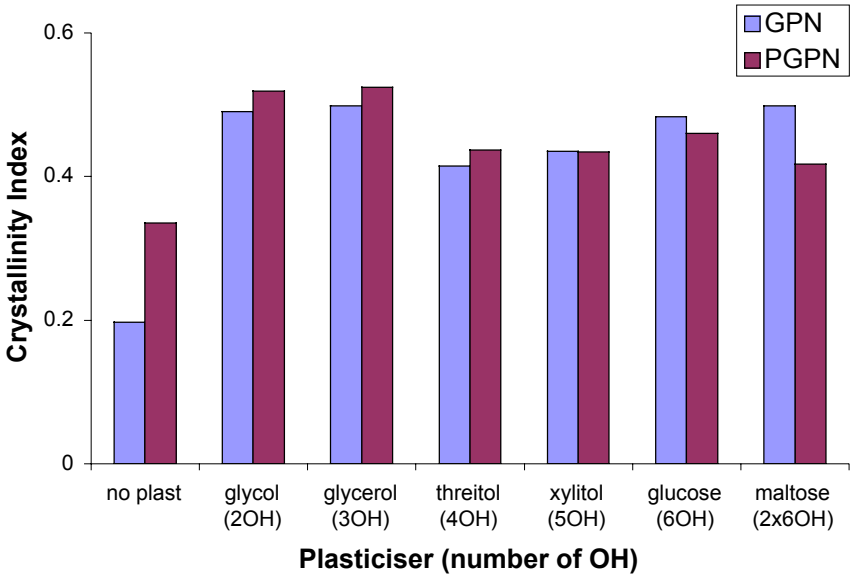

Figure 7.2 Final recrystallisation of completely (GPN) and partly gelatinised (PGPN) potato starch without added plasticiser, and with plasticisers varying in size and in number of OH groups.

Potato starch recrystallisation

As shown in Figure 7.2, the recrystallisation of (partly) gelatinised potato starch reaches a crystallinity index of ~0.5. With increasing plasticiser size, the largest reduction in recrystallisation is found for threitol (4 OH) and xylitol (5 OH). For bakery or other food industry, the use of xylitol instead of glucose would probably be too expensive for a small improvement in reducing retrogradation. In non-food products based on tuber starches (with B-type crystallinity), using threitol instead of glycerol can be interesting for reducing retrogradation. For controlled release applications of starch, the plasticiser trend is interesting because of the influence of crystallinity on the release behaviour. Crystallinity slows down release and is needed

for capsule stability, but too high crystallinity causes capsules to crack when swelling or induces micropores in the capsule, increasing release [9-11].

Fully and partly gelatinised starch systems were compared, to investigate to which extent ghosts can act as nuclei for crystallisation. For small plasticisers, up to 4 OH groups, crystallisation proceeds further for partly than for fully gelatinised potato starch samples, corresponding with crystal nucleation by ghosts. For larger plasticisers, however, more crystallisation takes place for fully than for partly gelatinised samples. The larger the number of OH groups in the plasticiser, the better the plasticiser reduces the crystallisation inducing effect of remaining ghosts. It may be, that the larger plasticisers that contain more OH groups interact with the ghost structures and obstruct interaction of the polysaccharide chains, thus preventing recrystallisation of the remaining ghost structure. The smaller, linear plasticisers are better capable of mobilising starch chains. They are therefore also capable of mobilising the remaining ghost structure, enabling crystal propagation at the ghost structures. It is clear that in both food and non-food applications of starch, granular remnants can influence starch retrogradation, the effect depending on the plasticiser used.

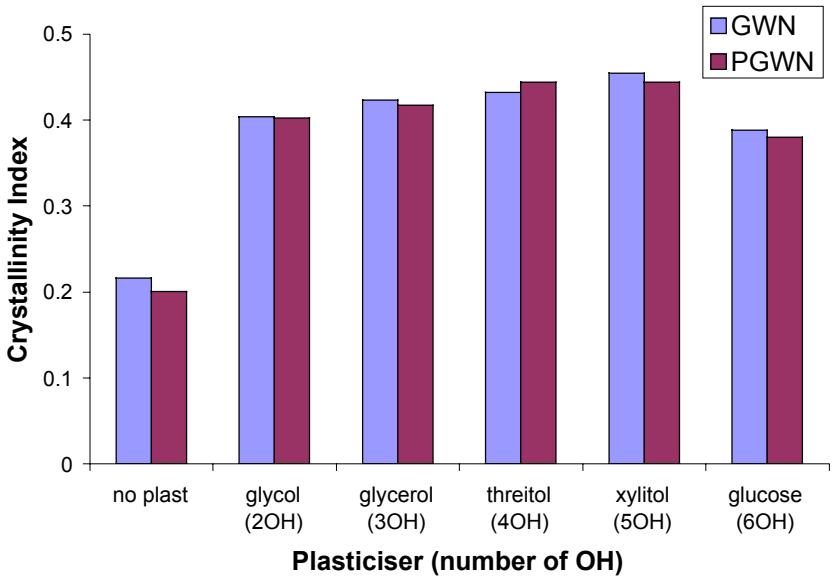

Figure 7.3 Final recrystallisation of completely (GWN) and partly gelatinised (PGWN) wheat starch without added plasticiser, and with plasticisers varying in size and in number of OH groups.

Wheat starch recrystallisation

Wheat starch recrystallises to a lesser extent than potato starch, resulting in crystallinity indices of ~0.4 (Figure 7.3). In contrast to potato starch, there are no clear trends in the recrystallisation with increasing plasticiser size or with the presence of ghosts for (partly) gelatinised wheat starch. Amidon Haussy wheat starch is, like potato starch, pure and contains little fat and protein. However, the amylopectin structure is different from that of potato starch. Native potato starch has B-type crystallinity, whereas native wheat starch has A-type crystals. Amylopectin chains are shorter for A-type starches, whereas B-type starches have a longer distance between the branch points [12,13]. In general, cereal amylopectin retrogrades to a lesser extent than pea and potato amylopectin, because of the shorter average chains of the cereal amylopectin [4,14-16]. Resulting from these shorter amylopectin chains, the remaining structures in wheat starch ghosts may resemble A-type crystallinity, which make it more difficult to form B-type crystals [17,18]. Since B-type crystals are formed during recrystallisation, the ghost structures can then not facilitate crystallisation, and no trend can be found with increasing plasticiser size. Alternatively, it may be that the trends as found for potato starch with increasing plasticiser size also occur for wheat starch, but are less manifest due to the lower degree of recrystallisation.

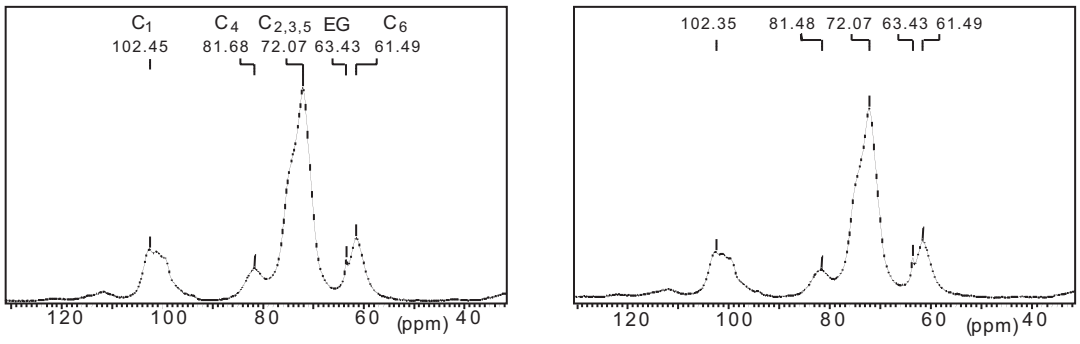

4a **4b**

Figure 7.4 Solid state ^{13}C CP/MAS NMR spectra of recrystallised partly (4a) and fully (4b) gelatinised wheat starch plasticised by ethylene glycol (63.4 ppm).

Solid state NMR spectroscopy

Further studies were performed by solid state CP/MAS NMR spectroscopy on the wheat starch samples containing ethylene glycol to gain better insight into the recrystallisation process and to compare completely and partly gelatinised systems. An ethylene glycol signal appeared at 63.4 ppm in the spectra of both preparations (Figure 7.4). This implies that the plasticiser is partly immobilised because of its interaction with starch.

Identical spectra were obtained with identical relative ethylene glycol signals, implying similar molecular organisation independent of the presence of ghosts. There is no influence of wheat starch ghosts on the mobility of the plasticiser. Since there is no obvious influence of ghosts on the molecular mobility in the sample, presumably there will be no influence of ghosts on wheat starch recrystallisation, which confirms the recrystallisation results. Apparently, wheat starch ghosts do not act as nuclei for crystallisation. HP/DEC NMR spectra were obtained as well, but did not lead to additional information, because of the large amount of mobile ethylene glycol.

Conclusions

Potato starch and wheat starch were fully or partly gelatinised, and aged in the presence of a range of plasticisers. The largest reduction in potato starch recrystallisation is found for threitol (4 OH) and xylitol (5 OH). The larger the number of OH groups in the plasticiser, when going from ethylene glycol to maltose, the better the plasticiser reduces the crystallisation inducing effect of remaining structure (ghosts) in potato starch. Up to 4 OH groups (the turning point), more recrystallisation takes place when ghosts are present. Smaller plasticisers facilitate crystallisation nucleated by ghosts, by mobilising the starch chains. Larger plasticisers intrude between the starch chains and thereby prevent crystal propagation. It is important for both food and non-food applications of starch that granular remnants can influence retrogradation, however, the effect is dependent on the plasticiser used.

Wheat starch recrystallises to a lesser extent than potato starch, probably because of the shorter amylopectin chains [14-16]. Recrystallisation of wheat starch does not show clear trends with increasing plasticiser size and number of OH groups. Solid state CP/MAS NMR spectra of wheat starch samples containing ethylene glycol confirm that the ghost structures do not influence wheat starch recrystallisation.

Especially in non-food products, e.g. controlled release systems, based on tuber starches (with B-type crystallinity), the use of threitol instead of glycerol can be interesting for reducing retrogradation.

References

1. N.J. Atkin, R.M. Abeysekera, A.W. Robards, 'The events leading to the formation of ghost remnants from the starch granule surface and the contribution of the granule surface to the gelatinization endotherm', *Carboh. Polym.* **36** (1998), p 193-204,
2. H. Levine, L. Slade, 'Water relationships in food', Plenum Press New York (1991),
3. N. Krog, S.K. Oleson, H. Toernaes, T. Joensson, 'Retrogradation of the starch fraction in wheat bread', *Cereal Foods World* **34** (1989), p 281-285,
4. M. Gudmundsson, 'Retrogradation of starch and the role of its components', *Thermochim. Acta* **246** (1994), p 329-341,
5. K. Kohyama, K. Nishinari, 'Effect of soluble sugars on gelatinization and retrogradation of sweet potato starch', *J. Agric. Food Chem.* **39** (1991), p 1406-1410,
6. K. Katsuta, A. Nishimura, M. Miura, 'Effects of saccharides on stabilities of rice starch gels: 1. Mono-and disaccharides', *Food Hydrocoll.* **6** (1992), p 387-398,
7. E. Chiotelli, A. Rolée, M. Le Meste, 'Effect of sucrose on the thermomechanical behavior of concentrated wheat and waxy corn starch-water preparations', *J. Agric. Food Chem.* **48** (2000), p 1327-1339,
8. J.J.G. van Soest, D. de Wit, H. Tournois, J.F.G. Vliegenthart, 'The influence of glycerol on structural changes in waxy maize starch as studied by FT-IR spectroscopy', *Polymer* **35** (1994), p 4722-4727,
9. M. Miyajima, A. Koshika, J. Okada, M. Ikeda, K. Nishimura, 'Effect of polymer crystallinity on papaverine release from poly(L-lactic acid) matrix', *J. Control. Release* **49** (1997), p 207-215,
10. S.K. Yadav, K.C. Khilar, A.K. Suresh, 'Release rates from semi-crystalline polymer microcapsules formed by interfacial polycondensation', *J. Membrane Sci.* **125** (1997), p 213-218,
11. P. Ispas-Szabo, F. Ravenelle, I. Hassan, M. Preda, M.A. Mateescu, 'Structure-properties relationship in cross-linked high-amylose starch for use in controlled release', *Carboh. Res.* **323** (2000), p 163-175,
12. S. Hizukuri, 'Relationship between the distribution of the chain length of amylopectin and the crystalline structure of starch granules', *Carboh. Res.* **141** (1985), p 295-306,
13. C. Gérard, V. Planchot, P. Colonna, E. Bertoft, 'Relationship between branching density and crystalline structure of A- and B-type maize mutant starches', *Carboh. Res.* **326** (2000), p 130-144,
14. M.T. Kalichevsky, P.D. Orford, S.G. Ring, 'The retrogradation and gelation of amylopectins from various botanical sources', *Carboh. Res.* **198** (1990), p 49-55,
15. H. Fredriksson, J. Silverio, R. Andersson, A.C. Eliasson, P. Åman, 'The influence of amylose and amylopectin characteristics on gelatinization and retrogradation properties of different starches', *Carboh. Polym.* **35** (1998), p 119-134,
16. J. Silverio, H. Fredriksson, R. Andersson, A.C. Eliasson, P. Åman, 'The effect of temperature cycling on the amylopectin retrogradation of starches with different amylopectin unit-chain length distribution', *Carboh. Polym.* **42** (2000), p 175-184,
17. A. Imberty, A. Buléon, V. Tran, S. Pérez, 'Recent advances in knowledge of starch structure', *Starch/Stärke* **43** (1991), p 375-384,
18. T.A. Waigh, A.M. Donald, F. Heidelbach, C. Riekel, M.J. Gidley, 'Analysis of the native structure of starch granules with small angle X-ray microfocus scattering', *Biopolymers* **49** (1999), p 91-105.

Chapter 8

The Influence of Various Malto-oligosaccharides on the Retrogradation of (partly) Gelatinised Wheat Starch

A.L.M. Smits, P.H. Kruiskamp, J.J.G. van Soest, J.F.G. Vliegenthart

[Submitted to be published]

Abstract

The influence of various malto-oligosaccharides in combination with granular remnants (ghosts) on starch ageing was investigated. Recrystallisation was determined, by using X-ray diffraction, of gelatinised and partly gelatinised wheat starch plasticised with maltose, maltotriose, maltotetraose, maltopentaose or maltohexaose. This resulted in crystallinity indices of ~0.2, with the largest reduction in recrystallisation for maltotriose and maltotetraose. No trend was found for the influence of ghosts. The presence of ghosts did not influence the ^{13}C solid state HP/DEC NMR spectra. Less recrystallisation took place than with the previously reported smaller plasticisers glycol, glycerol, threitol, xylitol or glucose that resulted in crystallinity indices of ~0.4. The finding that maltose was able to reduce retrogradation better than glucose could be of practical importance.

Introduction

Starch is one of the main energy providers in the human diet. Ageing of starch based foods causes staling, deteriorating the properties of food products. The ageing process is caused by starch crystallisation or retrogradation [1,2]. Low molecular weight carbohydrates, such as monosaccharides and malto-oligosaccharides, are significant components in many food products. Knowledge of their influence on the glass transition of foods has helped food scientists to control storage stability and food quality [3]. In bakery processes, low molecular weight malto-oligosaccharides are produced by enzymatic hydrolysis of starch by α-amylase. These sugars are known to reduce retrogradation, when comparing systems with equal total amounts of plasticiser, by interfering with starch recrystallisation [4,5].

In the present study, changes in the molecular organisation in starch-plasticiser systems during ageing and the influence of polyol plasticisers on ageing are investigated [6]. It would be interesting to know if there is an optimum in the reduction in retrogradation with a certain malto-oligosaccharide chain length. Much research has been done on starch gels, but for relevance to bakery products low water content gelatinised starch systems are examined in the present study. The influence of granular remnants on retrogradation is also interesting, since starch is often partly gelatinised when processing food products [3,7]. Therefore, the influence of maltose, maltotriose, maltotetraose, maltopentaose and maltohexaose on ageing was investigated, in combination with granular remnants, using fully and partly gelatinised wheat starch.

Experimental

Sample preparation

Gelatinisation is performed in a Brabender viscometer. 40.49 g wheat starch, WN (Amidon Haussy, Avebe), was mixed with de-ionised water to gain 350 g of a 10% dry weight starch dispersion. The mixture was poured into the Brabender and stirred at a frequency of 75 rpm, while heating from room temperature to 90°C with 2°C/min. The completely gelatinised mixture was obtained by keeping it at 90°C for 55 min. The partly gelatinised sample was prepared by stopping at the peak viscosity, which was reached after keeping it for 4 min at 90°C. The partly gelatinised sample was examined with polarised light microscopy for the presence of ghost structures, and for

the absence of granules. Granules would appear as Maltese crosses. Granular remnants appeared as non-crystalline ghost structures, as examined with X-ray diffraction.

The gelatinised mixtures were dried under reduced pressure in a vacuum-oven for 24 h at 50°C. Plasticisers were added to the WN samples at a dry starch / plasticiser ratio of 100:30 w/w. Equal plasticiser weight ratios were used in order to have added equal numbers of glucose residues. The plasticisers were dissolved in a small amount of water and mixed with the gel, when it was still humid. Plasticisers used were maltose (Merck), maltotriose, maltotetraose, maltomaltopenatose and maltohexaose (Sigma). The samples were ground after freezing with liquid nitrogen and conditioned at 20°C and 90% RH. Sample crystallinity was measured by using X-ray diffraction.

Analyses

Wide angle X-ray powder diffraction (XRD) was performed on a Philips PC-APD diffractometer in the reflection geometry in the angular range 4-40°(2θ). The CuK radiation from the anode operating at 40 kV and 50 mA was monochromised using a 15 µm Ni foil, leaving only the CuK_{α} radiation (1.54 Å). The diffractometer parameters were: divergence slit 1°, receiving slit 0.2 mm and scatter slit 1°. A proportional detector was used to detect the scattered radiation. Diffractograms were baseline corrected by drawing a straight line between the intensities at 7 and 40°(2θ). The ratio of the height of the crystalline diffraction at 17.3°(2θ) and the height of the total diffraction at this angle is defined as the crystallinity index, a measure for the B-type crystallinity of the sample.

Solid state high power decoupling (HP/DEC) NMR spectra were collected on a Bruker AMX 400 spectrometer operating at 100.63 MHz for ^{13}C. Samples were spun at the magic angle (54.7°) with respect to the static magnetic field. Carbon chemical shifts relative to tetramethylsilane (TMS) were determined from the spectra, using solid glycine at room temperature as external reference. Samples were packed into 7-mm ceramic rotors and spun at 4 kHz. The recycle delay was set to 4 s.

Results and Discussion

Recrystallisation was examined of fully and partly gelatinised wheat starch samples, using a range of malto-oligosaccharides with increasing number of glucose residues (Figure 8.1). Within two days of conditioning at 90%RH and 20°C, the samples are at

equilibrium moisture content. By that time most of the recrystallisation has already taken place. Therefore, focus is on the final recrystallisation. Experiments are well reproducible with a spread in crystallinity index of ±0.01.

Less recrystallisation takes place when no plasticiser is added. These samples have a different condition with respect to their glass transition temperature, because the content of plasticiser (including water) is lower. Therefore, it is only possible to compare the influence of plasticisers other than water.

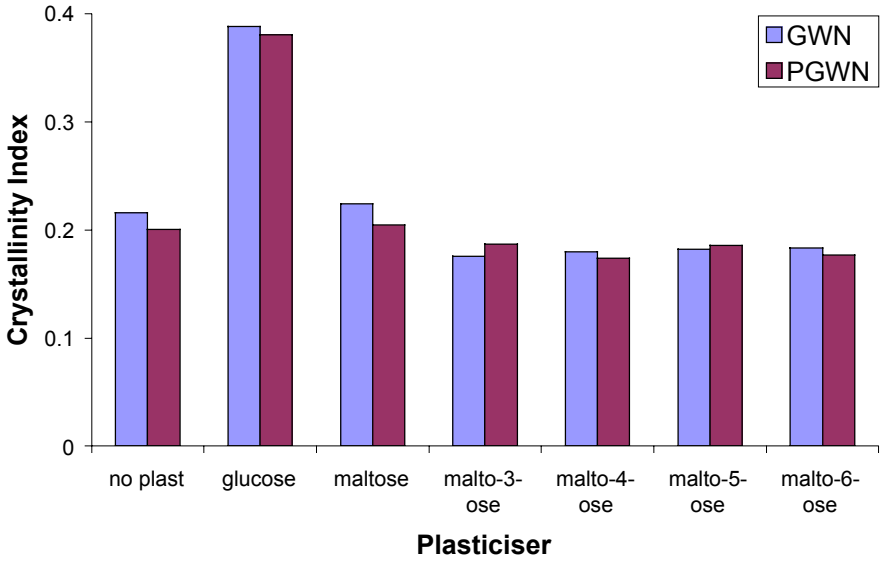

Figure 8.1 Final recrystallisation of completely (GWN) and partly gelatinised (PGWN) wheat starch without added plasticiser, with glucose [8], and with a range of malto-oligosaccharides.

Recrystallisation of wheat starch plasticised with maltose, maltotriose, maltotetraose, maltopentaose or maltohexaose is presented in Figure 8.1. With this range of malto-oligosaccharides, less recrystallisation takes place than with the smaller plasticisers ethylene glycol, glycerol, threitol, xylitol and glucose [8]. They resulted in crystallinity indices of ~0.4, whereas the malto-oligosaccharide plasticised systems gave crystallinity indices of ~0.2. The malto-oligosaccharides substantially reduce retrogradation. For comparison, the results for glucose have been added to Figure 8.1. The largest reduction in recrystallisation of (partly) gelatinised wheat starch is found for maltotriose and maltotetraose. The larger malto-oligosaccharides reduce retrogradation better than maltose. There is no obvious trend in the influence of ghosts on recrystallisation. A possible influence of ghosts may be not manifest, due to the low degree of recrystallisation.

Solid state HP/DEC NMR spectra were obtained from partly and completely gelatinised wheat starch with maltopentaose and maltohexaose to gain better insight into the recrystallisation process. No clear differences were found between completely and partly gelatinised systems (Figure 8.2), implying that there is no influence of wheat starch ghosts on the mobility of the malto-oligosaccharide. Since ghosts do not seem to influence the molecular mobility in the sample, presumably there will be no influence of ghosts on wheat starch recrystallisation, which confirms the recrystallisation results. CP/MAS NMR spectra did not lead to additional information, because the malto-oligosaccharides could not be revealed, due to complete overlap with the starch signals.

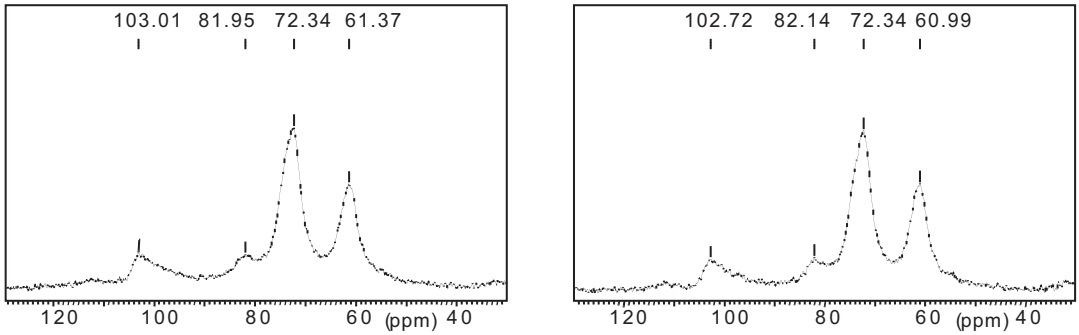

2a **2b**

Figure 8.2 Solid state HP/DEC NMR spectra of partly (2a) and completely (2b) gelatinised wheat starch containing maltohexaose.

Malto-oligosaccharides with a degree of polymerisation DP 3-6 reduce retrogradation better than maltose. However, these oligosaccharides are less available and more expensive than maltose. The limited reduction in retrogradation would therefore probably not justify the bulk application of these larger oligosaccharides. More importantly, maltose is found to reduce wheat starch retrogradation substantially better than glucose [8]. This makes it useful to add maltose instead of glucose to bakery products, for the prevention of retrogradation. It would be advisable to use an amylase type that cuts back up to maltose, but that does not create glucose, for example a ß-amylase [9]. Whereas α-amylase 'randomly' hydrolyses internal (1→4) bonds, finally producing glucose, maltose and small branched oligosaccharides, ß-amylase removes maltose units in a stepwise fashion at external (1→4) linkages, without hydrolysing or bypassing branch points (Figure 8.3).

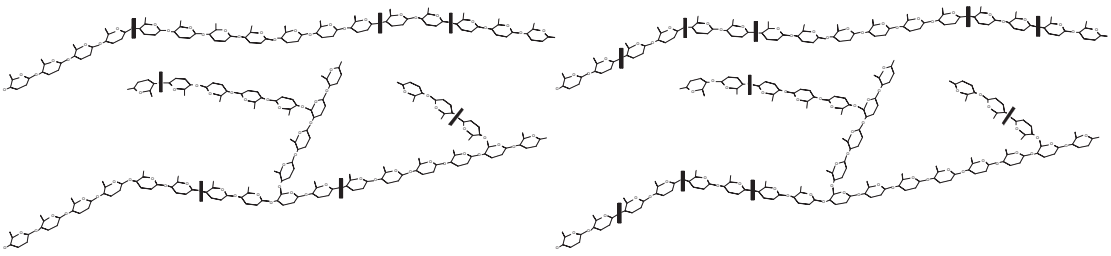

Figure 8.3 Enzymatic action on starch, shown by |. 'Random' attack by α-amylase (left), and external removal of maltose units by ß-amylase (right).

Recently, Durán *et al.* reported on the influence of malto-oligosaccharides on gelatinisation and retrogradation as studied by DSC [10]. Their systems probably recrystallised more than the systems reported here, because of the higher amount of water (1 starch : 2 water). Amounts of oligosaccharide were used (27% on starch base) that are comparable with the amounts in the present study. In wheat starch solutions with malto-oligosaccharides with DP 2-7, they found that up to DP5 the extent of retrogradation is reduced. At DP6 more retrogradation occurred than with DP5 but retrogradation was still reduced. And with DP7 retrogradation increases. Their results show a minimum in retrogradation at maltopentaose.

Starch crystal helices contain 6 sugar rings per helix turn. Sugiyama *et al.* showed that malto-oligosaccharides up to DP5 have conformation different from longer malto-oligomers, giving slightly different angles between the contiguous glucose residues [11]. This may be related to the reduction of recrystallisation of starch plasticised by malto-oligosaccharides up to DP6, and the increase in recrystallisation from DP7 onwards. The small malto-oligosaccharides interact with the starch chain, and may thus hinder helix formation. The larger the malto-oligosaccharide (DP 2-5), the better it reduces recrystallisation. Malto-oligosaccharides of DP6 can form just one helix turn, and as such may be less able to reduce retrogradation. The larger oligosaccharides (DP >6) may form small helices that can be incorporated into the starch helix and increase retrogradation. This is confirmed by Gidley *et al.*, who reported that for pure malto-oligosaccharides, the minimum chain-length required for crystallisation is DP10, but in the presence of longer chains, malto-oligomers as short as maltohexaose can co-crystallise [12].

Conclusions

Malto-oligosaccharides substantially reduce wheat starch recrystallisation. No trend was found for the influence of remaining granular structure (ghosts). The trend with increasing malto-oligosaccharide chain length relates to the number of glucose residues needed for helix formation. Malto-oligosaccharides of DP 2-5 may hinder helix formation, and are thus able to reduce retrogradation. Whereas larger malto-oligosaccharides of DP >6 may form small helices that co-crystallise with starch and thereby increase retrogradation. Maltose was found to reduce retrogradation better than glucose, which can be of practical importance for bakery products.

References

1. N. Krog, S.K. Oleson, H. Toernaes, T. Joensson, 'Retrogradation of the starch fraction in wheat bread', *Cereal Foods World* **34** (1989), p 281-285,
2. M. Gudmundsson, 'Retrogradation of starch and the role of its components', *Thermochim. Acta* **246** (1994), p 329-341,
3. H. Levine, L. Slade, 'Water relationships in food', Plenum Press New York (1991),
4. A. Léon, E. Durán, C. Benedito de Barber, 'Firming of starch gels and amylopectin retrogradation as related to dextrin production by α-amylase', *Z. Lebensm. Unters. Forsch. A* **205** (1997), p 131-134,
5. K. Katsuta, A. Nishimura, M. Miura, 'Effects of saccharides on stabilities of rice starch gels: 2. Oligosaccharides', *Food Hydrocoll.* **6** (1992), p 399-408,
6. A.L.M. Smits, F.C. Ruhnau, J.F.G. Vliegenthart, J.J.G. van Soest, 'Ageing of starch based systems as observed with FT-IR and solid state NMR spectroscopy', *Starch/Stärke* **50** (1998), p 478-483,
7. N.J. Atkin, R.M. Abeysekera, A.W. Robards, 'The events leading to the formation of ghost remnants from the starch granule surface and the contribution of the granule surface to the gelatinization endotherm', *Carboh. Polym.* **36** (1998), p 193-204,
8. A.L.M. Smits, P.H. Kruiskamp, J.J.G. van Soest, J.F.G. Vliegenthart, 'The influence of various plasticisers on the retrogradation of (partly) gelatinised starch', Chapter 7, to be published,
9. G.S. Nilsson, S. Richardson, A. Huber, N. Torto, T. Laurell, L. Gorton, 'Microdialysis clean-up and sampling in enzyme-based methods for the characterisation of starch', *Carboh. Polym.* **46** (2001), p 59-68,
10. E. Durán, A. Léon, B. Barber, C. Benedito de Barber, 'Effect of low molecular weight dextrins on gelatinization and retrogradation of starch', *Eur. Food Res. Technol.* **212** (2001), p 203-207,
11. H. Sugiyama, T. Nitta, M. Horii, K. Motohashi, J. Sakai, T. Usui, K. Hisamichi, J. Ishiyama, 'The conformation of α-(1→4)-linked glucose oligomers from maltose to maltoheptaose and short-chain amylose in solution', *Carboh. Res.* **325** (2000), p 177-182,
12. M.J. Gidley, P.V. Bulpin, 'Crystallisation of malto-oligosaccharides as models of the crystalline forms of starch: minimum chain-length requirement for the formation of double helices', *Carboh. Res.* **161** (1987), p 291-300.

Summary

Starch is produced by plants to store the energy-source glucose and consists of essentially linear amylose and highly branched amylopectin. When processing starch based food systems, starch is (partly) gelatinised or melted, using water and sugars as plasticisers. In starch based biodegradable plastics, adhesives or coatings, starch is plasticised, for example by glycerol or ethylene glycol, and (partly) melted or gelatinised. Plasticisers are needed to enable starch processing, by reducing the glass transition temperature of starch. Unfortunately, ageing causes retrogradation or recrystallisation of starch, which leads to staling of food products and embrittlement of non-food starch products. Some plasticisers are known to reduce retrogradation (as compared with equal amounts of other plasticisers), but it is not clear how. Therefore, it is difficult to control retrogradation, especially in new starch based products.

In the study described in this thesis, the location and mobility of the various components in starch systems containing polyol-type plasticisers (e.g. glycerol or sugars) have been investigated. Native potato starch is used, because of its purity, or wheat starch, which is mainly applied in bakery products. Emphasis is on retrogradation, the influence of polyol plasticisers and the influence of structure remaining due to incomplete melting or gelatinisation on retrogradation.

In chapter **1**, an overview is given of the present knowledge of starch structure, processing and ageing. In chapter **2**, the analytical techniques that are used in the study described in this thesis are presented, together with an overview of the applicabilities of these techniques in starch research.

In chapter **3**, retrogradation and sub-T_g physical ageing are described of gelatinised starch plasticised solely by water. Retrogradation caused changes in peak shapes and intensities in infrared spectra in the area 950-1150 cm^{-1}. Physical ageing as well as retrogradation caused an increase in the proton $T_{1\rho}$ relaxation times in solid state NMR relaxation experiments. Infrared and solid state NMR spectroscopy were shown to be good techniques for investigating these ageing processes.

Furthermore, the influence of processing temperature on initial crystallinity and subsequent recrystallisation are described of compression moulded starch, plasticised

by water and glycerol. Initial crystallinity, as determined by X-ray diffraction, was present irrespective of the crystallinity prior to processing. At higher processing temperatures, amylopectin crystallised only when amylose was present, and degradation was suggested to increase the initial crystallinity. Variation of the processing temperature can be used to control crystallisation and thereby change the mechanical properties of starch-based products.

In chapters **4-6**, the interaction between starch and the plasticisers glycerol or ethylene glycol in the absence of water are described. In chapter **4**, the investigation of the interaction of dry amylose and amylopectin with glycerol and ethylene glycol are described, as studied by DSC and solid state NMR spectroscopy. The interaction caused a strong exothermal transition in DSC. With solid state NMR spectroscopy, an immobilisation of the plasticiser was observed by a decrease in the HP/DEC signals and an increase in the CP/MAS plasticiser signals. Some mobilisation of starch was observed by an increase of starch HP/DEC signals. This mobilisation was suggested to enable starch crystal perfection, as a secondary process.

Upon storage at room temperature for several days, the interaction also occurred, but faster for ethylene glycol than for glycerol. Glycerol interacted mainly with the amorphous starch regions. However, ethylene glycol interacted with all starch regions, but possibly in a more ordered manner with amorphous than with crystalline starch. Upon storage at room temperature, less plasticiser molecules interacted, but they interacted in a more ordered manner than upon heating. This was suggested to imply interaction with more of the hydroxy groups of the plasticiser.

Due to the time dependent interaction between starch and plasticisers, varying the time between premixing ingredients and processing starch may influence processing conditions such as flow properties and resistance to shear.

In chapter **5**, a description is given of the interaction between dry amylopectin and ethylene glycol as studied by dielectric relaxation spectroscopy. Fresh mixtures consisted of a continuous ethylene glycol phase and a phase of amylopectin mixed molecularly with ethylene glycol. The interaction developed upon heating, as well as after storage at room temperature, leading to a polymer system with weak intermolecular interactions. Ethylene glycol was suggested to form intra-chain H-bonded bridges between the amylopectin chains, increasing chain stiffness and increasing the glass transition. As such, the plasticiser prevents retrogradation by intruding between the starch chains.

The ethylene glycol phase was reduced to nanometer sized droplets, as revealed by confinement effects of the α-relaxation of ethylene glycol, the dynamics changing from VFT towards Arrhenius behaviour. Confinement effects of ethylene glycol can occur in zeolitic pores or cages, but have not been previously reported to occur in polymer dispersed nanodroplets. The results lead to new insights into the influence of polyol plasticisers on the molecular organisation in starch.

In chapter **6**, the interaction between dry amylopectin and ethylene glycol or glycerol are described as studied by Inverse Recover Cross Polarisation solid state NMR spectroscopy. The results show that this is a useful technique for examining changes in the molecular mobility in starch systems. New insights were gained on how starch-plasticiser interactions take place at a molecular level. Upon storage at room temperature for a period of days up to months, the interaction developed. The plasticiser mobility decreased, for ethylene glycol as well as for glycerol, and the amylopectin carbon C6 mobility increased. The mobilities of the other amylopectin carbons did not change, showing that the interaction mainly occurs at carbon C6. Chemical modification at the amylopectin carbon C6 can be used to increase the affinity to plasticiser molecules, in order to reduce starch retrogradation.

Upon heating, the interaction develops fast, after which crystal perfection is assumed to take place during storage at room temperature. The process of crystal perfection is slower for glycerol than for ethylene glycol. Furthermore, it is suggested that the small ethylene glycol molecules, which can easily penetrate the ordered amylopectin chains, prevent the amylopectin chains from becoming immobilised. The larger glycerol molecules are hindered in penetrating the crystal structure of amylopectin and primarily interact at the edges of the crystalline lamellae. Therefore, they are unable to prevent immobilisation of the amylopectin chains due to ageing.

When ingredients are premixed prior to processing, the resulting increase in molecular mobility of amylopectin may influence the flow properties and resistance to shear. After processing, the occurrence of crystal perfection gives the product more strength. The interactions between starch and ethylene glycol or glycerol may reduce starch retrogradation or recrystallisation, which would improve the control of the mechanical properties of the product.

In chapters **7** and **8**, retrogradation is described of fully and partly gelatinised starch systems, plasticised by water and several plasticisers. Due to partial gelatinisation, some granular structure remained, appearing as non-crystalline ghosts. It was

investigated to which extent they can act as nuclei for crystallisation. In chapter **7**, retrogradation is described of fully and partly gelatinised potato starch and wheat starch, plasticised by water and a range of plasticisers, increasing in size and number of hydroxy groups (ethylene glycol, glycerol, threitol, xylitol, glucose and for potato starch also maltose). By using X-ray diffraction, the largest reduction in potato starch recrystallisation was found for threitol (4 OH) and xylitol (5 OH). The larger the number of OH groups in the plasticiser molecule, the better the plasticiser reduced the crystallisation inducing effect of ghosts in potato starch. Smaller plasticisers facilitate crystallisation nucleated by ghosts, by mobilising the starch chains. Larger plasticisers were suggested to intrude between the starch chains, thereby preventing crystal propagation. Wheat starch recrystallised to a lesser extent (crystallinity indices of ~0.4 vs. ~0.5 for potato starch), probably because of the shorter amylopectin chains. Recrystallisation of wheat starch did not show clear trends for the influence of plasticiser size and of ghosts.

In non-food products based on tuber starches (with B-type crystallinity), the use of threitol instead of glycerol can be interesting for reducing retrogradation. It is important for both food and non-food applications of starch that granular remnants can influence retrogradation, however the effect is dependent on the plasticiser used.

In chapter **8**, retrogradation is described of fully and partly gelatinised wheat starch, plasticised by water and a range of malto-oligosaccharides (maltose, maltotriose, maltotetraose, maltopentaose and maltohexaose). In bakery processes, these malto-oligosaccharides are produced by enzymatic hydrolysis of starch. By using X-ray diffraction, crystallinity indices of ~0.2 were found, with the largest reduction in recrystallisation for maltotriose and maltotetraose. No trend was found for the influence of ghosts that remained due to incomplete gelatinisation, by using X-ray diffraction as well as solid state NMR spectroscopy. Malto-oligosaccharides substantially reduced retrogradation, as can be seen when comparing the crystallinity indices with those described in chapter **7** (~0.4) for a range of smaller plasticisers. The finding that maltose reduced retrogradation substantially better than glucose (chapter **7**), is of practical importance for starch based foods. Maltose could be added instead of glucose, and a ß-amylase type could be used that affords maltose units from starch chains, instead of α-amylase that also produces glucose.

The trend with increasing malto-oligosaccharide chain length was suggested to be due to the need of 6 glucose residues for helix formation. Malto-oligosaccharides

consisting of 6 or more glucose residues were proposed to increase retrogradation because of co-crystallisation. The smaller malto-oligosaccharides were assumed to reduce retrogradation by intruding between the starch chains, the larger molecules giving the largest reduction.

Samenvatting

Zetmeel wordt door planten geproduceerd voor de opslag van de energiebron glucose en bestaat uit hoofdzakelijk lineair amylose en sterk vertakt amylopectine. Bij het verwerken van voedsel op zetmeelbasis wordt zetmeel (deels) verstijfseld of gesmolten, waarbij water en suikers worden gebruikt als weekmakers. In biodegradeerbare plastics, lijmen of coatings op zetmeelbasis wordt zetmeel weekgemaakt, door bijvoorbeeld glycerol of ethyleen glycol, en (deels) gesmolten of verstijfseld. Weekmakers zijn nodig om het verwerken van zetmeel mogelijk te maken, door de glasovergangstemperatuur van zetmeel te verlagen. Helaas veroorzaakt veroudering retrogradatie of herkristallisatie van zetmeel, wat leidt tot het oudbakken worden van voedingsproducten en het bros worden van niet-voedings zetmeelproducten. Van sommige weekmakers is bekend dat zij retrogradatie verminderen (in vergelijking met gelijke hoeveelheden van andere weekmakers), maar het is niet duidelijk hoe. Daarom is het moeilijk retrogradatie te beheersen, vooral in nieuwe zetmeelproducten.

In het in dit proefschrift beschreven onderzoek worden de locatie en mobiliteit bestudeerd van de verschillende componenten in zetmeelsystemen die polyol-type weekmakers (b.v. glycerol of suikers) bevatten. Natief aardappelzetmeel is gebruikt vanwege zijn zuiverheid, of tarwezetmeel dat hoofdzakelijk wordt toegepast in bakkerijproducten. De nadruk ligt op retrogradatie, de invloed van polyol weekmakers en de invloed van reststructuur door onvolledig smelten of verstijfselen op retrogradatie.

In hoofdstuk **1** wordt een overzicht gegeven van de huidige kennis op het gebied van de structuur, verwerking en veroudering van zetmeel. In hoofdstuk **2** worden de analysetechnieken besproken die worden gebruikt in het onderzoek dat wordt beschreven in dit proefschrift. Daarbij wordt een overzicht gegeven van de mogelijkheden van deze technieken in zetmeelonderzoek.

In hoofdstuk **3** worden retrogradatie en sub-T_g veroudering beschreven van verstijfseld zetmeel dat uitsluitend door water is weekgemaakt. Retrogradatie veroorzaakt veranderingen in de vorm en intensiteit van pieken in infrarood spectra in

het gebied 995-1050 cm^{-1}. Zowel fysische veroudering als retrogradatie veroorzaakt een toename in de proton $T_{1\rho}$ relaxatietijden in vaste stof NMR relaxatie experimenten. Er is aangetoond dat infrarood en vaste stof NMR spectroscopie goede technieken zijn voor het bestuderen van deze verouderingsprocessen.

Daarnaast wordt de invloed van de verwerkingstemperatuur op de aanvankelijke kristalliniteit en de daaropvolgende herkristallisatie beschreven van compression moulded (in een mal geperst) zetmeel dat is weekgemaakt door water en glycerol. Aanvankelijke kristalliniteit, bepaald met Röntgendiffractie, was aanwezig onafhankelijk van de kristalliniteit voor het verwerken. Bij hogere verwerkingstemperaturen kristalliseerde amylopectine uitsluitend wanneer amylose aanwezig was, en er werd voorgesteld dat degradatie de aanvankelijke kristalliniteit verhoogt. Variatie van de verwerkingstemperatuur kan gebruikt worden om kristallisatie en daarmee de mechanische eigenschappen van zetmeelproducten te beheersen.

In de hoofdstukken **4-6** wordt de interactie tussen zetmeel en de weekmakers glycerol of ethyleen glycol in afwezigheid van water beschreven. In hoofdstuk **4** wordt het onderzoek beschreven naar de interactie tussen droog amylose en amylopectine met glycerol en ethyleen glycol, zoals bestudeerd met DSC en vaste stof NMR spectroscopie. De interactie veroorzaakte een sterke exotherme overgang in DSC. Met vaste stof NMR spectroscopie werd een afname van de HP/DEC signalen en een toename van de CP/MAS weekmakersignalen waargenomen. Enige mobilisatie van zetmeel werd waargenomen door middel van een toename van de HP/DEC zetmeelsignalen. Er werd voorgesteld dat deze mobilisatie kristalperfectie mogelijk maakt, als een secundair proces.

Tijdens opslag bij kamertemperatuur gedurende enkele dagen vindt de interactie tevens plaats, maar sneller voor ethyleen glycol dan voor glycerol. Glycerol gaat vooral interactie aan met de amorfe gebieden in zetmeel. Echter, ethyleen glycol gaat interactie aan met alle zetmeelgebieden, maar mogelijk op een meer geordende wijze met amorf dan met kristallijn zetmeel. Tijdens opslag bij kamertemperatuur gingen minder weekmakermoleculen interactie aan, maar de interactie was meer geordend dan na verhitten. Er werd voorgesteld dat dit inhoudt, dat de interactie plaatsvindt met meer van de hydroxy-groepen van de weekmaker.

Vanwege de tijdafhankelijke interactie tussen zetmeel en weekmakers kan het variëren van de tijd tussen het premixen van ingrediënten en het verwerken van zetmeel, verwerkingcondities beïnvloeden zoals vloei en weerstand tegen shear (afschuiving).

In hoofdstuk **5** wordt de interactie tussen droog amylopectine en ethyleen glycol beschreven, zoals bestudeerd met diëlektrische relaxatie spectroscopie. Verse mengsels bestonden uit een continue ethyleen glycol fase en een fase van amylopectine moleculair gemengd met ethyleen glycol. De interactie vond zowel plaats door verhitting als door opslag bij kamertemperatuur, en leidde tot een polymeersysteem met zwakke intermoleculaire interacties. Er werd voorgesteld dat ethyleen glycol intramoleculaire H-gebonden bruggen vormt binnen de amylopectine ketens, waarmee de ketenstijfheid en de glasovergangstemperatuur verhoogd worden. Zodoende voorkomt de weekmaker retrogradatie door tussen de zetmeelketens in te dringen.

De ethyleen glycol fase werd gereduceerd tot druppels van nanometergrootte, wat wordt weegegeven door confinement (opsluitings) effecten van de α-relaxatie van ethyleen glycol, waarbij de dynamica verandert van VFT naar Arrhenius gedrag. Confinement effecten van ethyleen glycol kunnen plaatsvinden in poriën of holtes van zeolieten, maar werden niet eerder gerapporteerd in polymeer gedispergeerde nanodruppels. De resultaten leidden tot nieuwe inzichten in de invloed van polyol weekmakers op de moleculaire organisatie in zetmeel.

In hoofdstuk **6** wordt de interactie beschreven tussen droog amylopectine en ethyleen glycol of glycerol, zoals bestudeerd met Inverse Recovery Cross Polarisation vaste stof NMR spectroscopie. De resultaten tonen aan dat dit een zeer nuttige techniek is om veranderingen in de moleculaire mobiliteit in zetmeelsystemen te onderzoeken. Nieuwe inzichten werden verworven over de manier waarop zetmeel-weekmaker interacties plaats vinden op een moleculair niveau. De interactie vond plaats tijdens opslag bij kamertemperatuur gedurende enkele dagen tot maanden. De mobiliteit van de weekmaker nam af, zowel voor ethyleen glycol als voor glycerol, en de mobiliteit van de amylopectine koolstof C6 nam toe. De mobiliteit van de andere amylopectine koolstoffen veranderde niet, wat aangeeft dat de interactie voornamelijk bij koolstof C6 plaats heeft. Chemische modificatie aan amylopectine koolstof C6 kan gebruikt worden om de affiniteit voor weekmakermoleculen te verhogen en daarmee retrogradatie van zetmeel tegen te gaan.

Door verhitting vindt de interactie snel plaats, waarna er wordt aangenomen dat kristalperfectie optreedt tijdens opslag bij kamertemperatuur. Het proces van kristalperfectie is langzamer voor glycerol dan voor ethyleen glycol. Bovendien wordt voorgesteld dat de kleine ethyleen glycol moleculen, die gemakkelijk kunnen doordringen in de geordende amylopectine ketens, voorkomen dat de amylopectine ketens worden geïmmobiliseerd. De grotere glycerol moleculen kunnen moeilijker doordringen in de kristalstructuur van amylopectine en hebben alleen interactie aan de randen van de kristallijne lamellen. Daarom zijn zij minder goed in staat te voorkomen dat de amylopectine ketens immobiliseren door veroudering.

Wanneer ingrediënten worden gemengd voor de verwerking, kan de resulterende toename in moleculaire mobiliteit van amylopectine de vloei en weerstand tegen shear (afschuiving) beïnvloeden. Na verwerking geeft het plaatsvinden van kristalperfectie het product meer sterkte. De interactie tussen zetmeel en ethyleen glycol of glycerol kan retrogradatie of herkristallisatie van zetmeel verminderen, wat de beheersing van de mechanische eigenschappen van het product zou verbeteren.

In de hoofdstukken **7** en **8** wordt de retrogradatie beschreven van volledig en deels verstijfselde zetmeelsystemen die zijn weekgemaakt door water en verscheidene weekmakers. Door het deels verstijfselen blijft enige granulaire structuur achter in de vorm van niet-kristallijne ghosts. Er werd onderzocht in hoeverre deze kunnen fungeren als nucleus voor kristallisatie. In hoofdstuk **7** wordt retrogradatie beschreven van volledig en deels verstijfseld aardappelzetmeel en tarwezetmeel, weekgemaakt door water en een reeks weekmakers met toenemende grootte en aantal hydroxy-groepen (ethyleen glycol, glycerol, threitol, xylitol, glucose en voor aardappelzetmeel ook maltose). Met behulp van Röntgendiffractie werd de grootste reductie in herkristallisatie van aardappelzetmeel gevonden voor threitol (4 OH) en xylitol (5 OH). Hoe groter het aantal OH groepen in het weekmakermolecuul, des te beter vermindert de weekmaker het kristallisatie veroorzakend effect van ghosts in aardappelzetmeel. Kleinere weekmakers vergemakkelijken kristallisatie waarbij ghosts optreden als nucleus voor kristallisatie, door de zetmeelketens te mobiliseren. Er wordt voorgesteld dat grotere weekmakers tussen de zetmeelketens dringen en daarmee kristalpropagatie voorkomen. Tarwezetmeel herkristalliseert minder (kristalliniteits-indices van ~0.4 vs. ~0.5 voor aardappelzetmeel), waarschijnlijk vanwege de kortere amylopectine ketens. Herkristallisatie van tarwezetmeel liet geen trends zien voor de invloed van de weekmakergrootte en van ghosts.

In niet-voedings producten op basis van knol-zetmelen (met B-type kristalliniteit) kan het gebruik van threitol in plaats van glycerol interessant zijn om retrogradatie tegen te gaan. Het is belangrijk voor zowel voedings als niet-voedings toepassingen van zetmeel, dat granulaire resten retrogradatie kunnen beïnvloeden, waarbij het effect echter afhankelijk is van de gebruikte weekmaker.

In hoofdstuk **8** wordt retrogradatie beschreven van volledig en deels verstijfseld tarwezetmeel, weekgemaakt door water en een reeks malto-oligosachariden (maltose, maltotriose, maltotetraose, maltopentaose en maltohexaose). In bakkerijprocessen worden deze malto-oligosachariden geproduceerd door enzymatische hydrolyse van zetmeel. Met behulp van Röntgendiffractie werden kristalliniteits-indices gevonden van ~0.2, met de grootste reductie in herkristallisatie voor maltotriose en maltotetraose. Er werd geen trend gevonden voor de invloed van ghosts die overblijven door onvolledige verstijfseling, zowel met Röntgendiffractie als met vaste stof NMR spectroscopie. Malto-oligosachariden reduceerden retrogradatie substantieel, wat gezien kan worden door de kristalliniteits-indices te vergelijken met die beschreven in hoofdstuk **7** (~0.4) voor een reeks kleinere weekmakers. De bevinding dat maltose retrogradatie substantieel beter reduceert dan glucose (hoofdstuk **7**), is van praktisch belang voor voeding op basis van zetmeel. Maltose zou kunnen worden toegevoegd in plaats van glucose, en een ß-amylase type kan worden gebruikt dat maltose eenheden van zetmeelketens af haalt, in plaats van α-amylase dat tevens glucose produceert.

Er werd voorgesteld dat de trend met toenemende malto-oligosacharide ketenlengte wordt veroorzaakt door de noodzaak van 6 glucose residuen voor helixvorming. Malto-oligosachariden die bestaan uit 6 of meer glucose residuen werden voorgesteld retrogradatie te doen toenemen vanwege co-kristallisatie. Er werd aangenomen dat de kleinere malto-oligosachariden retrogradatie tegen gaan doordat zij indringen tussen de zetmeelketens, waarbij de grotere moleculen de grootste reductie geven.

Samenvatting voor Niet-Chemici

Met behulp van licht zetten planten koolstofdioxide (koolzuur, CO_2) uit de lucht met water om in zuurstof (O_2) en suiker (glucose). Dit proces wordt koolzuurassimilatie genoemd. Glucose is een energiebron voor de plant. Het wordt tijdelijk opgeslagen in de vorm van zetmeel, om het weer om te zetten in glucose wanneer energie nodig is. Zetmeel bestaat uit twee polymeren (lange moleculen) van aan elkaar geregen glucose moleculen: lineair amylose en sterk vertakt amylopectine.

Zetmeel is een van de belangrijkste bestanddelen in voedsel. In de voedselverwerking wordt zetmeel vaak verwarmd met water, waardoor het uiteindelijk oplost. Dit proces heet verstijfselen. Van zetmeel kunnen ook biologisch afbreekbare plastics, lijmen en coatings worden gemaakt. Hierbij kan gedacht worden aan bijvoorbeeld bloempotten, kleiduiven, hondenbotten, verpakkingsfolie, kinderlijm of milieuvriendelijke verf. Om deze producten van zetmeel te kunnen maken, moeten weekmakers worden toegevoegd. Dit zijn als het ware smeermiddelen voor de grote zetmeelmoleculen, die het smelten of oplossen vergemakkelijken. Bij voedingsmiddelen worden suikers en water toegevoegd, en bij niet-voedings producten worden bijvoorbeeld glycerol en water als weekmakers gebruikt.

Helaas worden op den duur voedingsproducten oudbakken en niet-voedings zetmeelproducten bros en breekbaar. Dit wordt veroorzaakt door zogeheten retrogradatie van zetmeel, waarbij het materiaal kristallijn en dus hard wordt. Van sommige weekmakers is bekend dat zij deze veroudering verminderen, maar het is niet duidelijk hoe. Daarom is het, vooral voor nieuwe zetmeelproducten, moeilijk retrogradatie te beheersen.

In het in dit proefschrift beschreven onderzoek worden de locatie en mobiliteit bestudeerd van zetmeel en weekmakers in zetmeelsystemen. De gebruikte weekmakers (b.v. glycerol en suikers) zijn zogeheten polyolen, wat betekent dat ze hydroxy (OH) groepen bevatten. De nadruk ligt op retrogradatie, de invloed van polyol weekmakers en de invloed van reststructuur door onvolledig smelten of verstijfselen op retrogradatie. Verschillende analysetechnieken worden hiervoor

gebruikt. Het nut van deze technieken, waaronder een aantal minder gangbare technieken, voor zetmeelonderzoek wordt aangetoond.

Resultaten in hoofdstuk **3** laten zien dat variatie van de verwerkingstemperatuur gebruikt kan worden om kristallisatie, en daarmee bijvoorbeeld de brosheid van zetmeelproducten, te beheersen.

In de hoofdstukken **4-6** wordt de interactie beschreven tussen zetmeel en de weekmakers glycerol of ethyleen glycol, zonder water. Deze interactie ontstaat snel door het materiaal te verhitten, maar onstaat ook (langzamer) bij kamertemperatuur. Het variëren van de tijd tussen het premixen van ingrediënten en het verwerken van zetmeel, blijkt in hoofdstuk **4** verwerkingcondities zoals vloei te beïnvloeden. Er wordt aangetoond in hoofdstuk **5** hoe weekmakermoleculen retrogradatie kunnen tegengaan. De weekmakermoleculen hechten aan de zetmeelketens, zodat deze ketens niet aan elkaar kunnen hechten en niet meer kunnen kristalliseren. In hoofdstuk **6** worden nieuwe inzichten verworven over de manier waarop zetmeel-weekmaker interacties plaats vinden op een moleculair niveau. Zo wordt aangegeven met welke atomen van het zetmeel de weekmaker de interactie aangaat, namelijk met de zogeheten koolstof C6. Chemische modificatie aan deze koolstof C6 kan gebruikt worden om de affiniteit voor weekmakermoleculen te verhogen, om daarmee retrogradatie van zetmeel tegen te gaan.

In de hoofdstukken **7** en **8** wordt de invloed van verschillende weekmakers op retrogradatie beschreven. Ook wordt bekeken in hoeverre reststructuren door onvolledig verstijfselen kristallisatie kunnen verergeren. In hoofdstuk **7** blijkt dat in niet-voedings producten op basis van knol-zetmelen (met B-type kristalliniteit) het gebruik van de weekmaker threitol in plaats van glycerol interessant kan zijn om retrogradatie tegen te gaan. Verder blijkt dat reststructuren (genaamd ghosts) retrogradatie kunnen beïnvloeden, waarbij het effect afhangt van de gebruikte weekmaker.

In hoofdstuk **8** worden zogeheten malto-oligosachariden gebruikt als weekmaker. In bakkerijprocessen worden deze suikermoleculen en glucose gemaakt door enzymen. Deze weekmakers gaan retrogradatie beter tegen dan de weekmakers uit hoofdstuk **7**. Het blijkt, dat maltose retrogradatie veel beter tegengaat dan glucose. Dit is van praktisch belang voor voeding op basis van zetmeel. Maltose zou kunnen worden toegevoegd in plaats van glucose, en een ander enzym kan worden gebruikt dat maltose maakt, in plaats van glucose.

Dankwoord

Langs deze weg wil ik iedereen bedanken die mij tijdens mijn promotie gesteund heeft. In de eerste plaats mijn promotor Prof. Vliegenthart, voor de begeleiding, het begrip en het vertrouwen tijdens het onderzoek en voor alle hulp en kennis bij het schrijven van dit proefschrift. En Jeroen van Soest, voor alle begeleiding, kennis en steun gedurende deze jaren bij ATO.

Mijn collegae en vrienden bij ATO. Met name mijn paranimfen Peter Kruiskamp en Renée van Schijndel vergrootten het plezier waarmee ik aan mijn promotie gewerkt heb. Ik heb genoten van de rust en het gezelschap van Peter; zijn kennis was soms onmisbaar. Via Renée ben ik bij ATO terecht gekomen; we hebben samen een erg leuke tijd gehad. Verder Frank Giezen (Frenk), Frans Kappen, Bastiaan van Voorn, Peter Stuut, Yannick Dziechciarek, Ed Westerweele, Casper van de Pol, Erik Kroeze, Patrick van Doeveren en Richard van der Walle. En mijn mede bestuursleden van de Personeels Vereniging, vooral Jan Stoutjesdijk, Rolf Blaauw, Liesbeth Dorama, Stephan Hulleman en Huug de Vries.

Mijn collegae bij de BOC, met name Anne Marie Partridge. Jan den Boesterd van de audiovisuele dienst, voor het drukklaar maken van dit proefschrift. En Michael Wübbenhorst van de TU Delft; ik heb veel bijgeleerd op dielectrisch gebied.

Mijn vrienden. Job Verpoorte, Auke Snijder, Walter Gruijters, Erik Littmann, Jacques Huppertz, Bastiaan van de Kerkhove en Bas Moorthaemer, voor o.a. de Whisky trails in Schotland en Ierland. Willy Zelen, Reidar Timmermans en de rest van de Stiefelcommissie. Paul Veldhuis en Joanne Cheung San. En mijn Primulastraat oud-huisgenoten, voor de zeilweekenden en Kerstklaasdiners.

Mijn ouders, voor hun zorg en mijn doorzettingsvermogen. Mijn broers Eric, Rudy en Marty. En bovenal Bram, zonder zijn liefde, aandacht en relativering zou het leven een stuk lastiger zijn. Ook zijn familie: Diny, Eric en Victor.

Allemaal bedankt. Ook een ieder van wie het me ontschoten is ze hier te noemen. Tot slot wil ik stilstaan bij diegenen van wie ik tijdens mijn promotie afscheid moest nemen. Opa en oma, ome Wim en Theo.

Curriculum Vitae

De auteur van dit proefschrift werd geboren op 9 mei 1974 te Den Dungen. Na het behalen van het VWO diploma aan het 'Rodenborch College' te Rosmalen in 1992, werd datzelfde jaar een aanvang gemaakt met de studie scheikundige technologie aan de Technische Universiteit Eindhoven. In maart 1997 werd het doctoraal examen afgelegd met als keuzevakken o.a. Procesontwerp, Polymeertechnologie, Biochemie, Coatingstechnologie, Oppervlaktechemie en Organische chemie. Zij studeerde af bij de vakgroep Polymeerchemie en Kunststoftechnologie onder begeleiding van Prof. Dr. P.J. Lemstra.

In juni 1997 trad zij, via de stichting Technische Wetenschappen (STW), in dienst van de Nederlandse Organisatie voor Wetenschappelijk Onderzoek (NWO) en was als onderzoeksmedewerker werkzaam bij de vakgroep Bio-organsiche Chemie van het Bijvoet Centrum voor biomoleculair onderzoek aan de Universiteit Utrecht. Het in dit proefschrift beschreven onderzoek werd uitgevoerd onder leiding van Prof. Dr. J.F.G. Vliegenthart. Het onderzoek werd mede uitgevoerd bij het Agrotechnologisch Onderzoeksinstituut ATO te Wageningen. Tijdens haar promotie heeft zij deelgenomen aan het 'VIIth European Polymer Federation Symposium on Polymer Materials' in Szczecin, Polen (1998), de 'Workshop on Biopolymer Science' in Montpellier, Frankrijk (1998), de 'Stärke Tagung' in Detmold, Duitsland (1999), de 'International Conference on Biopolymer Technology' in Coimbra, Portugal (1999), de 'Royal Society of Chemistry meeting on Molecular Aspects of Polysaccharide Behaviour' in Norwich, Engeland (2000) en de '1st International Conference on Polymer Modification, Degradation and Stabilisation' in Palermo, Italië (2000).